CALCIUM HOMEOSTATIC MECHANISMS OPERATING IN CULTURED POST-NATAL RAT HIPPOCAMPAL NEURONS

by

ADAM OMAR SIDKY

B.Sc. (Biochemistry), The University of British Columbia, 1994

A THESIS SUBMITTED IN PARTIAL FULFILLMENT OF

THE REQUIREMENTS FOR THE DEGREE OF

MASTER OF SCIENCE

in

THE FACULTY OF GRADUATE STUDIES

(Department of Physiology)

We accept this thesis as conforming to the required standard

THE UNIVERSITY OF BRITISH COLUMBIA

July, 1997

© Adam Omar Sidky, 1997

In presenting this thesis in partial fulfilment of the requirements for an advanced degree at the University of British Columbia, I agree that the Library shall make it freely available for reference and study. I further agree that permission for extensive copying of this thesis for scholarly purposes may be granted by the head of my department or by his or her representatives. It is understood that copying or publication of this thesis for financial gain shall not be allowed without my written permission.

Department of PHYSIOLOGY

The University of British Columbia
Vancouver, Canada

Date August 6 1997

ABSTRACT

In neurons, calcium (Ca^{2+}) is used for a variety of processes and, as a result, its intracellular regulation is an important factor in determining which messenger systems are activated and the extent of that activation. To date two principal methods have been used to induce increases in the free intracellular Ca^{2+} concentration ($[Ca^{2+}]_i$) in populations of neurons. These are the activation of either voltage or ligand gated Ca^{2+}-channels by superfusions with either high K^+-solutions or solutions containing ligand gated Ca^{2+}-channel agonists. Unfortunately, with the use of either of these methods, substantial Ca^{2+}-gradients are formed and decay kinetics are difficult to measure as a result of the lag time between agonist application and peak $[Ca^{2+}]_i$. In order to circumvent these problems a novel method has been developed to examine potential Ca^{2+}-homeostatic mechanisms in cultured post-natal rat hippocampal neurons. The method requires the monitoring of the recovery of background subtracted fluorescence levels of the Ca^{2+}-indicator dye fluo-3 at 20-22 °C immediately following a rapid increase in $[Ca^{2+}]_i$ induced by flash photolysis of the caged Ca^{2+}-compound nitrophenyl-EGTA (NP-EGTA).

A variety of methods or drugs were used in an attempt to block efflux of Ca^{2+} by the plasma membrane Na^+/Ca^{2+} exchanger (PM-Na^+/Ca^{2+}) or uptake of Ca^{2+} into mitochondria. We found that many of the experimental manipulations produced a decrease in intracellular pH (pH_i) measured in sister cultures using the pH sensitive dye 2',7'-bis-(2-carboxyethyl)-5-(and-6)-carboxyfluorescein (BCECF). These changes in pH_i are likely to influence neuronal Ca^{2+}-homeostatic mechanisms directly by decreasing mitochondrial Ca^{2+}-uptake, decreasing the affinity of Ca^{2+}-binding proteins for Ca^{2+}, and inhibition of the PM-ATPase. Accordingly, for each experimental situation we determined the appropriate amount of the weak base trimethylamine (TMA) required to restore baseline pH_i prior to flash photolysis.

When the Na^+/Ca^{2+} exchanger was inhibited by replacement of all extracellular Na^+ with *N*-methyl-D-glucamine (NMDG) we observed a significant prolongation in the rate of recovery to baseline Ca^{2+}-levels. However, this treatment markedly reduced pH_i and when this effect was corrected with 5 mM TMA, the resulting recovery rates of fluo-3 fluorescent intensities were virtually identical to those seen in control situations. Similar results were found when all external Na^+ was replaced by Li^+. These experiments were particularly revealing since the effects of Li^+ on pH_i were time dependent. At early time intervals pH_i was reduced and there was an apparent reduction in the rate of recovery of fluo-3 fluorescent intensities. At later times pH_i was restored towards normal values and no effect of blockade of the Na^+/Ca^{2+} exchanger on Ca^{2+} recovery rates was observed. It is concluded therefore that, in our neuronal preparations, the Na^+/Ca^{2+} exchanger is relatively unimportant in the removal of Ca^{2+}-loads induced by the caged Ca^{2+}-compound NP-EGTA.

Inhibition of mitochondrial Ca^{2+}-uptake, using the protonophore carbonyl cyanide *m*-chlorophenylhydrazone (CCCP), resulted in a reduction in pH_i which could be restored with 2 mM TMA. Under these conditions the rate of recovery of Ca^{2+}-levels was significantly slower than controls. Similar results were found using the respiratory chain inhibitor rotenone. In order to avoid the potentially confounding effects that mitochondrial Ca^{2+}-uptake inhibitors such as CCCP have on ATP-levels, oligomycin was added to the superfusate to block reverse activity of the ATP-synthase in order to sustain ATP levels, over the short term. Under these conditions we still observed a significant prolongation in the rates of recovery to baseline values. We conclude therefore that the uptake of Ca^{2+} into mitochondria is an important homeostatic mechanism in cultured post-natal rat hippocampal neurons following a Ca^{2+}-load induced by photolysis of NP-EGTA.

TABLE OF CONTENTS

Page

Abstract ii

Table of Contents iv

List of Tables vi

List of Figures vii

Acknowledgments ix

INTRODUCTION

Overview of neuronal Ca^{2+}-homeostasis 1
Calcium entry into neurons 2
    Voltage gated calcium channels 3
    Ligand gated calcium channels 4
    Intracellular calcium stores 5
Intracellular calcium homeostasis 6
    Calcium ATPases 6
        Plasma Membrane ATPase 7
        Endoplasmic Reticulum ATPase 8
    PM-Na^+/Ca^{2+} exchanger 9
    Mitochondria 10
    Calcium binding proteins 12
Overview of calcium homeostatic methods 13
Experimental methods for increasing$[Ca^{2+}]_i$ 14
Effects of pH on Ca^{2+}-homeostatic mechanisms 16
Goals of this study 18

MATERIALS AND METHODS

Tissue Culture 19
Ca^{2+}-imaging with fluo-3 and the use of NP-EGTA 19
    Loading 19
    Imaging 20
    NP-EGTA data analysis 22
Ca^{2+}-imaging using fura-2 23
    Loading 23
    Fura-2 data analysis 24

Ca^{2+}-imaging using fura-red 25
    Loading 25
    Fura-red data analysis 26
pH imaging using BCECF 27
    Loading 27
    BCECF data analysis 27

RESULTS

Loading conditions for fluo-3 and NP-EGTA 29
Neuronal calcium response to NMDA and caged calcium compound 30
    Comparison of Room Temperature and 37 °C rates of recovery 46
Role of the PM-Na^+/Ca^{2+} exchanger 49
Role of Mitochondria 54
Role of the Endoplasmic Reticulum ATPase 68
Summary and statistical analysis of data 81

DISCUSSION

Loading with fluo-3 and NP-EGTA 85
NP-EGTA as a method for increasing $[Ca^{2+}]_i$ 87
Rates of recovery of $[Ca^{2+}]_i$ at 22° and 37° C 93
The influence of pH on Ca^{2+}-homeostatic mechansims 94
The role of the PM-Na^+/Ca^{2+} exchanger 96
The role of mitochondria 97
The role of the Endoplasmic Reticulum 101
Conclusions, limiatations and future directions 101
REFERENCES 104

LIST OF TABLES

Page

Table 1 Loading parameters investigated for fluo-3-AM and NP-EGTA-AM 29

Table 2 Comparison of Room Temperature vs. 37 °C rates of recovery 49

Table 3 Statistical analysis of potential calcium homeostatic mechanisms 82

LIST OF FIGURES

Page

Figure 1 Typical control response in a field of neurons to NMDA application and flash photolysis 32

Figure 2 Typical response in a field of neurons to NMDA followed by two consecutive uncages 34

Figure 3 The influence of pH on NP-EGTA 36

Figure 4 The effects of the caged Ca^{2+}-compound nitr-5 39

Figure 5 Response seen to 0.4 s flash in fura-2 and NP-EGTA loaded neurons ... 41

Figure 6 Response seen to 0.5 s flash in fura-2 and NP-EGTA loaded neurons ... 43

Figure 7 Response seen to a field of neurons loaded with fura-red and NP-EGTA .. 45

Figure 8 Typical response seen at 37 °C 48

Figure 9 The effects of $0Na^{+}$-NMDG on pH_i 51

Figure 10 The effects of $0Na^{+}$-Li^{+} on pH_i 53

Figure 11 Background subtracted normalized data showing the influence of the PM-Na^{+}/Ca^{2+} exchanger on Ca^{2+}-homeostasis 56

Figure 12 The effects of CCCP on resting pH_i 58

Figure 13 The effects of CCCP and CCCP + TMA on pH_i 61

Figure 14 The effects of CCCP on resting Ca^{2+}-levels 63

Page

Figure 15 The effects of CCCP and CCCP + TMA on Ca^{2+}-levels 66

Figure 16 Background subtracted normalized data showing the influence of CCCP on Ca^{2+}-homeostasis 67

Figure 17 The effect of Rotenone on pH_i 70

Figure 18 The effect of rotenone on Ca^{2+}-levels 71

Figure 19 Background subtracted normalized data showing the influence of rotenone on Ca^{2+}-homeostasis 74

Figure 20 The effect of thapsigargin on pH_i 76

Figure 21 The effect of CPA on pH_i 78

Figure 22 The effect of Ryanodine on pH_i 80

Figure 23 The effect of clamping pH_i using high K^+-nigericin during NMDA application 84

ACKNOWLEDGMENTS

First and foremost I would like to thank Dr. Kenneth G. Baimbridge for his guidance over these past three years. As a result of his care and concern for his students, my past three years have been an altogether enjoyable experience and will be looked back upon fondly. His support of both my academic and extracurricular endeavours was immeasurable and I truly appreciate his patience and understanding of my numerous absences. Secondly, I would like to thank Dr. John Church for his invaluable advice and expertise on numerous aspects of pH and Ca^{2+} imaging. His suggestions and advice were indispensible and helped formulate the backbone for many aspects of my project. I would also like to thank Stella Atmadja for her technical expertise. Without her proficiency, none of this work would have been possible.

I would like to thank Dr. Edwin Moore and Dr. Steven Kehl who provided advice and helpful discussion on data analysis and a variety of technical aspects of my work along with the members of my supervisory committee who provided invaluable insights and suggestions. I would also like to thank the students and faculty of the Department of Physiology who have made the past three years extrordinarily enjoyable, and in particular, Dr. Raymond Pederson who makes graduate work in physiology an endless grad-retreat.

INTRODUCTION

I. Overview of neuronal Ca^{2+}-homeostasis

Mechanisms designed to regulate intracellular calcium ion concentration ($[Ca^{2+}]_i$) are pivotal in the control of a wide variety of cellular functions. In particular, neurons are known to use calcium ions (Ca^{2+}) as a trigger for diverse functions such as neurotransmitter release (Augustine *et al.*, 1987), the opening of potassium channels and the control of neuronal membrane excitability (Morita *et al.*, 1982), the induction of intracellular Ca^{2+}-release (Fabiato, 1983), the control of membrane permeability (Meech, 1978), the induction of long term potentiation (Lynch *et al.*, 1983) and the modulation of enzyme or gene activity (e.g. phospholipases, protein kinases, and endonucleases; Morgan and Curran, 1988). The mechanisms of Ca^{2+} entry, its subsequent short-term buffering and longer-term clearance, along with the mechanisms which affect the amplitude, shape and duration of the cytosolic Ca^{2+}-signal in neurons are therefore important factors in determining which messenger systems are activated and the extent of that activation (Benham *et al.*, 1992; Stuenkel, 1994). In addition, prolonged increases in $[Ca^{2+}]_i$ may lead to cell death (Randall and Thayer, 1992) and Ca^{2+}-signals intended to produce a particular physiological response (Werth *et al.*, 1996) may, if uncontrolled, have a similar result. Therefore a balance exists between the $[Ca^{2+}]_i$ needed in order to induce rapid Ca^{2+} signaling versus the $[Ca^{2+}]_i$ at which point toxicity becomes a factor. As a result, $[Ca^{2+}]_i$ regulation is a pivotal process in the control of neuronal functioning.

In neurons resting free $[Ca^{2+}]_i$ is in the range of 10^{-7}-10^{-8} M although the precise value is not well established (Kennedy and Thomas, 1996; Ross, 1993; Bassani *et al.*, 1995). Despite this low $[Ca^{2+}]_i$, the total concentration of Ca^{2+} within a neuron is often in the millimolar range due to the large amounts of Ca^{2+} existing conjugated to Ca^{2+} binding proteins and non-specific Ca^{2+} binding sites (Widdowson and Dickerson, 1964). This observation stems from experiments by Hodgkin and Keynes (1957) who injected radioactive Ca^{2+} into squid giant axons and compared the rate of diffusion in the axoplasm versus that in solution. In complete contrast to the low levels of free $[Ca^{2+}]_i$, the concentration of free extracellular Ca^{2+} ($[Ca^{2+}]_o$) is in the millimolar range, over four orders of magnitude (10,000 x) higher than $[Ca^{2+}]_i$. This extremely high ratio of $[Ca^{2+}]_o/[Ca^{2+}]_i$, combined with the negative resting membrane potential, results in a large inward acting electrochemical gradient across the plasma membrane, the largest for any common inorganic ion (McBurney and Neering, 1987). Any changes in the permeability of the plasma membrane to Ca^{2+} will therefore produce significant fluctuations in $[Ca^{2+}]_i$ which may lead to neuronal degeneration or neuronal death. A precise control of $[Ca^{2+}]_i$ is therefore crucial in maintaining neuronal viability and functioning (Farber, 1981; Nelson and Foltz, 1983; Carafoli, 1987).

II. Ca^{2+} entry into neurons

There are two principal mechanisms by which $[Ca^{2+}]_i$ is increased in neurons; Ca^{2+} may enter via gated channels or Ca^{2+} may be released from intracellular stores (Carafoli, 1987; Simpson *et al.*, 1995). Two principal types of gated Ca^{2+}-channels exist; voltage gated channels, activated by membrane depolarization, and ligand gated channels, activated by the binding of extracellular ligands.

Voltage Gated Ca^{2+}-Channels

Voltage gated Ca^{2+}-channels (VGCC) are the principal physiological entry point for Ca^{2+} during action potential conduction. The ability of VGCCs to translate action potentials into neurotransmitter release depends upon a variety of factors, such as the channels' conductance, proximity to release sites, density, response to depolarization and regulation by second messengers and transmitters (Regehr and Mintz, 1994). The four principal subtypes of VGCC can be distinguished based on their biophysical, pharmacological and structural properties (Bean, 1989; Hess, 1990; Miller, 1992; Tsien *et al.,* 1988). The first attempts at categorizing voltage gated channels were made by Nowycky *et al.* (1985) and were based on observations of Ca^{2+}-currents in chick dorsal root ganglion cells. Three channels were identified, a low threshold current which was named the T-type current, along with two higher threshold currents which were named the L and N-type currents. These channels were distinguishable not only on their structural properties but more importantly based on their blockade by pharmacological agents. T-type channels are sensitive to blockade by Ni^{2+}, verapamil, phenytoin and amiloride whereas L-type channels can be modulated by dihydropyridines (DHPs) along with a number of cardiovascular-regulating agents (Bean, 1989; Nowycky *et al.*, 1985; Miller, 1992). N-type channels are blocked by ω-conotoxin GVIA (ω-CgTx), a toxin derived from the venom of the piscivorous marine mollusk *Conus geographus* (Hirning *et al.*, 1988; Plummer *et al.*, 1989) and similar to the L-type channels, N-type channels are blocked by Cd^{2+} and Ni^{2+} (Tsien *et al.*, 1988). A fourth type of channel was later identified and, based on the high numbers found in Purkinje cells (as compared with the low numbers found in other neuronal cells), was termed the P-type channel (Llinas *et al.*, 1989; Regan *et al.*, 1991; Regan, 1991). P-type channels are insensitive to DHP's and ω-CgTx and are selectively blocked by ω-Aga-IVA, isolated from the venom of the funnel-web spider (Mintz *et al.*, 1992). Recently, with the advent of molecular cloning, attempts have been made to classify VGCC based on their structure and sequence. For example Snutch *et al.* (1990) classified channels into four groups (A, B, C and D) based on their hybridization patterns to rat brain mRNAs. These four groups can be directly correlated with previous classification gropus, for example group A channels correspond with P-type channels while groups C and D correspond with L-type channels. Southern blot analysis and DNA sequencing suggest that each class of cDNA represents a distinct gene or gene family with classes A and B along with classes C and D being virtually homologous to each other. This suggested that all Ca^{2+}-channels evolved from a single ancestral gene and the diversity in Ca^{2+}-channels has arisen through gene duplication and subsequent divergence (Tsien *et al.*, 1991).

Ligand Gated Ca^{2+}-Channels

Ligand gated Ca^{2+}-channels (LGCC) refer to channels which open in response to the binding of an extracellular ligand. The two subtypes of LGCC are those activated by the neurotransmitters glutamate or acetylcholine. Based on pharmacology, the glutamate receptor family can be further subdivided into two major subtypes; the NMDA and non-NMDA receptor activated channels. NMDA channels are opened by the agonist *N*-methyl-D-aspartate while non-NMDA channels open in response to α-amino-3-hydroxy-5-methyl-4-isoxazole priopionate (AMPA) or kainate. Some ligand gated channels are also voltage sensitive, for example, the NMDA channel responds to membrane depolarizations by releasing a Mg^{2+} block which normally prevents Ca^{2+} entry. It is this voltage-dependent Ca^{2+}-entry which gives the NMDA channel its distinct role in long-term potentiation (Mayer and Westbrook 1987; Tsien and Tsien, 1990).

Intracellular Ca^{2+} Stores

To date the general consensus is that a rise in $[Ca^{2+}]_i$ originates from the opening of VGCC or LGCC. However recent evidence indicates that a major component of the total Ca^{2+} signal appears to originate from intracellular Ca^{2+}-stores (Simpson *et al.*, 1993). As a result, intracellular Ca^{2+}-stores, in particular those associated with the endoplasmic reticulum, play a crucial role in Ca^{2+}-signaling as they not only act as a Ca^{2+}-source by initiating signals but may also act as a Ca^{2+}-sink by sequestering Ca^{2+} following an increase in $[Ca^{2+}]_i$. These stores are influenced by a variety of compounds, for example Ca^{2+} is released in response to adenosine triphosphate (ATP), inositol 1,4,5-trisphosphate (IP_3), cyclic adenosine diphosphate (ADP) ribose, caffeine, or low concentrations of ryanodine, while Ca^{2+}-release is inhibited by thapsigargin, cyclopiazonic acid (CPA), 2,5,-Di-(t-butyl)-1,4-benzohydroquinone (DBHQ), and high concentrations of ryanodine (Berridge, 1997). These stores may also be involved in a variety of neuronal processes, such as excitability, transmitter release, synaptic plasticity, gene expression and apoptosis (Holliday *et al.*, 1991; Simpson *et al.*, 1995).

As $[Ca^{2+}]_i$ often reaches micromolar levels following intense stimulation, neurons must possess effective mechanisms to sequester and extrude these potentially dangerous increases in $[Ca^{2+}]_i$ (Werth and Thayer, 1994). Mechanisms by which a neuron can regulate $[Ca^{2+}]_i$ include the plasma membrane Na^+/Ca^{2+} exchanger ($PM-Na^+/Ca^{2+}$), the plasma membrane Ca^{2+}-adenosine triphosphatase (PM-ATPase), the endoplasmic reticulum Ca^{2+}-adenosine triphosphatase (ER-ATPase), mitochondria, and Ca^{2+}-binding proteins (see Nicholls, 1986; Carafoli, 1987; Miller, 1991; Baimbridge *et al.*, 1992 for reviews). Since Ca^{2+} may be involved in multiple neuronal activities within different neuronal regions (soma, neurites, growth cones, and terminal boutons), there exist substantial spatial and temporal variations of $[Ca^{2+}]_i$ amongst these regions which are manifested in the form of a heterogeneous distribution of Ca^{2+}-channels and Ca^{2+}-homeostatic mechanisms within the neuron (Katz and Miledi 1969; Ross *et al.*, 1986; Miller, 1991; Carafoli, 1987; Reuter and Porzig, 1995). As a result of these spatial and temporal variations, little is known about the modulation of Ca^{2+}-homeostatic mechanisms. Despite this uncertainty, the general principles of Ca^{2+}-regulation, such as the mechanisms involved and their kinetics, should be applicable to different parts of the neuron and in general to most neurons (Blaustein, 1988).

III. Intracellular Ca^{2+}-homeostasis

Initially the Ca^{2+} which enters via VGCC or LGCC may be buffered by 'short-term' buffers such as Ca^{2+}-binding proteins or intracellular Ca^{2+}-stores but eventually the increase in Ca^{2+} must be extruded across the plasma membrane. Mechanisms designed to regulate $[Ca^{2+}]_i$ can be categorized as being either short-term buffers (1 and 2 below) or long term extruders (3 below):

1. Pumps which sequester Ca^{2+} into organelles such as the mitochondria or endoplasmic reticulum (ER).
2 Proteins, or other buffers, which bind Ca^{2+} within the cytoplasm.
3. Pumps or exchangers which extrude Ca^{2+} from the cell.

1. Ca^{2+} ATPase

There are two principal Ca^{2+}-ATPases found within neurons; those located on the plasma membrane which pump Ca^{2+} out of the cell (PM-ATPases) and those located on intracellular compartments which pump Ca^{2+} into intracellular stores (for example the ER-ATPase). Both of these ATPases use the energy generated by the hydrolysis of ATP to pump Ca^{2+} 'uphill' against its electrochemical gradient.

a) PM-ATPase

The first clue suggesting the presence of a Ca^{2+}-dependent ATPase in eukaryotic cells was seen over thirty-five years ago by Dunham and Glynn (1961) who noticed a relationship between ATP activity and the movement of alkali metal ions. Schatzmann (1966) later showed that erythrocyte ghosts loaded with Ca^{2+} and ATP had a much higher Ca^{2+} efflux rate compared with erythrocyte ghosts loaded only with Ca^{2+}. Since this efflux occurred against a concentration gradient Schatzmann inferred the presence of a pump which used energy to overcome this gradient. The PM-ATPase has since been shown to be present on the plasma membrane of all eukaryotic cells and its mechanism has been shown to involve ATP-phosphorylation of an aspartic acid residue in a Ca^{2+}-dependent manner followed by the translocation of one Ca^{2+} across the plasma membrane (Knauf *et al.*, 1974; Katz and Blostein, 1975; Carafoli, 1991).

The PM-ATPase is in fact a Ca^{2+}/H^{+} exchanger, exchanging one extracellular H^{+} with one intracellular Ca^{2+} (Niggli *et al.*, 1982; Smallwood *et al.*, 1983; Milanick *et al.*, 1990; Carafoli 1991; Schwiening *et al.*, 1993). The PM-ATPase has an essential requirement for Mg^{2+} and is inhibited by vanadate (Kd ~ 2-3 μM), which blocks an aspartic acid phosphorylated intermediate, La^{3+}, which increases the steady-state level of the phosphoenzyme and intracellular acidification and extracellular alkalinization, which influence the H^{+}-gradient (Carafoli 1987 and 1991). Calmodulin, by way of a direct interaction with the ATPase, increases the activity of the PM-ATPase (Gopinath and Vincenzi, 1977) and increases the affinity for Ca^{2+} by up to 30 fold and the V_{max} by up to 10 fold (Lynch and Cheung, 1979; Carafoli, 1991). The PM-ATPase is also activated by a variety of factors such as phospholipids from the inositol phosphate pathway (phosphatidyl inositol and its mono and di-phosphate derivatives), along with long chain polyunsaturated fatty acids (Ronner *et al.,* 1977).

b) endoplasmic reticulum ATPase

Many tissues possess ATP-dependent Ca^{2+} sequestration mechanisms. The first ATP-dependent intracellular Ca^{2+} pump to be discovered was the Ca^{2+}-ATPase of the sarcoplasmic reticulum (SR) (Ebashi and Lippman, 1962). Using X-ray microanalysis it was later shown that a similar ATPase existed in the ER. Following the cloning of cDNA's encoding homologous ATPases, the presence of several isoforms of this Ca^{2+}-pumping ATPase was discovered in both the SR and the ER (MacLennan *et al.,* 1985; Brandl *et al.,* 1986). With the exception of the SR in muscle, these stores have a small Ca^{2+}-sequestration capacity and are insensitive to the mitochondrial inhibitor ruthenium red. These ER Ca^{2+}-stores are influenced by a variety of factors; they are released by A23187 and high $[Ca^{2+}]_i$, while their uptake of Ca^{2+} is modulated by calmodulin, cAMP-dependent protein kinases, vanadate and ryanodine (Carafoli, 1987). A variety of specific inhibitors to the ER-ATPase exist, the most potent being thapsigargin (Tg). This tumor-promoting lactone was originally extracted from the resin of the umbelliferous plant *Thapsia garganica* and used initially for its ability to increase $[Ca^{2+}]_i$. Later, it was determined to be a specific inhibitor of the ER-ATPase and not other cation ATPases such as the PM-Na^+, K^+ and Ca^{2+}-ATPases (Rasmussen *et al.,* 1978; Thastrup *et al.*, 1990; Inesi and Sagara, 1994). Other inhibitors of the ER-ATPase include CPA, a toxic metabolite produced by the molds *Pencillium cylopium* and *Aspergillus flavus* and DBHQ (Holzapfel, 1968; Goeger *et al.*, 1988; Moore *et al.*, 1987).

2. PM-Na^+/Ca^{2+} exchanger

The PM-Na^+/Ca^{2+} exchanger was first identified in heart muscle (Reuter and Seitz, 1968) and neuronal tissue (Blaustein and Hodgkin, 1969), and has since been found on the plasma membrane of all cell types, with the exception of erythrocytes. The PM-Na^+/Ca^{2+} exchanger was originally postulated to be an electroneutral exchanger with 2 Na^+ being imported for every 1 Ca^{2+} extruded, but Blaustein and Hodgkin (1969) demonstrated that the energy content of the transmembrane Na^+ gradient was not large enough to maintain the large Ca^{2+}-gradient across the plasma membrane. Following this revelation, experiments by Reeves and Sutko (1979) on sarcolemmal vesicles unequivocally demonstrated that the PM-Na^+/Ca^{2+} exchanger exchanged 3 Na^+ for every 1 Ca^{2+} extruded from the cytosol, producing one inward positive charge per cycle. The PM-Na^+/Ca^{2+} exchanger is sensitive to changes in the Na^+ or Ca^{2+}-gradient or changes in the membrane potential and by changing either of these factors it is possible to induce the reverse mode of the exchanger, thereby promoting Ca^{2+}-influx (Carafoli, 1987). ATP is needed indirectly as the Na^+ which enters the neuron via the exchanger must eventually be extruded across the PM by the Na^+/K^+-ATPase.

The Na^+/Ca^{2+} exchanger has an absolute requirement for Na^+, and Na^+ substitutes such as Tris, choline, *N*-methyl-D-glucamine, or Li^+ are ineffective. There are no potent and specific inhibitors of the Na^+/Ca^{2+} exchanger, although some compounds such as doxorubicin and its derivatives along with amiloride and its derivatives such as 3',4'-dichlorobenzamil (DCB) have been shown to have inhibitory actions on the exchanger (Caroni *et al.*, 1981; Siegl *et al.*, 1984).

3. Mitochondria

The principal role of mitochondria is to produce ATP, the common organic cellular fuel. Mitchell (1966) postulated the following series of reactions in order to explain ATP production. Products from the metabolism of sugars, carbohydrates, amino acids and lipids are used as carbon sources in the tricarboxylic acid (TCA) cycle. NADH and $FADH_2$, products from the TCA cycle, serve as reducing equivalents in the electron transport chain (ETC) located on the inner mitochondrial membrane. At 3 points along the ETC, energy obtained from oxidation is used to pump H^+ outwards across the inner mitochondrial membrane thereby creating an inward acting electrochemical gradient. When H^+ passes down this electrochemical gradient, through a pore in the ATP-synthase, ADP is phosphorylated forming ATP. Mitochondria take up calcium via a uniporter driven by the large electrochemical gradient across the inner membrane (Akerman *et al.*, 1977; Carafoli, 1987; Gunter and Pfeiffer, 1990; Werth and Thayer, 1994). Calcium exits the mitochondria via a Na^+/Ca^{2+} exchanger and Na^+ is then removed via a Na^+/H^+ exchanger, the net result being that two H^+ ions are prevented from entering the mitochondria via the ATP-synthase. As a result of mitochondrial Ca^{2+} sequestration, ATP production is decreased and the cycling of Ca^{2+} back and forth across the inner mitochondrial membrane will uncouple electron transport from ATP synthesis.

Mitochondria are believed to sequester Ca^{2+} for two principal reasons. Firstly, they protect the neuron against the damaging effects of prolonged Ca^{2+} elevation, and secondly, they control metabolic processes such as the activation of Ca^{2+}-sensitive dehydrogenases which influence ATP production (Gunter *et al.*, 1994; Rizzuto *et al.*, 1994; Hehl *et al.*, 1996). The observation that mitochondria take up Ca^{2+} was made by De Luca and Engström (1961) and Vassington and Murphy (1962), and has since been demonstrated in a variety of neuronal preparations (Sanchez and Blaustein, 1987; Stuenkel, 1994; Thayer and Miller, 1990; White and Reynolds, 1995). Early evidence, using isolated mitochondria, suggested that there existed a mitochondrial 'set-point' below which Ca^{2+}-sequestration does not occur. However, above this 'set-point' in $[Ca^{2+}]_i$, traditional neuronal homeostatic mechanisms are saturated and mitochondria begin to sequester Ca^{2+}. Mitochondria persist in sequestering Ca^{2+} until $[Ca^{2+}]_i$ is reduced to a level below this 'set-point' at which time Ca^{2+} is released by the mitochondria to be extruded by the now unsaturated neuronal homeostatic mechanisms (Thayer and Miller, 1990). In experiments on isolated mitochondria, this set-point has been estimated to be in the range of 0.75 - 1.0 μM suggesting that mitochondria only sequester Ca^{2+} in rare pathological situations where $[Ca^{2+}]_i$ is raised above physiologically 'normal' levels (Nicholls 1985; Carafoli 1987; Kostyuk *et al.*, 1989; Thayer and Miller, 1990). However more recent evidence, obtained in whole cells, demonstrates that firstly, this mitochondrial 'set-point' may be lower than previously reported (Werth & Thayer, 1994), and secondly, that microdomains of high $[Ca^{2+}]_i$ exist close to the mitochondria (Rizzuto *et al.*, 1994) lending credence to the idea that mitochondria may take up Ca^{2+} following apparently minimal increases in $[Ca^{2+}]_i$ (Gunter *et al.*, 1994; Werth and Thayer, 1994; Kiedrowski and Costa, 1995; White and Reynolds, 1995; Hehl *et al.*, 1996; Herrington *et al.*, 1996; Park *et al.*, 1996).

The role of mitochondria in Ca^{2+}-homeostasis can be examined by the use of cell-permeant mitochondrial Ca^{2+}-uptake inhibitors. Rotenone, an electron transport chain inhibitor, slowly decreases the mitochondrial electrochemical gradient, whereas the uncouplers carbonylcyanide *p*-trifluoromethoxyphenylhydrazone (FCCP) and carbonylcyanide *m*-chlorophenylhydrazone (CCCP), both protonophores, permeabilize the inner mitochondrial membrane thereby rapidly eliminating the mitochondrial electrochemical gradient.

4. Ca^{2+} Binding Proteins

The ability of Ca^{2+}-binding proteins to buffer rises in intracellular Ca^{2+} depends on a number of factors. Firstly, the amount of protein present within the neuron, secondly, the K_d of the protein for Ca^{2+}, thirdly, the forward rate constant K_{on} ('speed' of binding to Ca^{2+}), and fourthly, the mobility or distribution of the protein within the cytoplasmic compartment (Sala and Hernandez-Cruz, 1990). The first Ca^{2+}-binding protein to be studied in detail was parvalbumin, a muscle protein found at high concentrations in fish, amphibia, reptiles and mammals. Kretsinger and Nelson (1973) deduced the mechanism by which parvalbumin binds Ca^{2+} and in doing so established some general principles for the interaction of Ca^{2+} with Ca^{2+}-binding proteins. From crystallized parvalbumin they deduced the existence of repeat domains which bound Ca^{2+} specifically and effectively; each domain contained a loop of 10-12 amino acid residues with two α-helixes aligned perpendicularly to each other, this helix/loop/helix peptide sequence, coined the 'EF-hand', has been found in over twenty Ca^{2+}-binding proteins and is crucial for the high affinity binding of Ca^{2+} to Ca^{2+}-binding proteins

Based on function, Ca^{2+}-binding proteins can be divided into two groups. Those which modulate the activity of enzymes and other cellular functions are known as 'trigger' proteins, while those whose primary function is thought to be the buffering of increases in $[Ca^{2+}]_i$ are known as 'buffer' proteins (Baimbridge *et al.,* 1992). An example of a 'trigger' protein is calmodulin, present in all eukaryotic cells. When complexed with Ca^{2+}, calmodulin interacts with a variety of cellular enzymes such as adenylate cyclase, cyclic nucleotide phosphodiesterase, phosphorylase b kinase, phospholamban, and of particular importance to Ca^{2+}-homeostasis, the PM-ATPase. An example of the 'buffer' variety of Ca^{2+}-binding proteins is calbindin-D28K (CaBP), first identified in the chick gut but later found to exist predominantly in the nervous system of mammals (Wasserman and Taylor, 1966; Baimbridge *et al.*, 1992). Lledo *et al.* (1992) found that GH_3 cells transfected with CaBP exhibited lower Ca^{2+}-entry through VGCC and were better able to reduce Ca^{2+}-transients evoked by voltage depolarizations as compared with 'CaBP -free' control cells. In addition, cells containing CaBP showed no changes in baseline Ca^{2+}-levels as compared with CaBP free cells, suggesting that CaBP is only important during situations in which $[Ca^{2+}]_i$ is above resting levels. Despite this lack of an effect on baseline Ca^{2+}-levels, CaBP, as a result of its high affinity for Ca^{2+} ($K_d \sim 500$ nM) and high intracellular levels (up to 0.1 - 0.2 mM in some neuronal populations), could affect many aspects of the kinetics of Ca^{2+}-transients. For example the peak $[Ca^{2+}]_i$ achieved, the rate of rise and decay of $[Ca^{2+}]_i$, neuronal excitability, action potential duration, neuronal 'bursting' activity (by inhibiting the Ca^{2+}-dependent inactivation of voltage gated Ca^{2+}-channels) and neuronal protection against the harmful effects of high $[Ca^{2+}]_i$ may all be influenced by CaBP (Oberholtzer *et al.*, 1988; Baimbridge *et al.*, 1992; Chard *et al.*, 1993)

IV. Overview of Ca^{2+}-homeostatic methods

Although the presence of the above mentioned Ca^{2+}-homeostatic mechanisms has been well documented, the relative contribution of each of these processes to overall Ca^{2+}-homeostasis is not well understood. Depending on the cell type studied, different groups have found diverse roles for individual Ca^{2+}-homeostatic mechanisms. Initial work by Dipolo and Beauge (1979) suggested that the PM-Na^+/Ca^{2+} exchanger and the PM-ATPase acted in tandem to reduce increases in $[Ca^{2+}]_i$. They characterized the PM-ATPase as a high affinity/low capacity pump and the PM-Na^+/Ca^{2+} exchanger as a low affinity/high capacity exchanger. As a result, the PM-Na^+/Ca^{2+} exchanger was postulated to be responsible for the initial fast phase of the removal of large Ca^{2+}-loads while the PM-ATPase was postulated to be responsible for the secondary restoration of $[Ca^{2+}]_i$ to baseline levels (Dipolo and Beauge, 1979; Sanchez-Armass and Blaustein, 1987; Ahmed and Connor, 1988; Blaustein, 1988; Thayer and Miller, 1990; Benham *et al.*, 1992; Gleason *et al.*, 1995; Werth *et al.*, 1996). Others have shown that the Na^+/Ca^{2+} exchanger plays a secondary role in reducing $[Ca^{2+}]_i$ levels while other mechanisms, such as mitochondria or the PM-ATPase, form the principal Ca^{2+}-extrusion mechanisms (Bleakman *et al.*, 1993; Kiedrowski and Costa, 1995; Mironov, 1995; Herrington *et al.*, 1996). Mitochondria, initially thought to buffer $[Ca^{2+}]_i$ only during pathological conditions of $[Ca^{2+}]_i$ overload (Kostyuk *et al.*, 1989; Thayer and Miller, 1990), have recently been implicated as an important mechanism for the removal of minimal increases in $[Ca^{2+}]_i$ (Rizzuto *et al.*, 1992; Gunter *et al.*, 1994; Werth and Thayer, 1994; Kiedrowski and Costa, 1995; White and Reynolds, 1995; Hehl *et al.*, 1996; Herrington *et al.*, 1996; Park *et al.*, 1996). As a result, it is clear that Ca^{2+}-homeostasis is a complicated and dynamic process involving a large number of mechanisms, each of which may be activated at different times by differing factors.

V. Experimental methods for increasing $[Ca^{2+}]_i$

In order to study the Ca^{2+}-homeostatic mechanisms present within neurons, it is necessary to induce an increase in $[Ca^{2+}]_i$, which is in turn controlled by an interplay between the influx and efflux of Ca^{2+}. To date, when imaging changes in $[Ca^{2+}]_i$ from multiple neurons simultaneously, two principal methods have been used to increase $[Ca^{2+}]_i$. Both of these methods require the superfusion of solutions containing either high K^+, which depolarizes the membrane and activates VGCC, or specific ligands whose receptors are coupled to Ca^{2+}-permeable channels (LGCC), such as the *N*-methyl-D-aspartate (NMDA) channel. In either case, the responses are relatively slow and during the period when Ca^{2+} is entering via VGCC or

LGCC, Ca^{2+} -homeostatic mechanisms are already initiated in an attempt to reduce the increase in $[Ca^{2+}]_i$. The concurrence of these two opposing effects therefore makes Ca^{2+}-decay kinetics very difficult to interpret. Additionally, it has been suggested that the mechanism(s) of Ca^{2+}-homeostasis may be dependent upon the method used to increase $[Ca^{2+}]_i$. For example, White and Reynolds (1995) demonstrated that, depending on whether glutamate or high K^+ was used to increase $[Ca^{2+}]_i$, neurons utlized different Ca^{2+}-homeostatic mechanisms.

Ideally it would be best to examine Ca^{2+}-homeostasis following a very rapid increase to peak $[Ca^{2+}]_i$ and this has been made possible with the development of caged Ca^{2+}-compounds. Following a brief exposure to UV light, $[Ca^{2+}]_i$ can be raised above physiological levels virtually instantaneously, thereby negating the slow rise to peak Ca^{2+}-levels. These caged compounds are particularly useful because the flash of light can be easily controlled with respect to timing, location, duration, and amplitude (Adams and Tsien, 1993). Numerous properties of caged Ca^{2+}-compounds must be taken into consideration when they are used in an intracellular environment. These include their pH sensitivity, their affinity for Ca^{2+} and selectivity of Ca^{2+}-binding with respect to other ions, especially Mg^{2+}, the relative binding of the native molecules with respect to their photolysis products and the quantum yield for Ca^{2+}-release (i.e. the proportion of caged Ca^{2+}-compound photolysed by UV light). Currently the two most popular caged Ca^{2+}-compounds are DM-nitrophen and nitr-5 (Nerbonne, 1996).

A relatively new caged Ca^{2+}-compound, nitrophenyl-EGTA (NP-EGTA), meets a number of important criteria not previously attained by molecules such as nitr-5 or DM-nitrophen. NP-EGTA has been used successfully to induce the endocytosis of secretory granules in mouse pancreatic β-cells (Eliasson *et al.*, 1996), contract chemically skinned skeletal muscle fibres in rabbit (Ellis-Davies and Kaplan, 1994) and induce exocytosis in rat pituitary melanotrophs (Parsons *et al.*, 1996). Due to the low affinity for Mg^{2+}, the low affinity of the photolysis products for Ca^{2+} and the large percentage of NP-EGTA broken down during photolysis, NP-EGTA was the compound of choice for inducing increases in $[Ca^{2+}]_i$ for the purposes of this study.

VI. Effects of pH on Ca^{2+} homeostatic mechanisms.

Neurons possess a variety of mechanisms designed to regulate intracellular pH (pH_i). These mechanisms can be subdivided into two categories based upon their abilities to acidify or alkalinize the cytoplasm; acid extruders increase pH_i while acid loaders decrease pH_i. The predominant acid extruders are the Na^+/ H^+ exchanger (NHE), which exchanges one extracellular Na^+ ion for one intracellular H^+, and the Na^+-dependent $Cl^-/HCO3^-$ exchanger which exchanges one extracellular Na^+ and one extracellular HCO_3^- for one intracellular Cl^- ion. The principal acid loaders are the Na^+-independent $Cl^-/HCO3^-$ exchanger, which exchanges one extracellular Cl^- with one intracellular HCO_3^- and the Na^+/HCO_3^- co-transporters, which transports one extracellular Na^+ ion and one extracellular HCO_3^- ion out of the cell. Different cell types rely on different pH regulatory mechanisms in order to maintain a constant pH_i. For example, in rat sympathetic neurons, rat brain synaptosomes, cultured rat cerebellar Purkinje cells and rat neocortical neurons, the NHE appears to be the dominant acid extrusion mechanism, whereas in CA1 hippocampal pyramidal neurons, the NHE along with other mechanisms such as the Na^+-dependent HCO_3^-/Cl exchanger appears to be the dominant acid extrusion mechanisms (Schwiening and Boron, 1994; Baxter and Church, 1996; Bevensee *et al.*, 1996).

Intracellular pH in the majority of cell types is kept constant within the range of 6.8 to 7.2 (Putnam, 1995). Any prolonged deviations from this range are known to result in cellular toxicity and/or cellular death (Kraig *et al.*, 1987). In neurons, changes in pH_i have been shown to affect the activity of many enzymes or ion channels, the activities of VGCC or LGCC and the excitability of neurons (Chesler and Kaila, 1992). Additionally, cytoskeletal properties (cell shape and motility), cell-cell coupling, and membrane conductance are all dependent upon pH_i (Putnam, 1995). Of particular importance to the present study is the influences of pH_i on Ca^{2+}-regulatory mechanisms within neurons. For example, lowering pH_i inhibits the PM-ATPase (Carafoli, 1987), decreases the affinity of Ca^{2+}-binding proteins for Ca^{2+} (Ingersoll and Wasserman, 1971), and decreases mitochondrial Ca^{2+}-uptake (Gambassi *et al.*, 1993). Additionally the K_d for Ca^{2+} of fluorescent Ca^{2+}-indicator dyes along with caged Ca^{2+}-compounds increases significantly (i.e. becomes less sensitive) as acidity increases (Martínez-Zaguilán *et al.*, 1996)

Researcher-induced changes in pH_i have many times been overlooked and may produce uninterpretable and confusing results. For example, due to the lack of a specific blocker for the PM-Na^+/Ca^{2+} exchanger, many groups have simply removed extracellular Na^+ (Na^+_o) (Na^+ substituted by choline, *N*-methyl-D-glucamine, or Li^+) and in doing so have assumed that only the PM-Na^+/Ca^{2+} exchanger is blocked (Benham *et al.*, 1992; Sanchez-Armass and Blaustein, 1987). However, the NHE is also blocked leading to a decrease in pH_i. Therefore, in any neuron in which the NHE is a major component of pH_i regulation, pH_i will be influenced by Na^+_o substitution and the interpretation of Ca^{2+} recovery kinetics may be incorrect. This was demonstrated by Koch and Barish (1994) who found that acidification of the cytoplasm, due to blockade of the Na^+/H^+ exchanger using Na^+ free media, resulted in a two-fold increase in the time required for $[Ca^{2+}]_i$ to return to baseline levels following glutamate activation. As a result, it is crucial for pH_i to be maintained in order to ensure that the intracellular environment is kept constant and undisturbed.

VII. Goals of this study

This study had three purposes, firstly, to develop a reproducible method for loading both NP-EGTA and the fluorescent indicator dye fluo-3 into neurons, secondly, to develop a photolysis protocol which allowed for significant increases in $[Ca^{2+}]_i$ following flash photolysis of NP-EGTA and thirdly, to investigate which Ca^{2+}-homeostatic mechanisms are responsible for reducing $[Ca^{2+}]_i$ back to baseline values following flash photolysis of NP-EGTA with particular emphasis of the relative roles of the PM-Na^+/Ca^{2+} exchanger and the mitochondria.

METHODS AND MATERIALS

I. Tissue culture

All experiments were performed on primary cultures of 4-day postnatal hippocampal neurons derived from Wistar rats using the method of Huettner and Baughman (1986) as modified and described previously (Abdel-Hamid and Baimbridge, 1997). Cultures were used after 7-10 days *in vitro* (DIV). Glial multiplication was inhibited by a single addition of cytosine arabinoside (10 μM) to the culture medium 48 hours after plating. In specifying culture age, the plating day was counted as day zero *in vitro* (0 DIV). The growth medium was Eagle's minimum essential medium with N2 supplement (insulin 5 μg ml^{-1}, transferrin 100 μg ml^{-1}, progesterone 20 nM, putrescine 100 μM, sodium selenite 30 nM). Media were obtained from Gibco (Grand Island, NY) and were replenished by replacing half the volume with fresh N2-supplemented medium twice weekly.

II. Ca^{2+}-imaging with fluo-3 and the use of NP-EGTA

i. Loading

Fluo-3 and NP-EGTA were both purchased as their acetoxymethyl (AM) esters from Molecular Probes Inc. (Eugene, Oregon). Fluo-3-AM was dissolved in dimethlysulfoxide (DMSO) to produce a 1 mM stock solution which was stored in 25 μl aliquots at -80 °C until use. NP-EGTA-AM was purchased in individually packaged 50 μg aliquots and similarly stored. To prepare the loading solution, a 25 μl aliquot of fluo-3-AM and an additional 25 μl of DMSO were added to a vial of NP-EGTA-AM and vortex mixed. Using a fine pipette tip, 25 μl of this mixture was added, while mixing vigorously with a vortex stirrer, to 4 ml of a balanced salt solution (BSS; NaCl 139 mM, KCl 3.5 mM, Na_2HPO_4 3 mM, $NaHCO_3$ 2 mM, HEPES acid 6.7 mM, HEPES-Na^+ 3.3 mM, D-Glucose 11 mM, $CaCl_2$ 1.8 mM, Glycine 2 μM, tetrodotoxin 1 μM; pH 7.35) containing 0.05% bovine serum albumin (Sigma). The final concentrations of fluo-3-AM and NP-EGTA-AM were 3.1 μM and 8 μM respectively. In one experiment, nitr-5-AM (Chemica Alta LTD, Edmonton, Alberta, Canada; final loading concentration 12.5 μM), was substituted for NP-EGTA-AM. Individual coverslips, plated with neurons, were placed in a well of a 6-well culture dish and incubated for 1 hour at room temperature in the dark in 2 ml of this loading solution. They were then transferred to fresh BSS for at least 15 minutes prior to, or after mounting on a superfusion chamber. After loading, and for the duration of the experiment, the cells were maintained at 20 - 22 °C. This loading protocol was established empirically to yield sufficient intracellular concentrations of fluo-3 for adequate imaging and sufficient NP-EGTA to yield a 2-4 fold increase in background corrected fluo-3 fluorescence following a 0.4 s exposure to UV light. Whenever possible, control and experimental data were collected from paired sister cultures loaded with identical solutions.

ii. Imaging

Fluo-3 fluorescence was measured using a Zeiss-Attofluor™ digital fluorescence imaging system controlled by Attofluor imaging software. The microscope used was a Zeiss Axiovert-10 fluorescent microscope which was equipped with a long distance 40x objective (Zeiss LD UV-Achroplan 0.6, Ph2) and a 100 W mercury arc lamp as a light source. The mercury lamp was used at full power for all of the experiments and no neutral density filters were in place. Excitation light for the fluo-3 was filtered through a 10 nm band pass 488 nm excitation filter whose position was determined by a computer-controlled solenoid filter changer. The filtered light passed through a long band-pass dichroic mirror (FT-495) before being focused through a 40 x Neofluar objective (numerical aperture 0.75) onto the cells in the superfusion chamber. The emitted light was passed through a dichroic beam splitter before being filtered by a 510 nm long-pass filter. The imaging software operated on a dual-monitor IBM-compatible 80486-33 MHz which controlled the filter changer, camera gain, image processor, data processor, data display and data storage. One of the monitors displayed a pseudocoloured image of the field of view while the second monitor gave the raw emission intensity plotted against time. The photosensitive detector was a high sensitivity, charge-coupled device (CCD) camera and images were digitized to 8 bit resolution with a 512 x 480 pixel frame size on a Matrox-AT image processor.

The coverslips containing the plated hippocampal neurons were mounted face-up in a superfusion chamber made in our departmental workshop. The inflow channel was connected to a perfusion pump while the outflow channel was connected to a suction line which removed all of the superfusate present above a level of 3 mm. Neurons were superfused at a rate of 2.4 ml min^{-1} at 20 - 22°C with Mg^{2+}-free BSS. In order to select an appropriate field of view, a 12 V 100W halogen lamp was used to visualize the cells under phase illumination. Regions of interest (ROIs) were set at 10 x 10 pixels and placed over the soma of up to 99 neurons in field of view. The camera gain was set at a level in order to minimize camera saturation while at the same time maximizing image intensity.

At the normal resting $[Ca^{2+}]_i$ of our neurons, the baseline fluo-3 fluorescence was often very low, thus making the identification of neurons and the placement of ROIs difficult. In such cases, 2 ml of a 40 μM NMDA solution in BSS was added through a pipette placed over the inlet of the chamber. A maximum increase in fluo-3 fluorescence was seen approximately 10 to 15 seconds later, at which time an image was stored and the flow rate was then increased for 10 s to maximum (about 10 ml min^{-1}) in order to wash out the NMDA. This stored image was then used for the placement of ROIs.

In order to uncage NP-EGTA, the acquisition of fluo-3 fluorescence data was interrupted and the cells exposed to unfiltered UV light for 0.4 s by the placement of an empty filter holder in the excitation light path. Fluo-3 fluorescence data acquisition then continued ~ 0.6 s after uncaging. To minimize photobleaching, for the first 30 s after uncaging the acquisition rate was one image per second, for the next two minutes it was one image every two seconds, and for the final thirty seconds it was one image every three seconds. This total time of three minutes was, in most experiments, more than enough for the fluo-3 fluorescence to decay back to baseline values. Data was recorded from up to three well-separated fields on a single coverslip, ensuring that neurons were only exposed to a singular 0.4 s flash of UV light.

iii. NP-EGTA data analysis

Using a stand-alone DOS-based program ATTOGRAF (Atto Instruments Inc., version 5.41), regions of interest deemed acceptable were chosen for analysis. Neurons were deemed acceptable if the background corrected fluo-3 fluorescence, firstly, increased by 50 % or greater in response to NMDA (thereby excluding glial cells), secondly, increased at least two-fold in response to flash photolysis of NP-EGTA and, thirdly, returned within three minutes to 110 % of that recorded prior to flash photolysis (with the exception of those neurons treated with CCCP; see results below). For each neuron, the fluorescence intensity was normalized between a value of 0 and 1 with 0 being the baseline value to which fluo-3 fluorescence decayed, and 1 being the fluorescence at the first time-point immediately following photolysis.

The data was processed for a best fit exponential decay curve using Table Curve-2D™ which, in the majority of situations, was a double-exponential decay curve with:

$$\text{Rate} = A_1 \exp^{(-t/\tau 1)} + A_2 \exp^{(-t/\tau 2)} + C$$

Where: t - time (s)

A_1 - amplitude of the first (fast) exponential

$\tau 1$ - time constant of the first (fast) exponential

A_2 - amplitude of the second (slow) exponential

$\tau 2$ - time constant of the second (slow) exponential

C - constant

Statistical analysis was carried out using Student's two-tailed *t* test with a 95 % confidence limit. In all cases unpaired *t* values were calculated with supplemental paired data added when appropriate.

III. Ca^{2+}-imaging using fura-2

i. Loading

Fura-2-AM was obtained from Molecular Probes Inc. (Eugene, Oregon) and stored in 30 μg aliquots. 25 μl of anhydrous DMSO was added to a vial of fura-2-AM which was then added slowly, while vortex mixing, to 4 ml of BSS which had been supplemented with 0.05% bovine serum albumin. The mixture was then vigorously vortex mixed in order to disperse the fura-2-

AM solution. Coverslips were then incubated for 1 hour at room temperature in 2 ml of this loading media. Neurons were transferred to fresh BSS for at least 15 minutes prior to, or after mounting on a superfusion chamber.

ii. fura-2 data analysis

Fura-2 measurements were made using a dual excitation ratiometric method on the same imaging system. Excitation light was filtered through either 334 nm or 380 nm (10 nm band pass) excitation filters. Briefly the dye was excited alternately at either 334 or 380 nm (10 nm band pass filters) and the resulting fluorescence above 510 nm was recorded. The frequency of image acquisition was varied between 1 image every second to 1 image every 15 seconds depending on the experiment. Less frequent acquisition were used whenever possible to eliminate photobleaching of the fura-2. The ratios of background corrected emission intensities (I_{334}/I_{380}) were converted to $[Ca^{2+}]_i$ using the method of Grynkievicz *et al.* (1985) which involved the use of the following equation:

$$[Ca^{2+}]_i = \beta K_d \frac{[R - R_{min}]}{[R_{max} - R]}$$

Where:

β - the ratio of the measured fluorescence intensity of Ca^{2+} free to Ca^{2+} bound indicator at 380 nm.

K_d - the dissociation constant of Fura-2 for Ca^{2+}.

R - the background corrected emission intensity ratio (I_{334}/I_{380}).

R_{min} - the limiting value of R when all the indicator is in the Ca^{2+}-free form.

R_{max} - the limiting value of R when all of the indicator is in the Ca^{2+}-bound form.

For our calibration experiment, the values of R_{min}, R_{max}, and β were 0.3, 8.6 and 11.9 respectively. These values were obtained by exposing neurons to 0 Ca^{2+} solutions (0 Ca^{2+}: NaCl 139 mM, KCl 3.5 mM, Na_2HPO_4 3 mM, $NaHCO_3$ 2 mM, HEPES acid 6.7 mM, HEPES-Na^+ 3.3 mM, D-Glucose 11 mM, Glycine 2 μM, tetrodotoxin 1 μM; EGTA 1 mM; pH 7.35) for 10 mins followed by the addition of 2 x 2 ml of this 0 Ca^{2+} solution which contained 10 μM of the Ca^{2+}-ionophore Br-A23187. Data was then collected for 30 min at an acquisition rate of 1 image/min at which time another 2 x 2 ml of this 0 Ca^{2+} solution with 10 μM Br-A23187 was added and data was collected for a further 15 min. The background subtracted ratio obtained following this 45 minute data acquisition period was considered R_{min}. Following this, 2 x 2 ml of BSS was added and the ratio obtained following 5 min incubation in this media was considered R_{max}.

IV. Ca^{2+}-imaging using fura-red

i. Loading

Fura-Red-AM was obtained from Molecular Probes Inc. (Eugene, Oregon) and dissolved in DMSO to give a 0.45 mM stock solution which was stored in 75 μM aliquots at -60 °C. 75 μl of this Fura-Red-AM solution was added to 4 mL of BSS to produce a final loading concentration of 8 μM Fura-Red-AM. This solution was used to load neurons on a single coverslip for 1 hour at room temperature. They were then transferred to fresh BSS for at least 15 minutes prior to, or after mounting on a superfusion chamber.

ii. *fura-red data analysis*

Fura-Red measurements were made using a dual excitation ratiometric method available on the same imaging system. Briefly, the dye was excited alternately at 452 nm and 488 nm and the resulting fluorescence above 510 nm was recorded. The frequency of data acquisition was kept to a minimum in order to avoid photo-bleaching the fura-red. The ratio of background corrected emission intensities (I_{452}/I_{488}) was then converted to $[Ca^{2+}]_i$ values with the following equation:

$$[Ca^{2+}]_i = \beta\, K_d \frac{[R - R_{min}]}{[R_{max} - R]}$$

Where: β - the ratio of the measured fluorescence intensity of Ca^{2+}-free to Ca^{2+}-bound indicator at 488 nm.

K_d - the dissociation constant of Fura-Red for Ca^{2+}.

R - the background corrected emission intensity ratio (I_{452}/I_{488}).

R_{min} - the limiting value of R when all the indicator is in the Ca^{2+}-free form.

R_{max} - the limiting value of R when all of the indicator is in the Ca^{2+}-bound form.

Using the same calibration method as for fura-2 (above), values of R_{min}, R_{max} and β were 1.28, 6 and 2.85 respectively.

V. pH imaging using BCECF

i. Loading

2',7'-bis-(2-carboxyethyl)-5-(and-6)-carboxyfluorescein (BCECF)-AM was obtained from Molecular Probes Inc. (Eugene, Oregon) and dissolved in DMSO to give a 1 mM stock solution which was stored in 60 μl aliquots at -60 °C. 5 μl of the BCECF-AM solution was taken from the stock solution and added, while vortex stirring, to 2.5 ml of BSS to produce a final concentration of 2 μM BCECF. This loading solution was transferred to one well of a six well tissue culture plate and used to load neurons on a single coverslip. Loading was for 30 minutes at room temperature (Baxter and Church, 1996). Neurons were then transferred to fresh BSS for at least 15 minutes prior to, or after mounting on a superfusion chamber.

ii. BCECF data analysis

BCECF measurements were made using a dual excitation ratiometric method available on the same imaging system. The advantages of a ratiometric method for estimating pH_i are that the ratio obtained is insensitive to changes in optical path length, local probe concentrations, illumination intensity and photobleaching (Bright *et al.*, 1987). Full details of the methodology can be found in Baxter and Church (1996). Briefly, the dye was excited alternately at 488 nm and 452 nm and the resulting fluorescence above 510 nm was recorded. The intensity of light illuminating the neurons was reduced by decreasing the power output of the mercury arc lamp to half that used for the fluo-3 experiments and by the addition of neutral density filters to the excitation light path. The frequency of image acquisition was kept constant at 1 image every 10 seconds and data was recorded until steady baseline readings were observed. Analysis was restricted to those neurons able to retain the fluorescent indicator (as judged by raw emission intensity values) throughout the entire course of the experiment (see Schwiening and Boron, 1994). In order to correct for minor differences in dye behavior between our *in vitro* calibration solution and the cytosol, BCECF ratios measured from each cell were normalized to an intracellular ratio recorded at the end of the experiment after a 15 minute exposure of the cell to a pH 7.0 medium containing 10 µM of the H^+-ionophore nigericin (Chaillet and Boron, 1985). This resulted in a normalization of the ratios with a value of 1.0 being equivalent to a pH_i of 7.0. The normalized ratios were then transformed into pH_i values using the equation:

$$pH_i = \log[(R_n - R_{n(min)})/(R_{n(max)} - R_n)] + pK_a$$

Where: R_n is the normalized ratio
$R_{n(min)}$ is the normalized minimum ratio obtained from the standard curve.
$R_{n(max)}$ is the normalized maximum ratio obtained from the standard curve.
pK_a is the acid dissociation constant.

In a total of nine calibration experiments, the mean values of $R_{n(min)}$, $R_{n(max)}$, and pK_a were 0.47 ± 0.07, 2.06 ± 0.20, and 7.30 ± 0.07 respectively. These values were obtained by exposing neurons to a variety of HEPES-buffered solutions of different pH's (ranging from 5.5 to 8.5) at room temperature. These solutions all contained 10 µM nigericin, a charged electron carrier ionophore which equilibrates pH_i with pH_o as long as the intracellular and extracellular K^+ activities are equal and high (Chaillet and Boron, 1985).

RESULTS

I. Loading conditions for fluo-3 and NP-EGTA

The first objective of this study was to develop a method which used NP-EGTA to induce increases in $[Ca^{2+}]_i$ with the fluorescent indicator fluo-3 being used to detect and record Ca^{2+}-levels. The fluorescent indicator fluo-3 was the indicator dye of choice as a result of complications which arise when more traditional ratiometric dyes are used in conjunction with NP-EGTA (see Discussion). In order to develop correct loading parameters for both fluo-3 and NP-EGTA, many empirical trials were performed and the following parameters were varied:

Table 1: Loading parameters investigated for fluo-3-AM and NP-EGTA-AM

PARAMETER	CONDITIONS	BEST CONDITION
1. Loading time	30, 45, 60, 80 and 120 mins	60 mins
2. [Fluo-3-AM]	~ 1, 3, 5, 10 µM	3 µM
3. [NP-EGTA-AM]	~ 1, 4, 6, 8, 10, 14 µM	8 µM
4. Loading temperature	23 °C and 37 °C	23 °C
5. Photolysis Wavelength	334 ± 5 nm, 360 ± 5 nm and Unfiltered UV light	Unfiltered UV light
6. Photolysis Time	0.1, 0.15, 0.2, 0.25, 0.35, 0.4 and 0.5 s	0.4 s
7. Pluronic F-127	Absent or 0.02 %	Absent

II. Neuronal Ca^{2+} responses to NMDA and caged Ca^{2+} compound

In all experiments, neurons were identified on the basis of their Ca^{2+} response to a transient (5 s) exposure to 40 μM NMDA (Fig. 1). This produced a peak in fluo-3 fluorescence 5-15 s after the onset of exposure and the recovery to baseline from the peak value was relatively slow and in the order of 250-400 s. For comparative purposes, responses to NMDA recorded with the ratiometric dye fura-2 yielded peak $[Ca^{2+}]_i$ in the range of 600 nM and resting $[Ca^{2+}]_i$ of ~ 80 nM in our neurons (see Fig. 5; Abdel-Hamid and Baimbridge-submitted, Abdel-Hamid and Baimbridge-in press). In contrast, a flash photolysis of NP-EGTA produced a rapid peak fluo-3 fluorescence which was already recovering at the time of the first measurement following photolysis (~ 0.6 s). Thereafter, the recovery was rapid and usually complete within 3 minutes.

Since unphotolysed and unbound NP-EGTA could contribute to Ca^{2+}-buffering following photolysis, we examined the effect of successive 0.4 s flashes. The maximum number of uncages on a single field was two; any subsequent uncages produced negligible increases in fluo-3 fluorescence over baseline values. A second uncage on the same field of neurons resulted in a smaller peak indicating that approximately 60% of the loaded NP-EGTA was photolysed by the first uncage (Fig. 2). When a similar experiment was repeated with continuous superfusion of a medium in which Na^+ was replaced by NMDG immediately after the first of two uncagings (Fig. 3), the second response was less than 25 % of the first, indicating that 0 Na^+ conditions, which reduce pH_i (see Fig. 9), also reduce the amount of releasable Ca^{2+} from NP-EGTA. This is consistent with the known sensitivity of EGTA (and its derivative NP-EGTA) to pH, especially below a value of pH 7.0 (Kao, 1994). Based upon the reported K_d values of NP-EGTA and nitr-5 (~ 80 nM and ~ 145 nM respectively) we would anticipate that approximately 50 % of the NP-EGTA molecules would be in a Ca^{2+} bound state at the resting $[Ca^{2+}]_i$ of our neurons (~80 nM, see Fig. 5 and 6)

Figure 1: Typical control response in a field of neurons to NMDA application and flash photolysis.

Mean response of a field of neurons (n=12) loaded with both fluo-3 and NP-EGTA exposed for 5 s to 40 μM NMDA followed by a 0.4 s flash of unfiltered UV light (Uncage). Resting Ca^{2+}-levels increased following NMDA application. In this, and all subsequent similar figures, an increase in $[Ca^{2+}]_i$ is indicated by an increase in background corrected fluo-3 fluorescence intensity. Following the removal of NMDA, Ca^{2+}-levels decayed back to baseline values over the course of the next 500s. When a 0.4 s flash of UV light was used to uncage the NP-EGTA, the resulting peak Ca^{2+} level decayed back to baseline values at a much quicker rate compared to the response following NMDA, with baseline Ca^{2+}-values being restored to within 300 s.

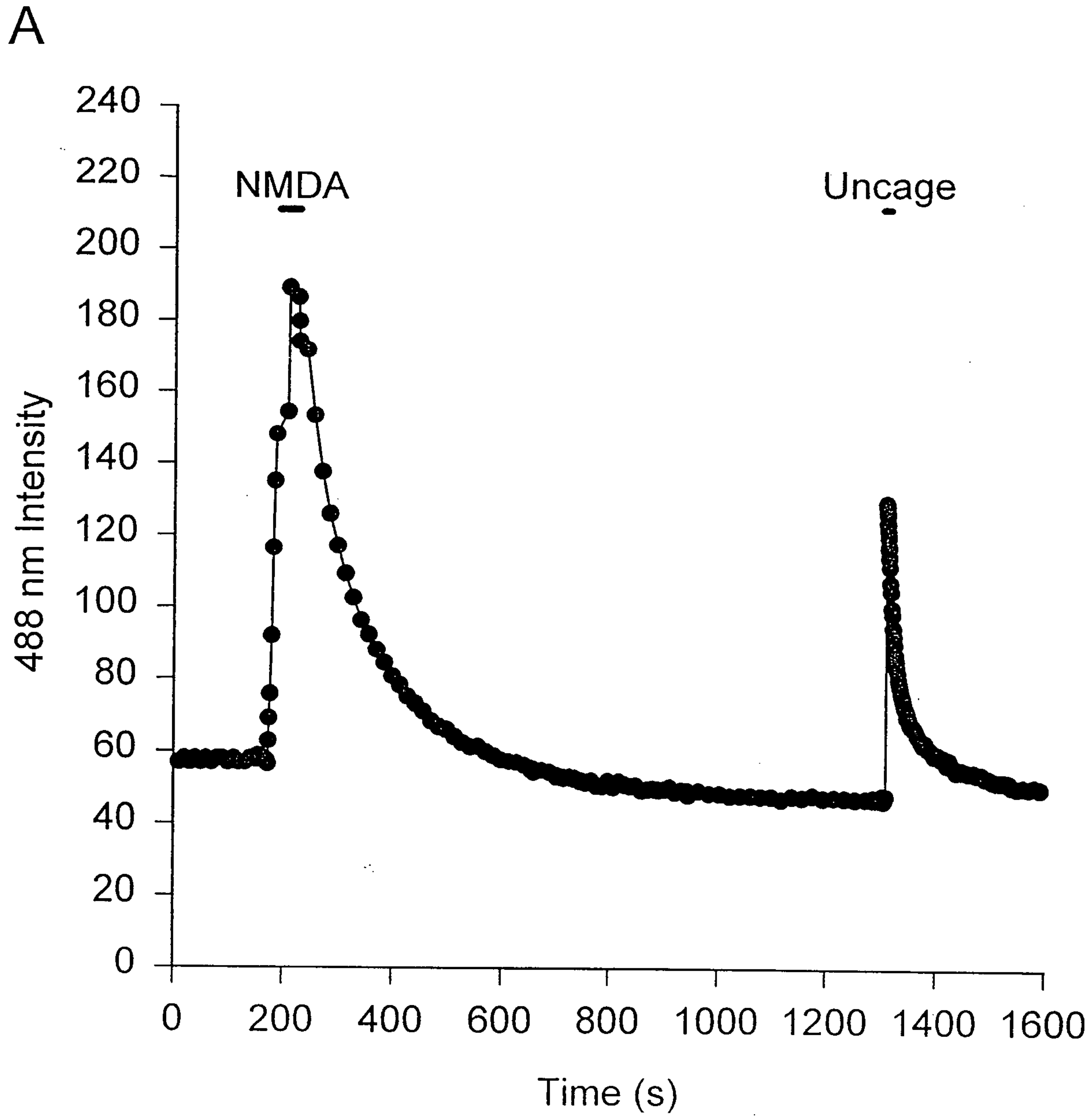
A
240
220
200
180
160
140
120
100
80
60
40
20
0
488 nm Intensity
NMDA
Uncage
0
200
400
600
800
1000
1200
1400
1600
Time (s)

Figure 2: Typical response in a field of neurons to NMDA followed by two consecutive uncages.

Mean response of a field of neurons (n=10) loaded with both fluo-3 and NP-EGTA exposed for 5 s to 40 μM NMDA followed by two consecutive 0.4 s flashes of unfiltered UV light (U). Ca^{2+}-levels increased following NMDA application and then returned to near baseline values. The two responses to uncaging of NP-EGTA decayed to near baseline values within 300 s. The markedly reduced peak reached as a result of the second uncaging demonstrates that the majority of the NP-EGTA was photolyzed during the initial 0.4 s flash.

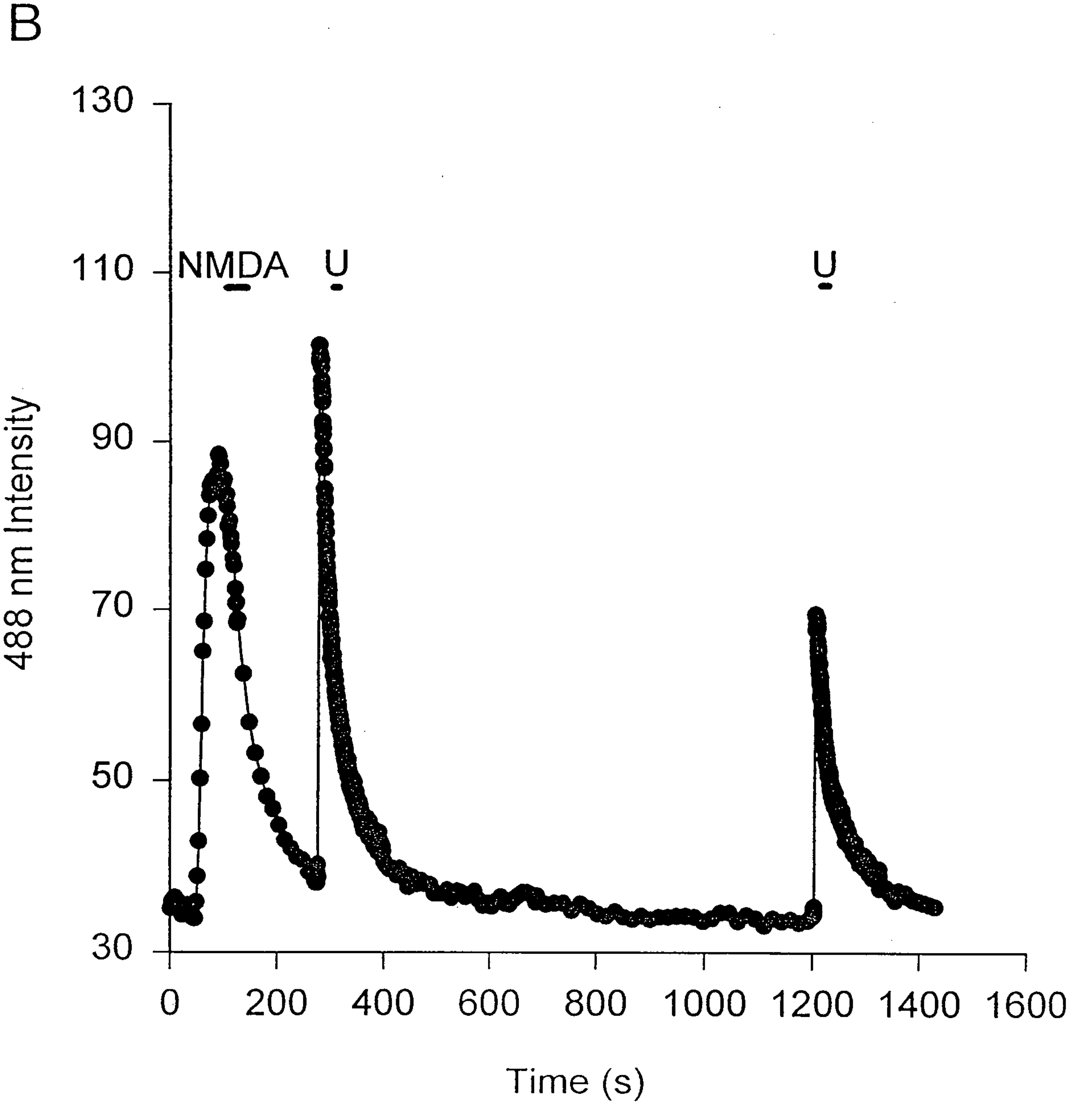
B
130
110
90
70
50
30
NMDA
U
U
488 nm Intensity
0
200
400
600
800
1000
1200
1400
1600
Time (s)

Figure 3: The influence of pH on NP-EGTA

Mean response of a field of neurons (n=14) loaded with both fluo-3 and NP-EGTA exposed for 5 s to 40 μM NMDA followed by two 0.4 s uncages (U). Following the first uncage, all external Na^+ was replaced with NMDG, as a result, the second uncaging was performed during a decrease in pH_i (see Fig. 9). The second photolysis peak is much smaller than is normally expected for a second uncage (see Fig. 2 for comparison) demonstrating the pH sensitivity of NP-EGTA binding with Ca^{2+}.

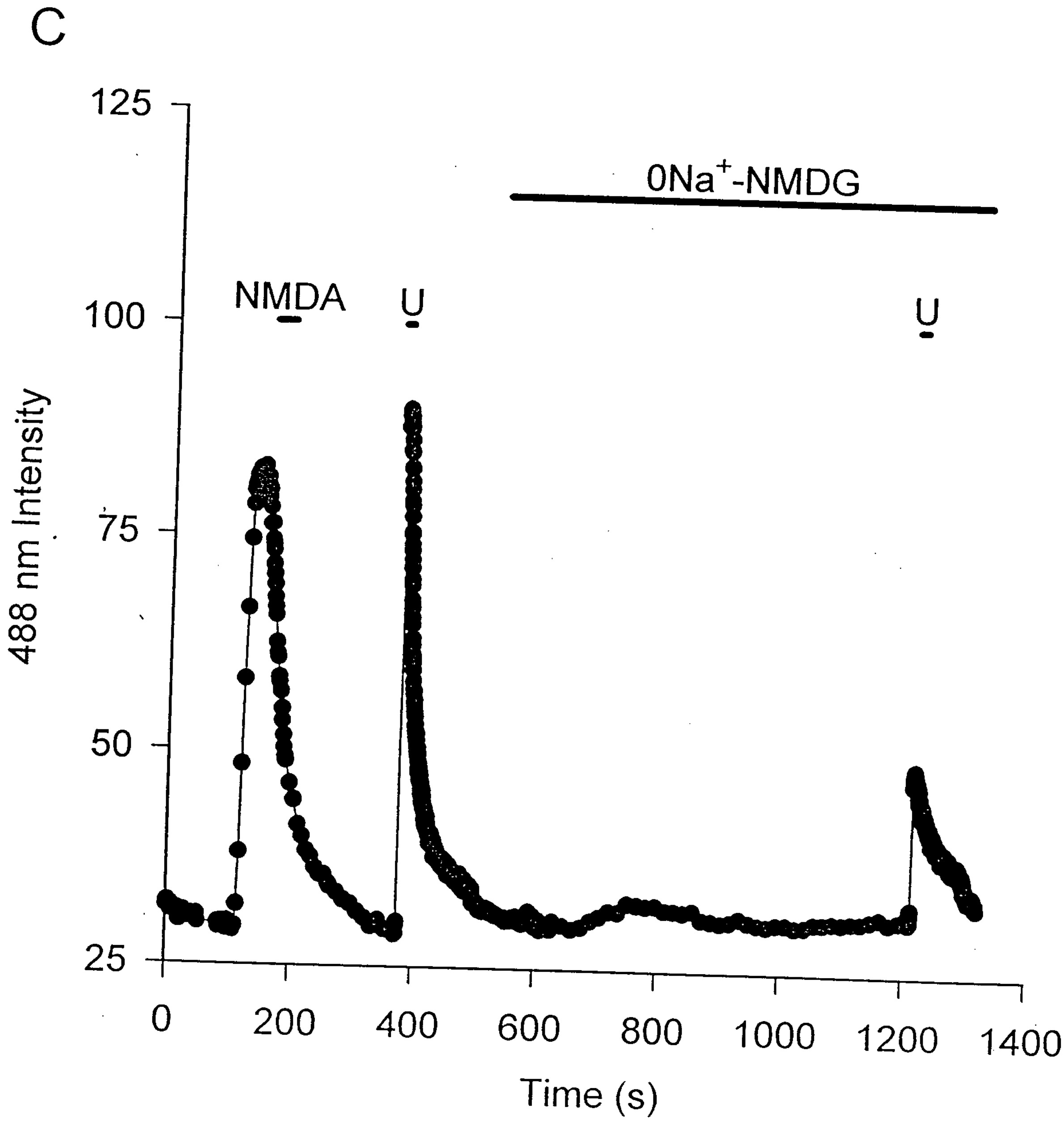
C
0Na$^+$-NMDG
NMDA
U
U
125
100
75
50
25
488 nm Intensity
0
200
400
600
800
1000
1200
1400
Time (s)

compared with < 25 % in the case of nitr-5 (Nerbonne, 1996). This is consistent with the relatively modest increase in fluo-3 fluorescence in response to photolysis of nitr-5 unless the uncaging was timed with the recovery phase of a substantial Ca^{2+} response to NMDA (Fig. 4). These results emphasize the advantage of using NP-EGTA rather than nitr-5.

Although the fluorescent indicator dye fluo-3 may be calibrated, the method is inaccurate and not widely accepted, and was not attempted in our experiments (Minta *et al.*, 1989; Kao *et al.*, 1989; Kao, 1994). In order to obtain an indication of the $[Ca^{2+}]_i$ reached during photolysis, the ratiometric and calibratable dye fura-2 was used. In 23 neurons loaded with fura-2 and NP-EGTA, resting $[Ca^{2+}]_i$ was ~ 90 nM (Fig. 5). Following 40 μM NMDA application, $[Ca^{2+}]_i$ reached 950 nM before decaying back to resting levels of ~ 90 nM. Uncaging using a 0.4 s flash of unfiltered UV light, produced a peak $[Ca^{2+}]_i$ of 530 nM which subsequently decayed back to baseline levels of ~ 100 nM. In a second experiment increasing the photolysis time to 0.5 s (Fig. 6), resulted in a peak $[Ca^{2+}]_i$ of 720 nM (n=12) before decaying back to resting $[Ca^{2+}]_i$ of ~ 100 nM,with NMDA application producing a peak of 1050 nM. As a result of the complications associated with simultaneous using fura-2 and NP-EGTA (see discussion), we attempted to use the ratiometric dye Fura-Red to determine the peak $[Ca^{2+}]_i$ reached following flash photolysis. Baseline $[Ca^{2+}]_i$ was found to be ~ 100 nM (Fig. 7), consistent with those found using fura-2, while peak $[Ca^{2+}]_i$ immediately following flash photolysis was seen to be ~ 800 nM. Both of these ratiometric dyes indicated that the peak $[Ca^{2+}]_i$ observed immediately following photolysis was similar to that found during a 5 s application of 40 μM NMDA, indicating that the loading parameters used in this study did not produce an excessive increase in $[Ca^{2+}]_i$. Although the $[Ca^{2+}]_i$ found immediately following flash photolysis was not excessive, it does not reflect the true peak $[Ca^{2+}]_i$ reached following flash photolysis as the first data point was obtained ~ 0.6 s

Figure 4: The effects of the caged Ca^{2+}-compound nitr-5.

Records from three individual neurons loaded with both nitr-5 and fluo-3 exposed for 5 s to 40 μM NMDA followed by a 0.4 s flash of UV light (U). Photolysis of nitr-5 produced negligible increases in Ca^{2+}-levels unless the $[Ca^{2+}]_i$ was elevated during the photolysis demonstrating the reduced affinity of nitr-5 for Ca^{2+}.

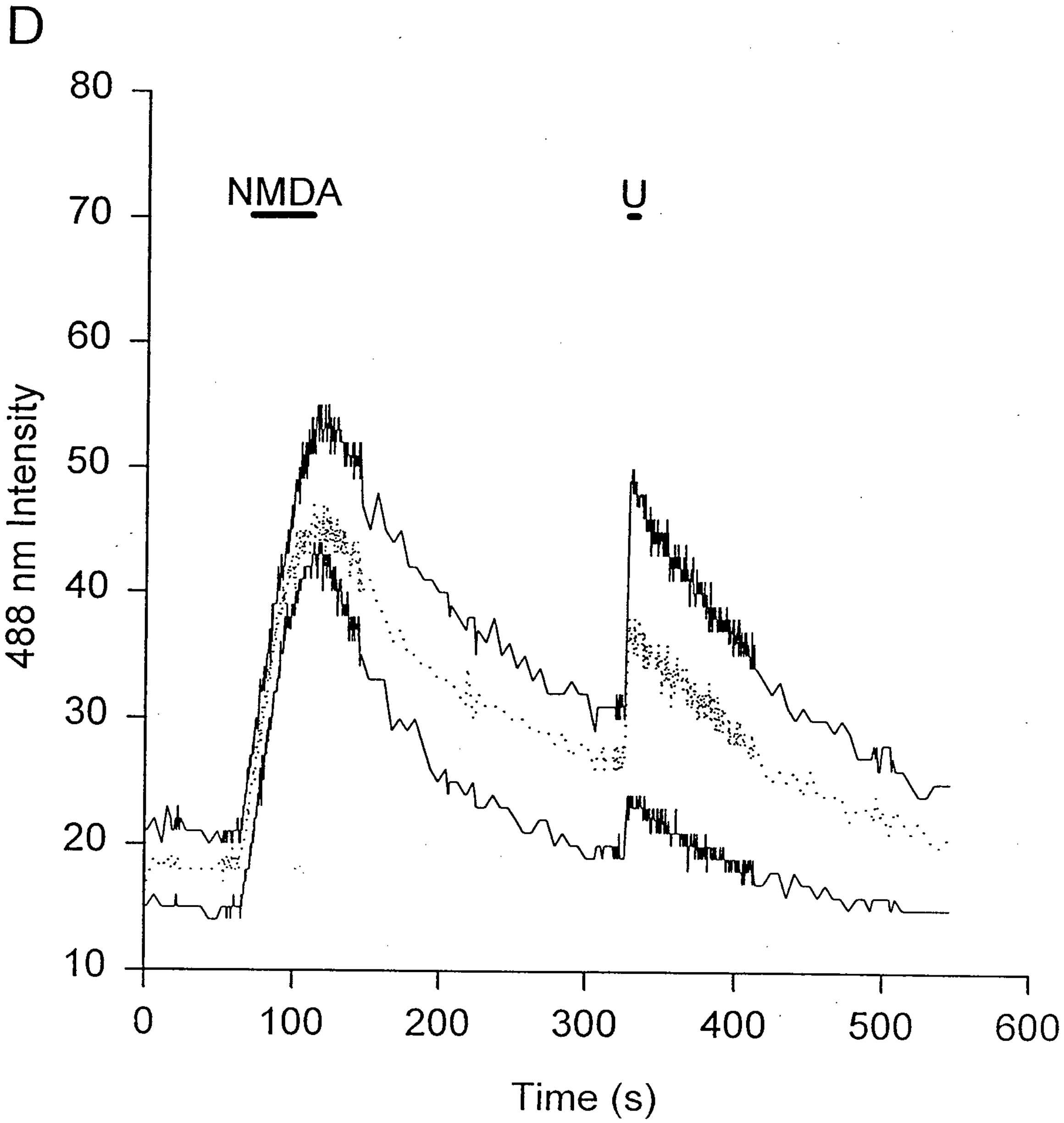
D
NMDA
U
80
70
60
50
40
30
20
10
488 nm Intensity
0
100
200
300
400
500
600
Time (s)

Figure 5: Response seen to 0.4 s flash in fura-2 and NP-EGTA loaded neurons.

Mean response of a field of neurons (n=14) loaded with both fura-2 and NP-EGTA exposed for 5 s to 40 μM NMDA followed by a 0.4 s flash of UV light (U). Baseline $[Ca^{2+}]_i$ was ~ 80 nM, following NMDA application $[Ca^{2+}]_i$ reached ~ 900 nM. Following flash photolysis of NP-EGTA $[Ca^{2+}]_i$ reached ~ 500 nM.

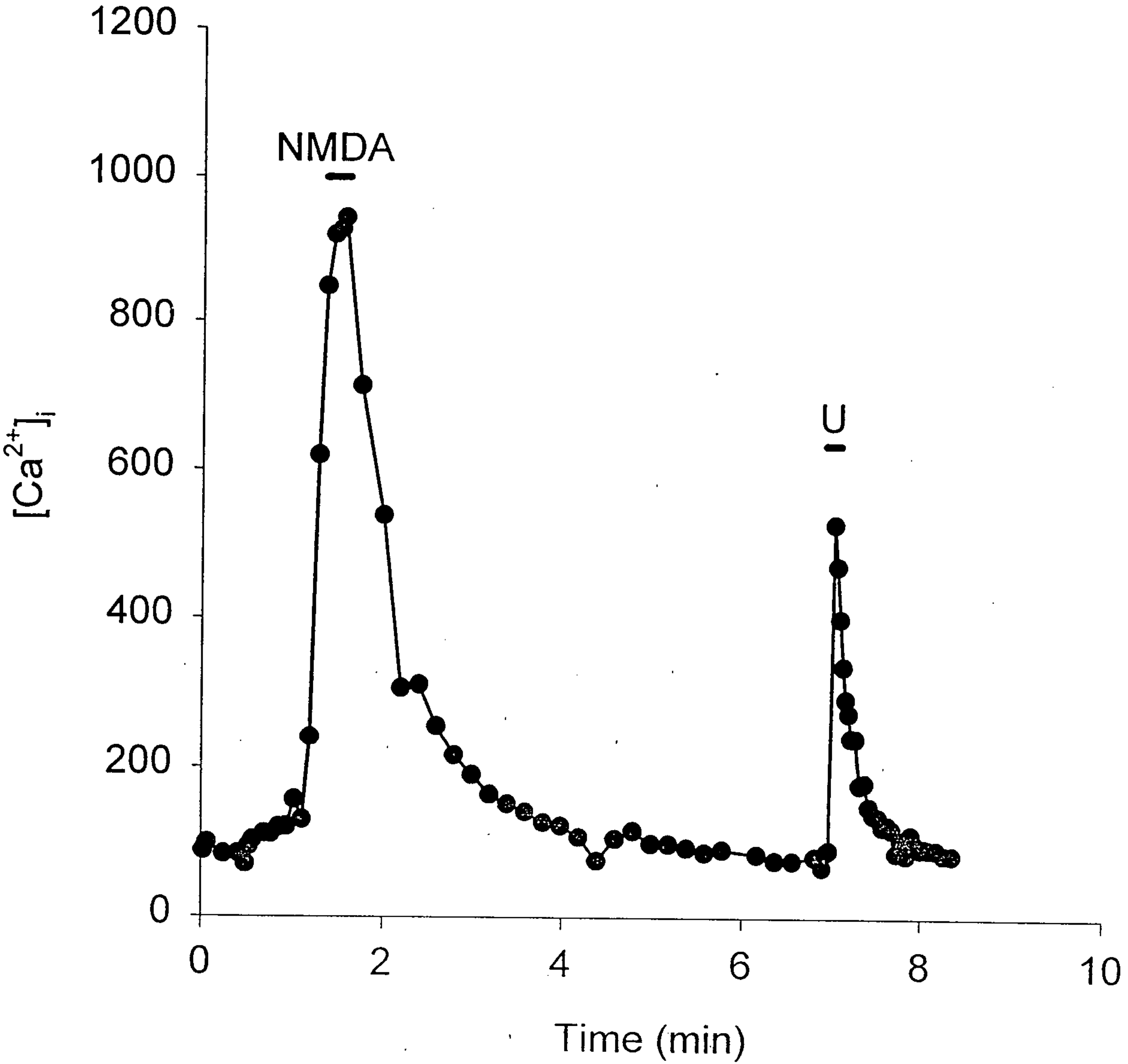
1200
1000
800
600
400
200
0
$[Ca^{2+}]_i$
NMDA
U
0
2
4
6
8
10
Time (min)

Figure 6: Response seen to 0.5 s flash in fura-2 and NP-EGTA loaded neurons.

Mean response of a field of neurons (n=10) loaded with both fura-2 and NP-EGTA exposed for 5 s to 40 μM NMDA followed by a 0.5 s flash of UV light (U). Baseline $[Ca^{2+}]_i$ was ~ 80 nM, following NMDA application $[Ca^{2+}]_i$ reached ~ 900 nM. Following flash photolysis of NP-EGTA $[Ca^{2+}]_i$ reached ~ 700 nM. This value of ~ 700 nM was similar to that obtained with the use of Fura-Red and was larger than the peak $[Ca^{2+}]_i$ reached following a 0.4 s flash (see Figure 5). Reasons for the decreased amount of Ca^{2+} released during the 0.4 s flash are outlined in the discussion.

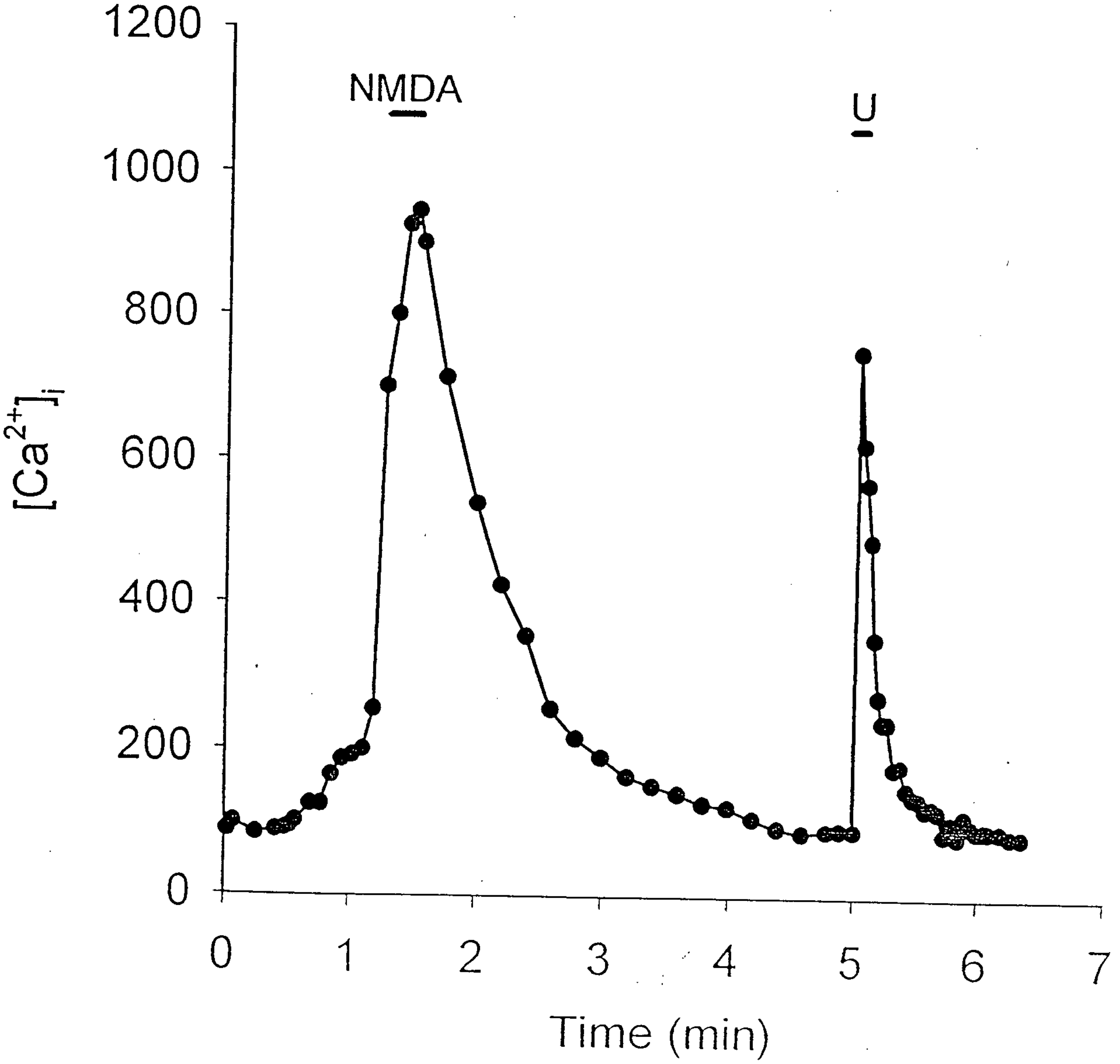
1200
1000
800
600
400
200
0
[Ca^{2+}]$_i$
NMDA
U
0
1
2
3
4
5
6
7
Time (min)

Figure 7: Response seen to a field of neurons loaded with fura-red and NP-EGTA.

Mean response of a field of neurons (n=16) loaded with both fura-red and NP-EGTA and exposed for 5 s to 40 µM NMDA followed by a 0.4 s flash of UV light (U). Baseline $[Ca^{2+}]_i$ was ~ 100 nM, following NMDA application $[Ca^{2+}]_i$ reached ~ 1000 nM and following flash photolysis of NP-EGTA $[Ca^{2+}]_i$ reached ~ 900 nM.

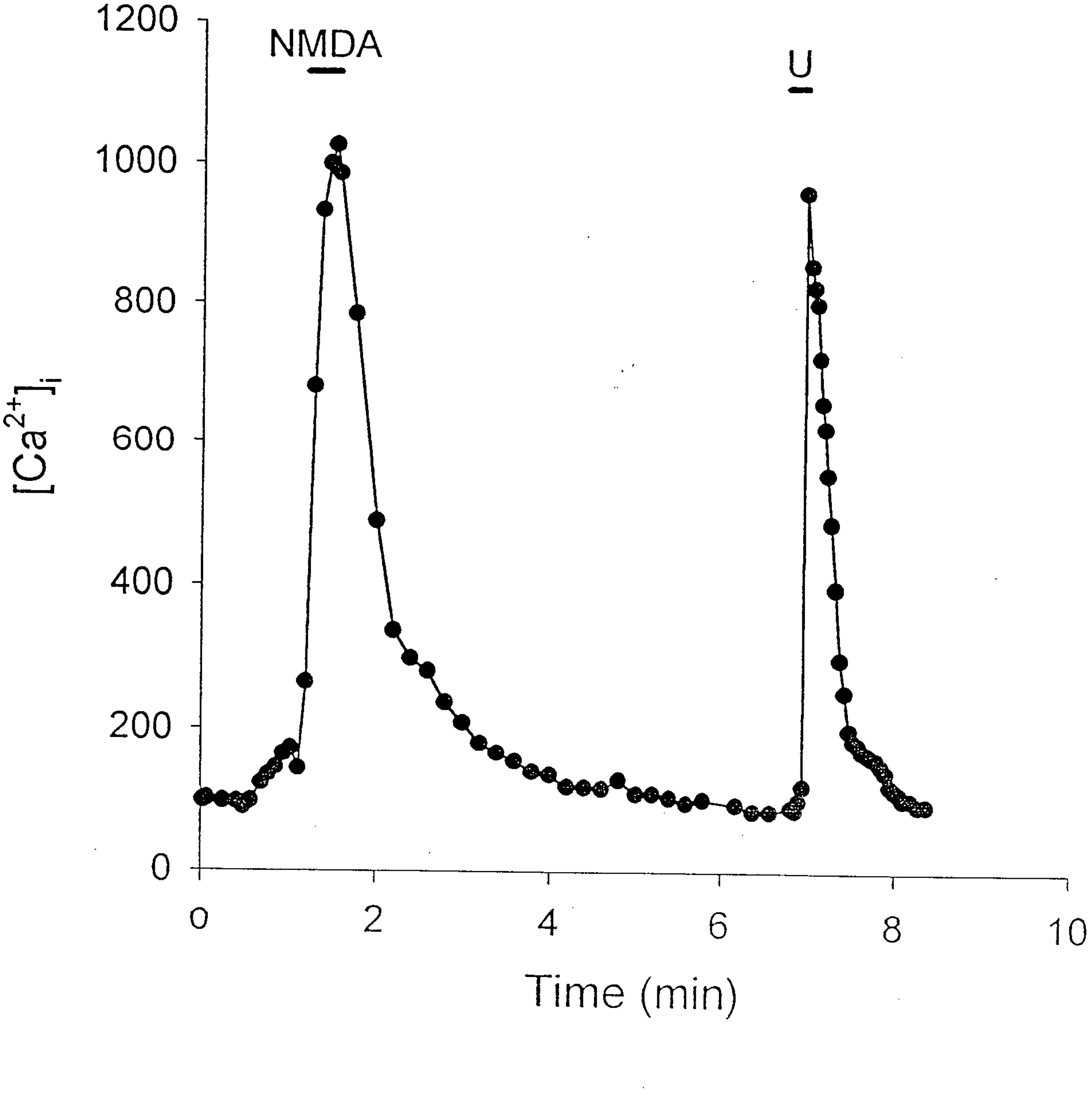
1200
1000
800
600
400
200
0
NMDA
U
$[Ca^{2+}]_i$
0
2
4
6
8
10
Time (min)

post-photolysis at which time $[Ca^{2+}]_i$ was already in the process of decaying back to baseline values.

Comparison of Room Temperature vs. 37 °C rates of recovery

Following flash photolysis of NP-EGTA, the resulting Ca^{2+}decay curve was, in the majority of situations, best fit by a double exponential decay curve, a result consistent with the observations of Kennedy & Thomas (1995) and Mironov (1995). In order to improve the resolution of the double exponential and to minimize the effects of dye leakage, all experiments were performed at room temperature (22 °C; Zavoico and Cragoe, 1988; Kao, 1994). The average control rates of recovery (N=92; N=number of cells) were 14.06 ± 3.52 for the fast component and 72.44 ± 32.19 for the slow component. These values are similar to those found by Mironov (1995) and reflect the slow nature of calcium transients at room temperature. Experiments were also performed at 37 °C in order to establish that decay curves at physiological temperatures were similar to those obtained at 22 °C. At 37 °C, the Ca^{2+} decay curve was also best fit by a double exponential with both a fast and a slow component; however, the noticeable difference was the much faster recovery to baseline $[Ca^{2+}]_i$ (Fig. 8 and Table 2). The following table lists the control values obtained at room temperature and 37 °C, two sets of values are shown, obtained on separate days, demonstrating the marked variability in decay rates between days. Despite this marked variability between days, within a single day there was no significant variability thus emphasizing the use of paired same-day controls obtained from sister-cultures.

Figure 8: Typical response seen at 37 °C.

Mean response of a field of neurons (n=12) loaded with both fluo-3 and NP-EGTA. Following a 5 s exposure to 40 µM NMDA, resting Ca^{2+}-levels increased and then decayed back to baseline levels within the next 200s. Following flash photolysis of NP-EGTA, Ca^{2+}-levels increased and then decayed back to baseline levels at a much quicker rate than observed at room temperature.

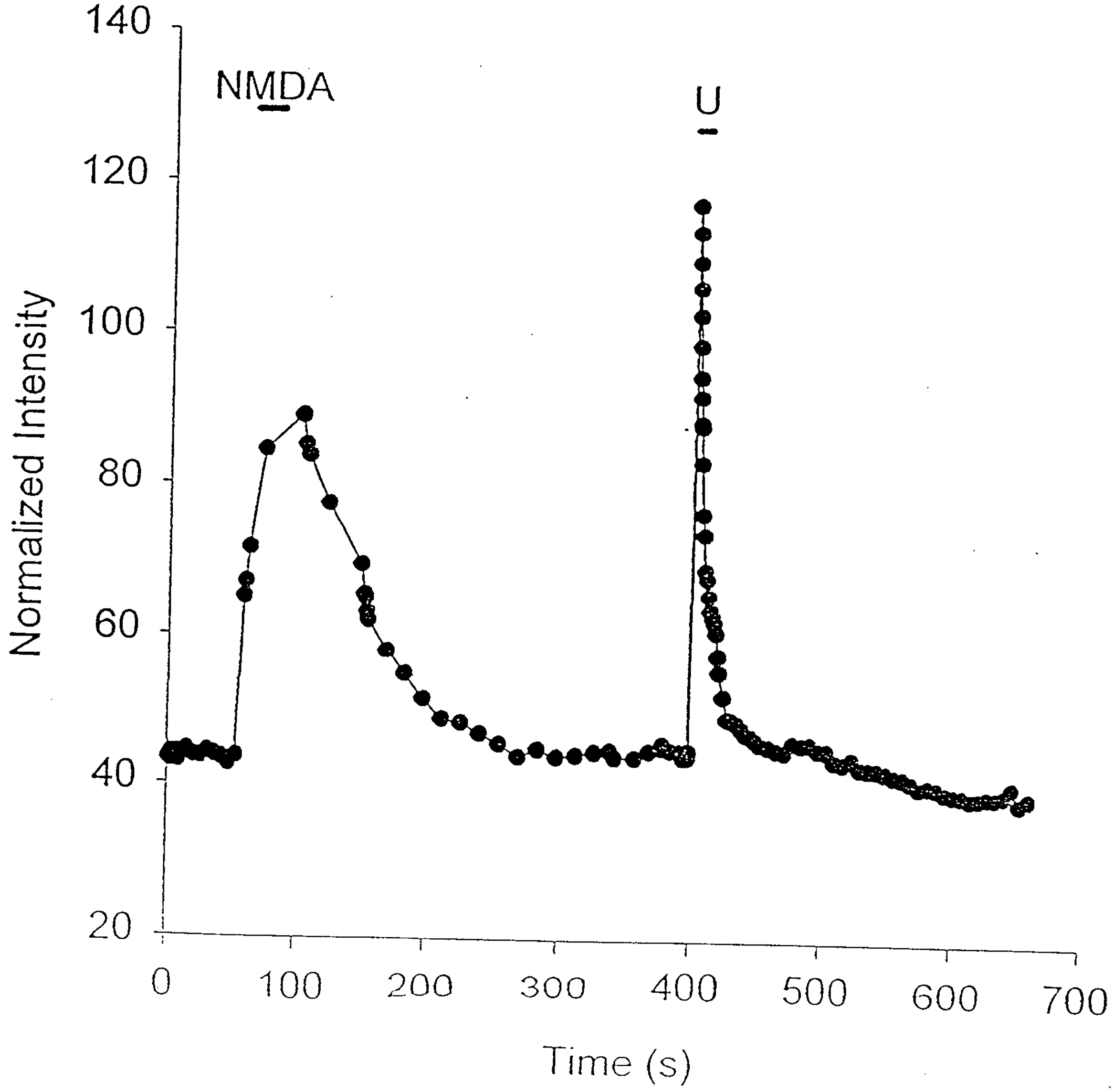
NMDA
U
Normalized Intensity
140
120
100
80
60
40
20
0
100
200
300
400
500
600
700
Time (s)

Table 2: Comparison of Room Temperature vs. 37 °C rates of recovery

			FAST			SLOW
	N	τ (s)	S.E.M.		τ (s)	S.E.M.
Control-RT	13	7.39	0.16		87.32	2.75
Control-37 °C	9	2.28	0.14		20.32	1.32
Control-RT	5	10.91	0.80		37.45	2.96
Control-37 °C	16	4.35	0.31		26.36	0.69

III. Role of the PM-Na^+/Ca^{2+} exchanger

In neurons loaded with the pH sensitive fluorescent indicator BCECF, removal of external Na^+ and replacement with either NMDG or Li^+ (Figs. 9 and 10 respectively), resulted in a rapid fall in pH_i from resting values of ~ 6.8 to values of ~6.4 or less. For 15 neurons, normal resting pH_i was 6.83 ± 0.04, following removal of all external Na^+ (replaced by NMDG) pH_i fell to statistically different levels of 6.38 ± 0.02 ($p<0.001$, paired *t*-test, Fig. 9), this effect lasted 20 minutes until 10 μM nigericin was added to the superfusate. In another field of 20 neurons, normal resting pH_i was 6.79 ± 0.04, following removal of external Na^+ (replaced by NMDG), pH_i fell to 6.25 ± 0.03 ($p<0.001$, paired *t*-test, Fig. 9). With the addition of 5 mM TMA, pH_i returned to 6.77 ± 0.02 which was not statistically different from the original resting pH_i (paired *t*-test). Without correcting for changes in pH_i, removal of all external Na^+ (replaced by NMDG) resulted in a significant prolongation of the recovery of background corrected fluo-3

Figure 9: The effects of $0Na^+$-NMDG on pH_i.

Record from two separate fields of neurons obtained from sister cultures loaded with BCECF. The solid line represents a field of neurones (n=15) exposed to 0 Na^+-NMDG for 27 minutes followed by a 15 minute exposure to 10 μM nigericin (*). Upon substitution of extracellular Na^+ with NMDG, pH_i falls from a resting value of 6.83 ± 0.04 to 6.38 ± 0.02. The dotted line represents a field of neurons (n=20) continuously exposed to 0 Na^+- NMDG for 26 min; after 15 minutes, pH_i fell to 6.25 ± 0.03 from its resting value of 6.79 ± 0.04; at this point (^), 5 mM TMA was added to the medium which restored pH_i to 6.77 ± 0.02 it was at this point, when pH_i was restored to baseline values, where the uncage was performed in sister cultures loaded with fluo-3 and NP-EGTA; 10 μM nigericin was then superfused (*) for calibration purposes.

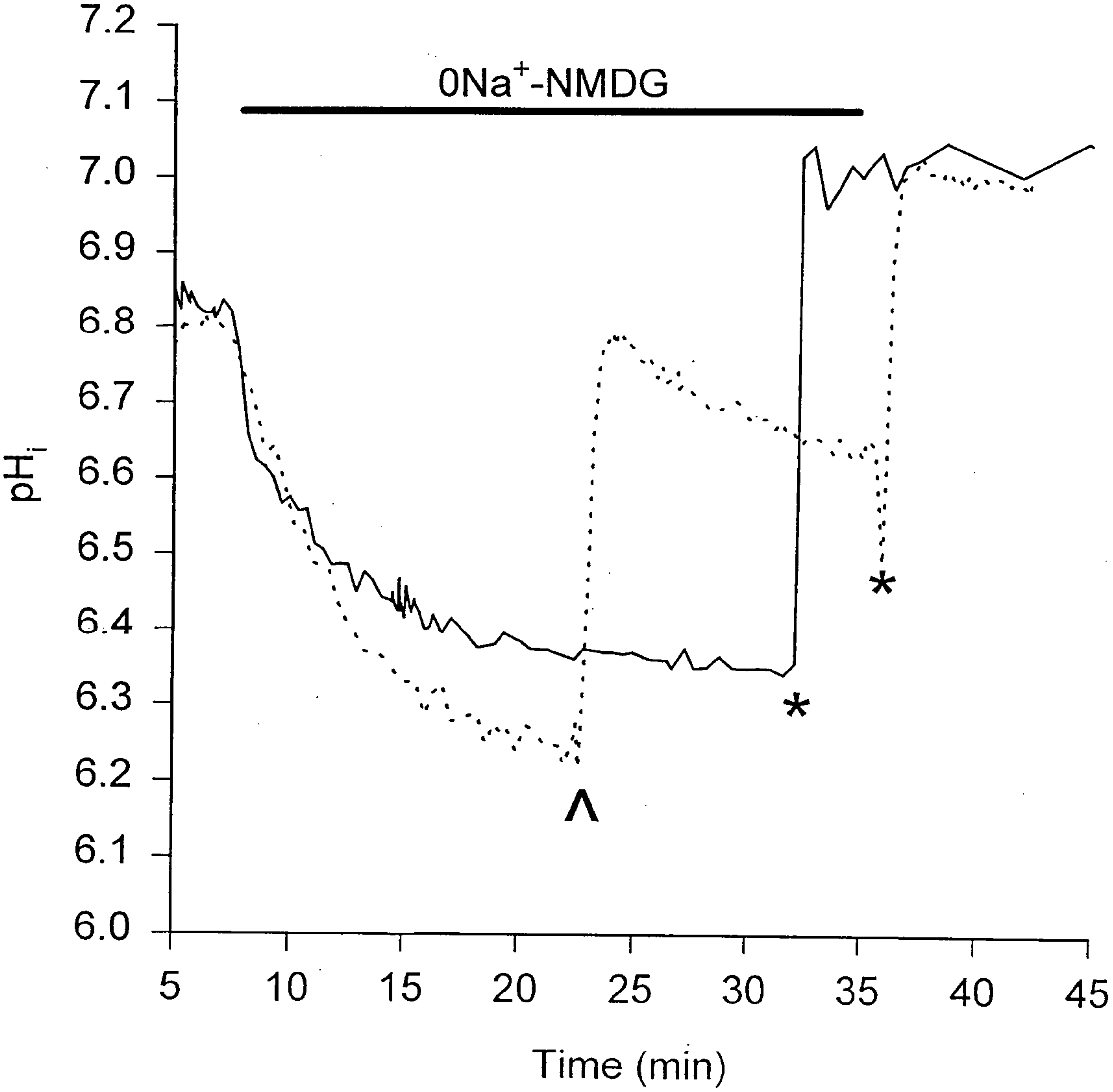
0Na$^+$-NMDG
pH$_i$
7.2
7.1
7.0
6.9
6.8
6.7
6.6
6.5
6.4
6.3
6.2
6.1
6.0
5
10
15
20
25
30
35
40
45
Time (min)
^
*
*

Figure 10: The effects of 0Na$^+$-Li$^+$ on pH$_i$.

Mean response of a field of neurons (n=20) loaded with BCECF. Following removal of external Na$^+$ (replaced by Li$^+$) resting pH$_i$ fell from a value of 6.97 ± 0.03 to 6.35 ± 0.04, pH$_i$ recovered slowly over the course of the next 30 min, 10 μM nigericin was then superfused (*) for calibration purposes.

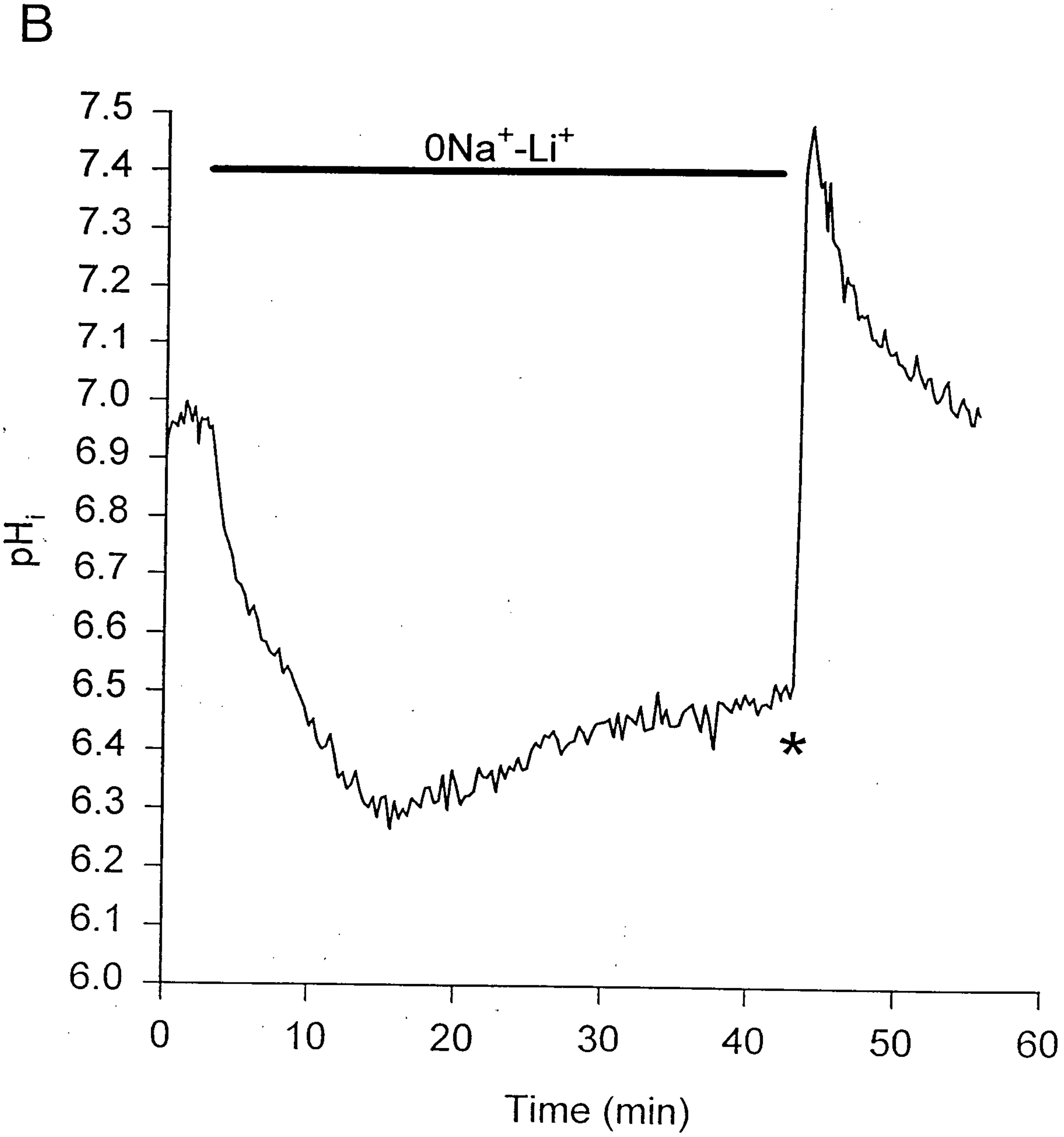
B
0Na+-Li+
*
pHi
7.5
7.4
7.3
7.2
7.1
7.0
6.9
6.8
6.7
6.6
6.5
6.4
6.3
6.2
6.1
6.0
0
10
20
30
40
50
60
Time (min)

fluorescence intensities to baseline values following photolysis of NP-EGTA (Fast, $p<0.001$; Slow, $p<0.001$; unpaired *t*-test, see Fig. 11 and Table 3). A slowing down of the initial fast recovery phase was particularly evident. However, restoring pH_i to normal values eliminated this effect of 0 Na^+. Under these conditions there was no evidence to support a role for the PM-Na^+/Ca^{2+} exchanger in the recovery of background corrected fluo-3 fluorescent intensities to baseline values (Fast, N/S; Slow, N/S; unpaired *t*-test, Table 3).

In 20 neurons, when Li^+ was used to replace external Na^+, we observed an immediate fall in pH_i from resting levels of 6.97 ± 0.03 to 6.30 ± 0.04 ($p<0.001$, paired *t*-test), pH_i levels then began to slowly recover (Fig. 10). We therefore examined the recovery of fluo-3 fluorescence following flash photolysis of NP-EGTA at four different time intervals after the onset of superfusion with Li^+-containing solutions. After 4 and 12 minutes, we observed a significant prolongation in the rate of recovery (4 min-Fast-$p<0.05$, Slow-$p<0.05$; 12 min- Fast-$p<0.05$, Slow-$p<0.001$, unpaired *t*-test), but with longer superfusions this effect declined and by 40 minutes there was no significant difference in the rates of recovery when compared to control values obtained in sister cultures (Fast-N/S, Slow-N/S, unpaired *t*-test; see Table 3).

IV. Role of mitochondria

In 21 neurons, when the protonophore CCCP (2 μM) was used to inhibit mitochondrial uptake of Ca^{2+} in neurons loaded with BCECF, within 4 minutes we observed a fall in pH_i from resting levels of 6.86 ± 0.04 to statistically different levels of 6.66 ± 0.04 ($p<0.001$; paired *t*-test, Fig. 12), this effect lasted for 15 minutes until 10 μM nigericin was added to the superfusate. In

Figure 11: Background subtracted normalized data showing the influence of the PM-Na^+/Ca^{2+} exchanger on Ca^{2+}-homeostasis.

Normalized mean response of three independent fields of neurons from sister cultures loaded with both fluo-3 and NP-EGTA. When Na^+ was replaced by NMDG (□) (n=11), the rate of recovery back to baseline values was much slower than that of the controls (o) (n=8). However if photolysis was performed 1 min after restoring pH_i to baseline values with 5 mM TMA, the resulting decay curve (Δ) (n=13) was virtually identical to that seen in controls (o). (□, o, and Δ represent actual data points while the solid line represents the best fit double exponential decay curve.)

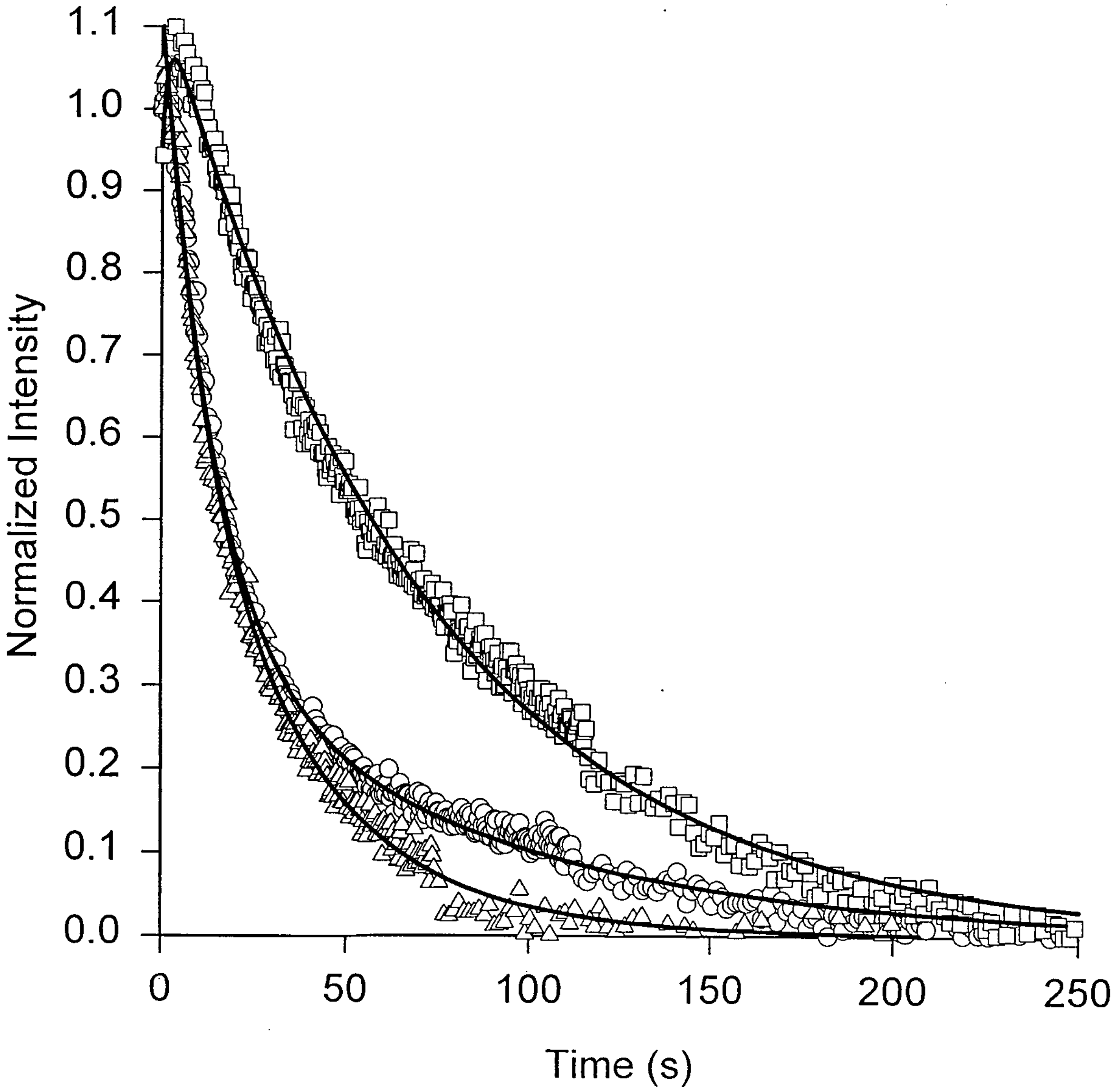
1.1
1.0
0.9
0.8
0.7
0.6
0.5
0.4
0.3
0.2
0.1
0.0
Normalized Intensity
0
50
100
150
200
250
Time (s)

Figure 12: The effects of CCCP on resting pH_i.

Mean response of a field of neurons (n=21) loaded with BCECF. When 2 μM CCCP was superfused, pH_i fell from 6.86 ± 0.04 to 6.66 ± 0.04. Nigericin (10 μM) was then superfused (*) for calibration purposes.

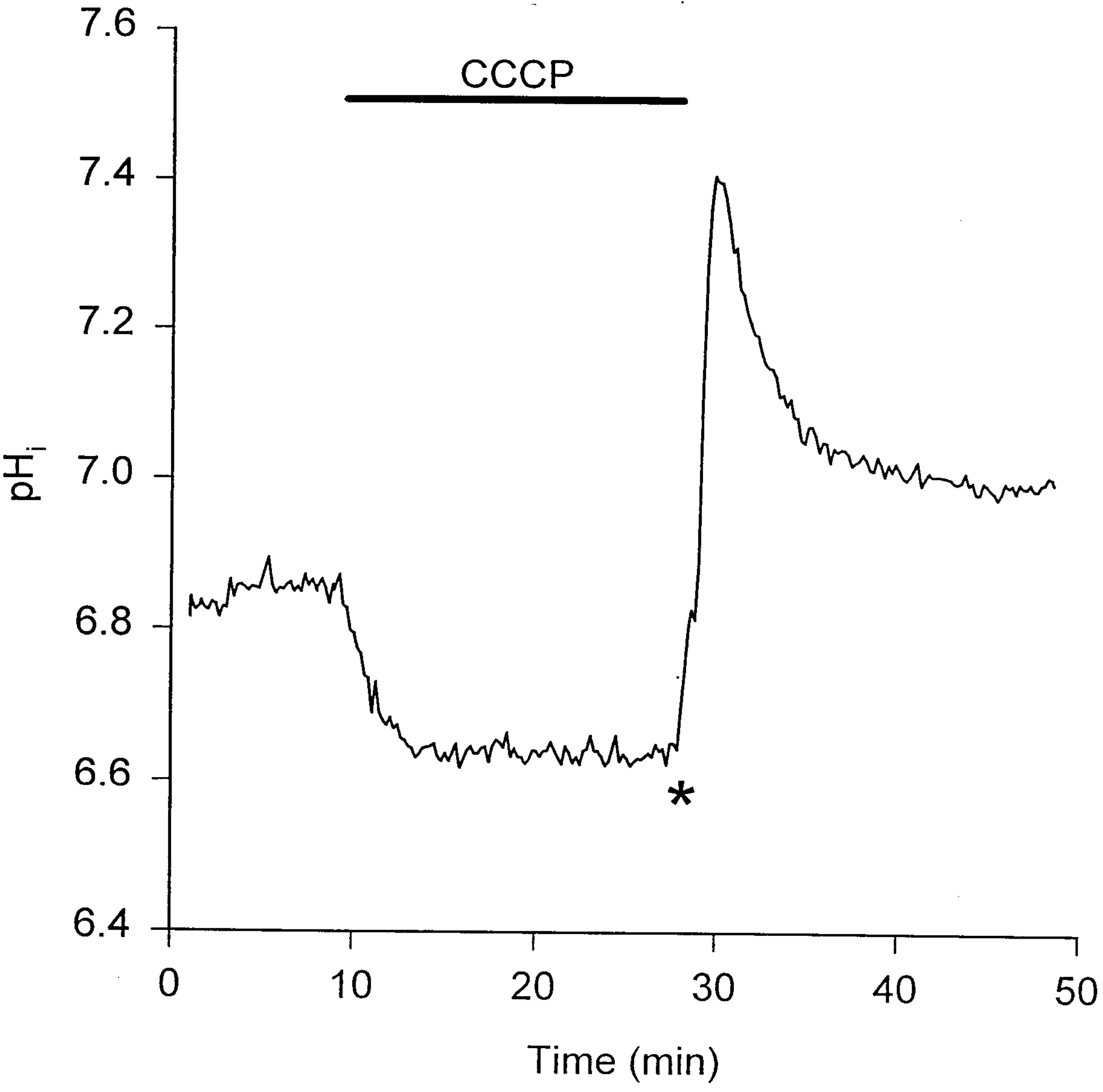
7.6
7.4
7.2
7.0
6.8
6.6
6.4
pH_i
CCCP
*
0
10
20
30
40
50
Time (min)

another field of 25 neurons, resting pH_i levels of 6.85 ± 0.04 fell, after 2 minutes, to statistically different levels of 6.67 ± 0.03 following superfusion of 2 μM CCCP ($p<0.001$; paired *t*-test, Fig. 13). Within 1 minute of the addition of 2 mM TMA to the superfusion medium pH_i was restored to 6.84 ± 0.03, which was not statistically different from the original resting levels obtained prior to superfusion with CCCP (paired *t*-test). This procedure was repeated using sister cultures loaded with fluo-3 and NP-EGTA to assess the effect of CCCP on the recovery of background corrected fluo-3 fluorescent intensities to baseline values following photolysis of NP-EGTA. Superfusion of CCCP alone produced an apparent rise in background corrected fluo-3 fluorescence (Fig. 14) which was rapidly eliminated when TMA was added to the medium (Fig. 15). Uncaging in CCCP resulted in a significantly slower recovery to baseline values (Fast, $p<0.001$; Slow, $p<0.05$; unpaired *t*-test, see Table 3). When the pH_i was restored to resting levels, uncaging (after 60 s of superfusion in TMA, 300 s in CCCP) resulted in a release of Ca^{2+} with a much slower recovery to baseline values well above prior resting levels (Fast, $p<0.05$; Slow, $p<0.05$; unpaired *t*-test). This effect of CCCP is evident in the normalized data shown in Fig. 16 and Table 3. Compared to control rates of recovery, CCCP treated neurons, with normal pH_i restored by TMA, had significantly slower rates of recovery (Fig. 16).

In view of the fact that CCCP will deplete ATP levels in addition to its action on mitochondrial Ca^{2+}-uptake, we performed additional experiments in the presence of 20 μM of the ATP-synthase inhibitor oligomycin. This served to inhibit the reverse activity of the ATP-synthase resulting from the collapse of the mitochondrial proton gradient. ATP/ADP levels will then be transiently maintained (most likely due to glycolysis) and any changes in Ca^{2+}-extrusion rates can be attributed to inhibition of mitochondrial Ca^{2+}-uptake rather than ATP depletion (Budd & Nicholls, 1996). Under these conditions we still observed a significant prolongation

Figure 13: The effects of CCCP and CCCP + TMA on pH_i.

Mean response of a field of neurons (n=25) loaded with BCECF. When 2 μM CCCP was superfused, resting pH_i fell from 6.85 ± 0.04 to 6.67 ± 0.03. Within 1 min of superfusion with 2 mM TMA pH_i was restored to its resting value of 6.85 ± 0.03, at this point the uncage was performed ensuring that pH_i was at resting values. Nigericin (10 μM) was then superfused (*) for calibration purposes.

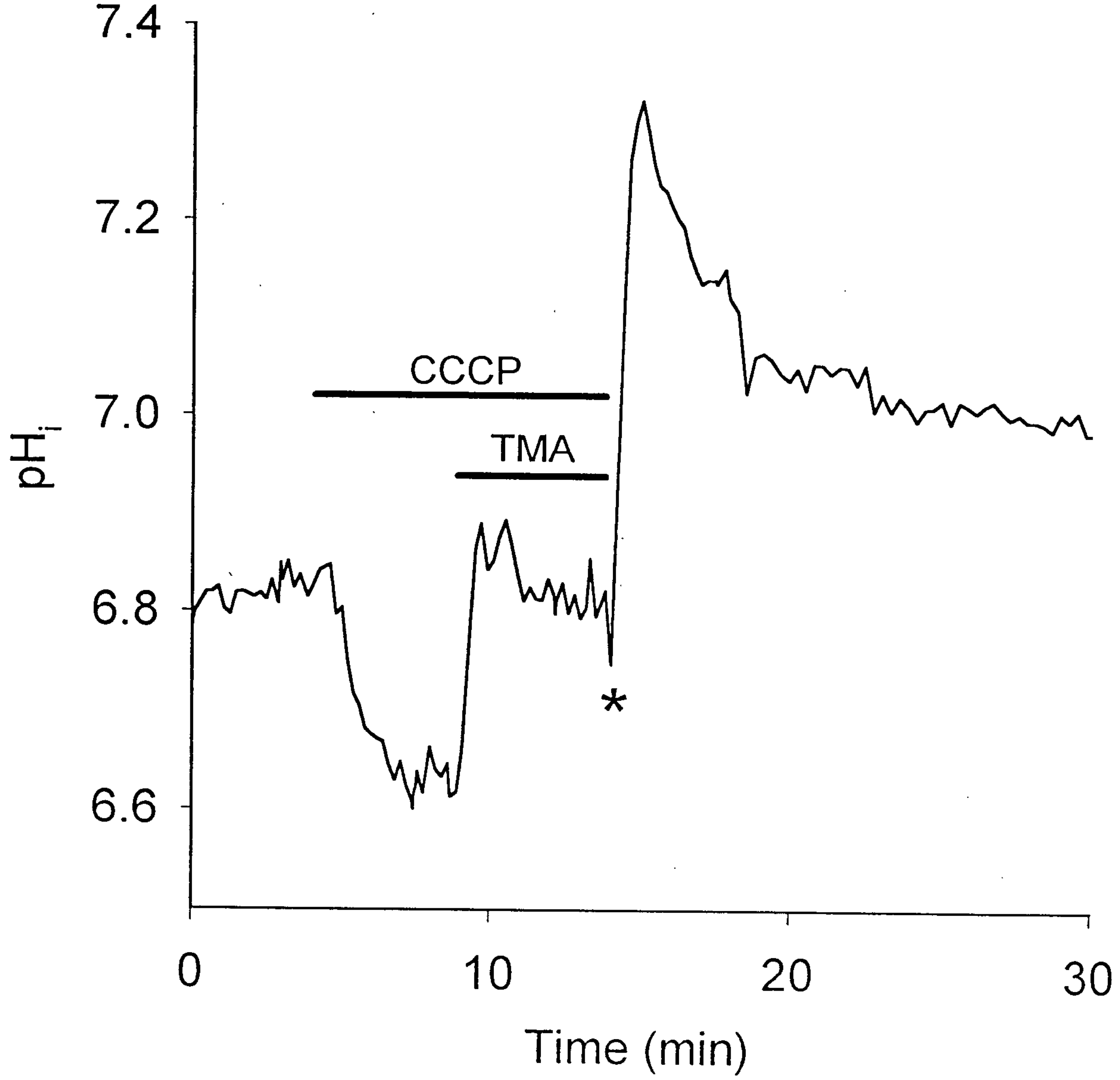
7.4
7.2
7.0
6.8
6.6
pH_i
CCCP
TMA
*
0
10
20
30
Time (min)

Figure 14: The effects of CCCP on resting Ca^{2+}-levels.

Mean response of a field of neurons (n=12) loaded with fluo-3 and NP-EGTA. Following a 5 s application of 40 μM NMDA, Ca^{2+}-levels increased before decaying back to baseline levels. Following superfusion of 2 μM CCCP, resting Ca^{2+}-levels increased and remained at this elevated level for the remainder of the experiment (700 s).

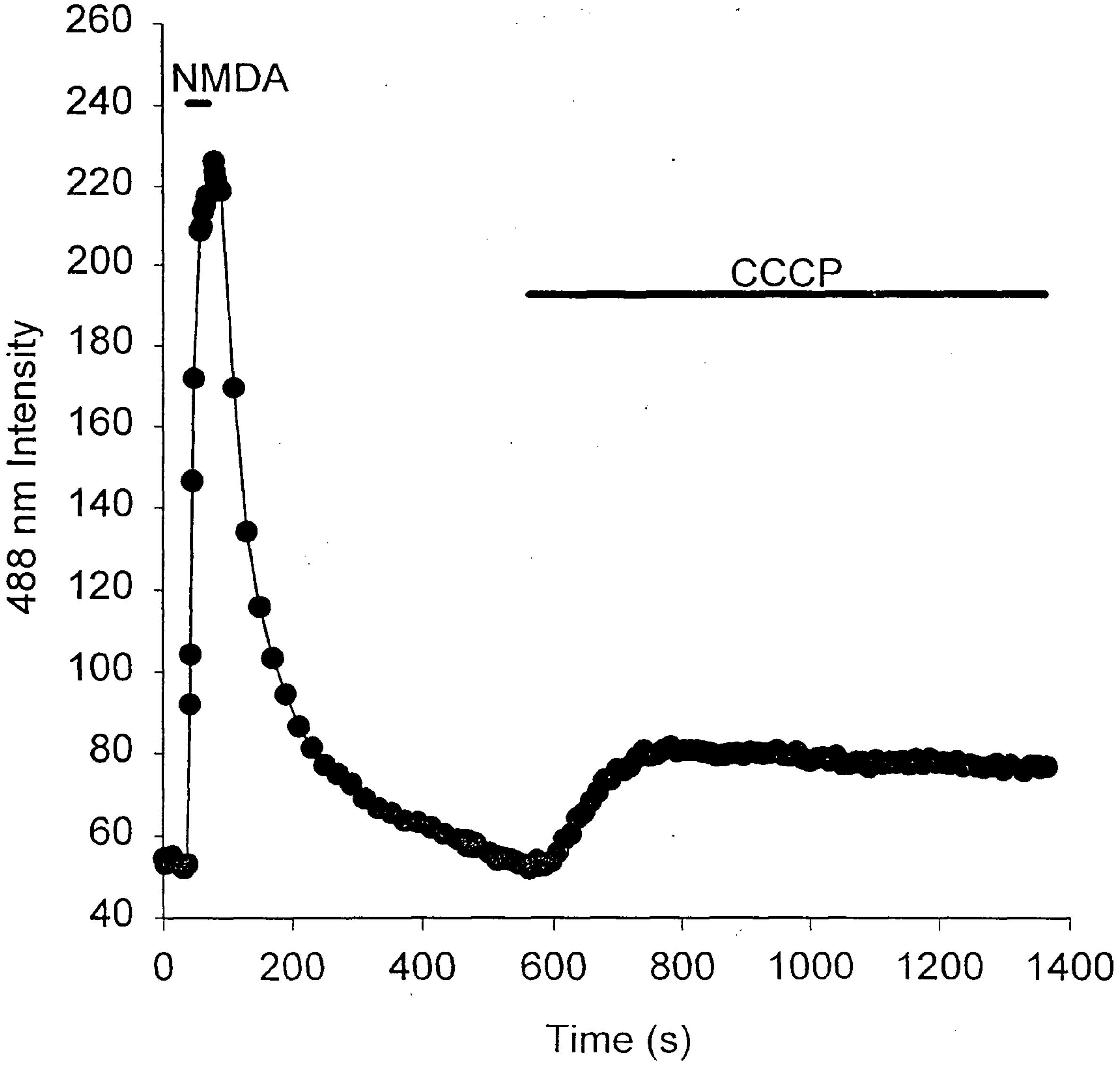
NMDA
CCCP
488 nm Intensity
260
240
220
200
180
160
140
120
100
80
60
40
0
200
400
600
800
1000
1200
1400
Time (s)

Figure 15: The effects of CCCP and CCCP + TMA on Ca^{2+}-levels

Mean response of a field of neurons (n=16) loaded with fluo-3 and NP-EGTA. Following a 5 s application of 40 µM NMDA, 2 µM CCCP was added to the superfusate. After 240 s in 2 µM CCCP, 2 mM TMA was added to the superfusate at which point Ca^{2+}-levels began to decay back to baseline values. Following 60 s of superfusion in TMA, 300 s in CCCP an uncage was performed (U). Background subtracted fluo-3 fluorescence values then decayed back to values similar to those seen immediately prior to photolysis.

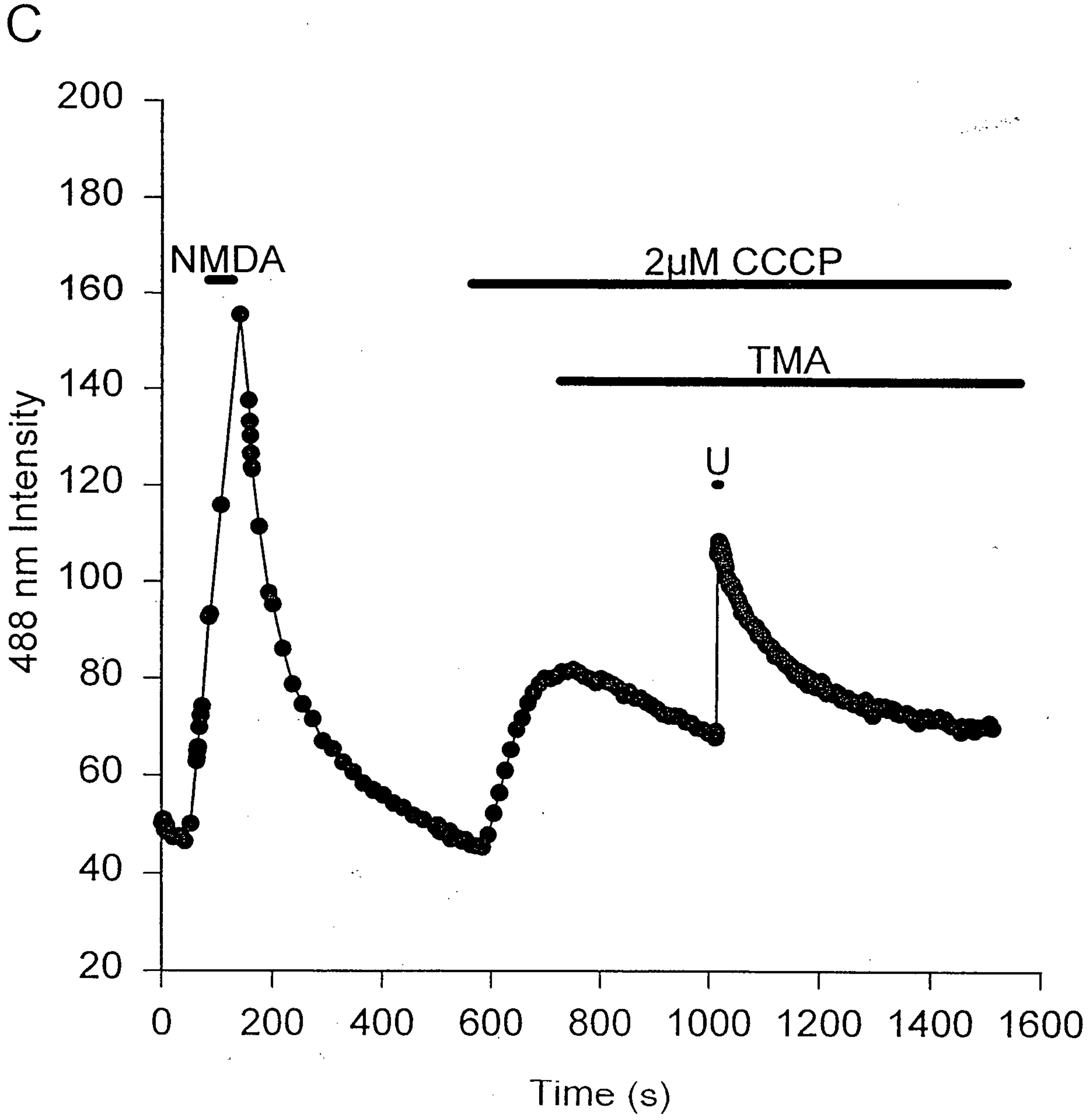
C
NMDA
2μM CCCP
TMA
U
488 nm Intensity
200
180
160
140
120
100
80
60
40
20
0
200
400
600
800
1000
1200
1400
1600
Time (s)

Figure 16: Background subtracted normalized data showing the influence of CCCP on Ca^{2+}-homeostasis.

Normalized mean response of two independent fields of neurons from sister cultures loaded with both fluo-3 and NP-EGTA. When 2 μM CCCP was superfused and pH_i was corrected for by the addition of 2 mM TMA (□) (n=7) the resulting decay curve was significantly slower than controls (o) (n=6). (□ and o represent actual data points while the solid line represents the best fit double exponential decay curve.)

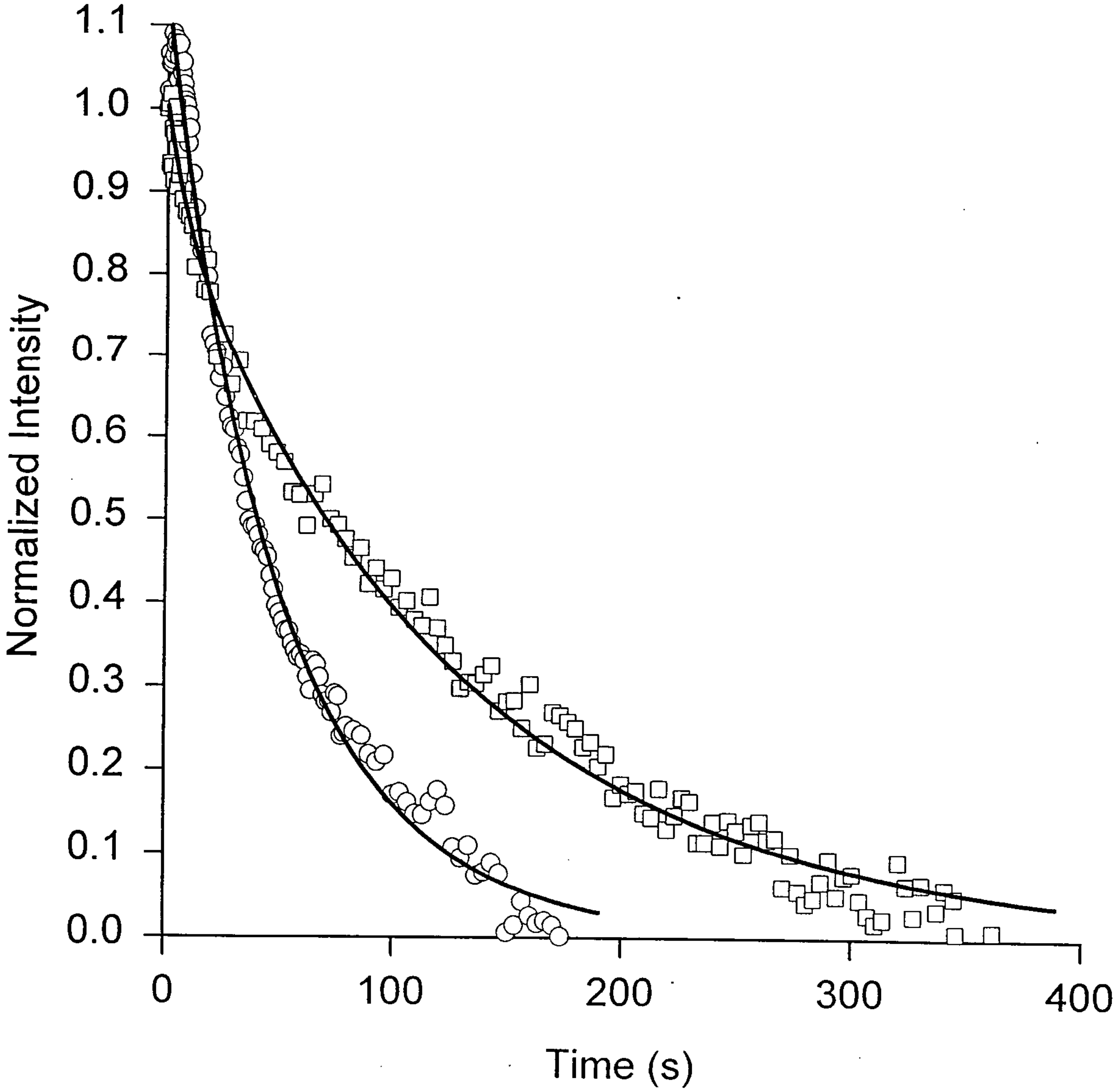
1.1
1.0
0.9
0.8
0.7
0.6
0.5
0.4
0.3
0.2
0.1
0.0
Normalized Intensity
0
100
200
300
400
Time (s)

(Fast-$p<0.001$, Slow- $p<0.001$, unpaired *t*-test) in the rate of recovery from a flash-photolysis-induced increase in $[Ca^{2+}]_i$ (see Table 3).

We also inhibited mitochondrial electron transport by superfusion of 5 μM rotenone (Budd and Nicholls, 1996). In 32 neurons, resting pH_i of 6.92 ± 0.02 remained at non-significantly different levels of 6.91 ± 0.02 after two minutes of rotenone superfusion (Fig. 17; paired *t*-test), at this point the uncage was performed. Unlike the effect of CCCP, rotenone alone had no effect on the baseline $[Ca^{2+}]_i$ and following flash photolysis of NP-EGTA, the $[Ca^{2+}]_i$ returned close to original resting levels (Fig. 18). Under these conditions we observed a significant prolongation in both the fast and slow component of the recovery (Fast-$p<0.05$, Slow-$p<0.001$, unpaired *t*-test) which is evident in the normalized data shown in Fig. 19 and Table 3.

V. Role of the ER-ATPase

In an attempt to assess the influence of Ca^{2+}-uptake into the ER following increases in $[Ca^{2+}]_i$ we superfused either 2 μM thapsigargin or 10 μM CPA in order to block the ER-ATPase (Mironov, Usachev and Lux, 1993; Bleakman, Roback, Wainer, Miller and Harrison, 1993; Seidler, Jona, Vegh, and Martonosi, 1989) or 20 μM ryanodine which, at this concentration, is sufficient to block ryanodine sensitive Ca^{2+} channels (Kiedrowski and Costa, 1995). Superfusion of thapsigargin, CPA, and ryanodine alone did not produce any significant changes in pH_i (Fig. 20, 21, 22). We found the results of these experiments to be highly variable and in some cases we even observed a small increase in the rate of recovery of fluo-3 fluorescence. However, we did not observe any consistent reduction in the rate of recoveries of either the fast or slow components.

Figure 17: The effect of rotenone on pH_i.

Mean response of a field of neurons (n=32) loaded with BCECF. Following the addition of 5 μM rotenone to the superfusate, pH_i began to slowly decrease. At (^) the uncage was performed to ensure that pH_i was at levels that were not statistically different from resting levels. Following 10 min of superfusion with rotenone, nigericin (10 μM) was added to the superfusate (*).

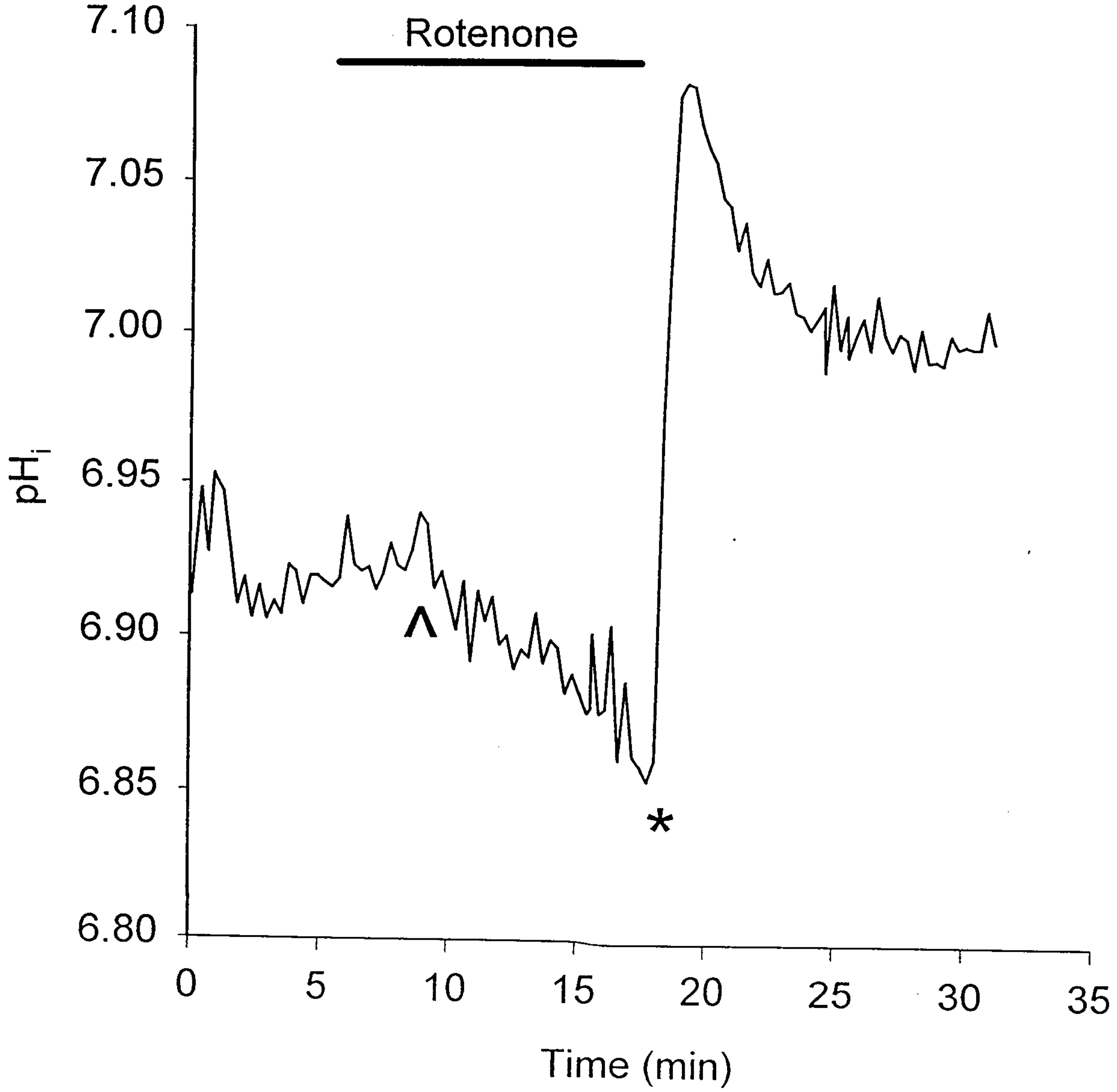
7.10
7.05
7.00
6.95
6.90
6.85
6.80
pH$_i$
Rotenone
^
*
0
5
10
15
20
25
30
35
Time (min)

Figure 18: The effect of rotenone on Ca^{2+}-levels.

Mean response of a field of neurons (n=10) loaded with both fluo-3 and NP-EGTA. Following a 5 s application of 40 μM NMDA, Ca^{2+}-levels returned to baseline values. At this point rotenone (5 μM) was added to the superfusate and 2 min later an uncage was performed (U). During rotenone superfusion, baseline intensities did not change and flash photolysis of NP-EGTA produced a large transient increase in intensity which returned to levels close to the initial baseline values.

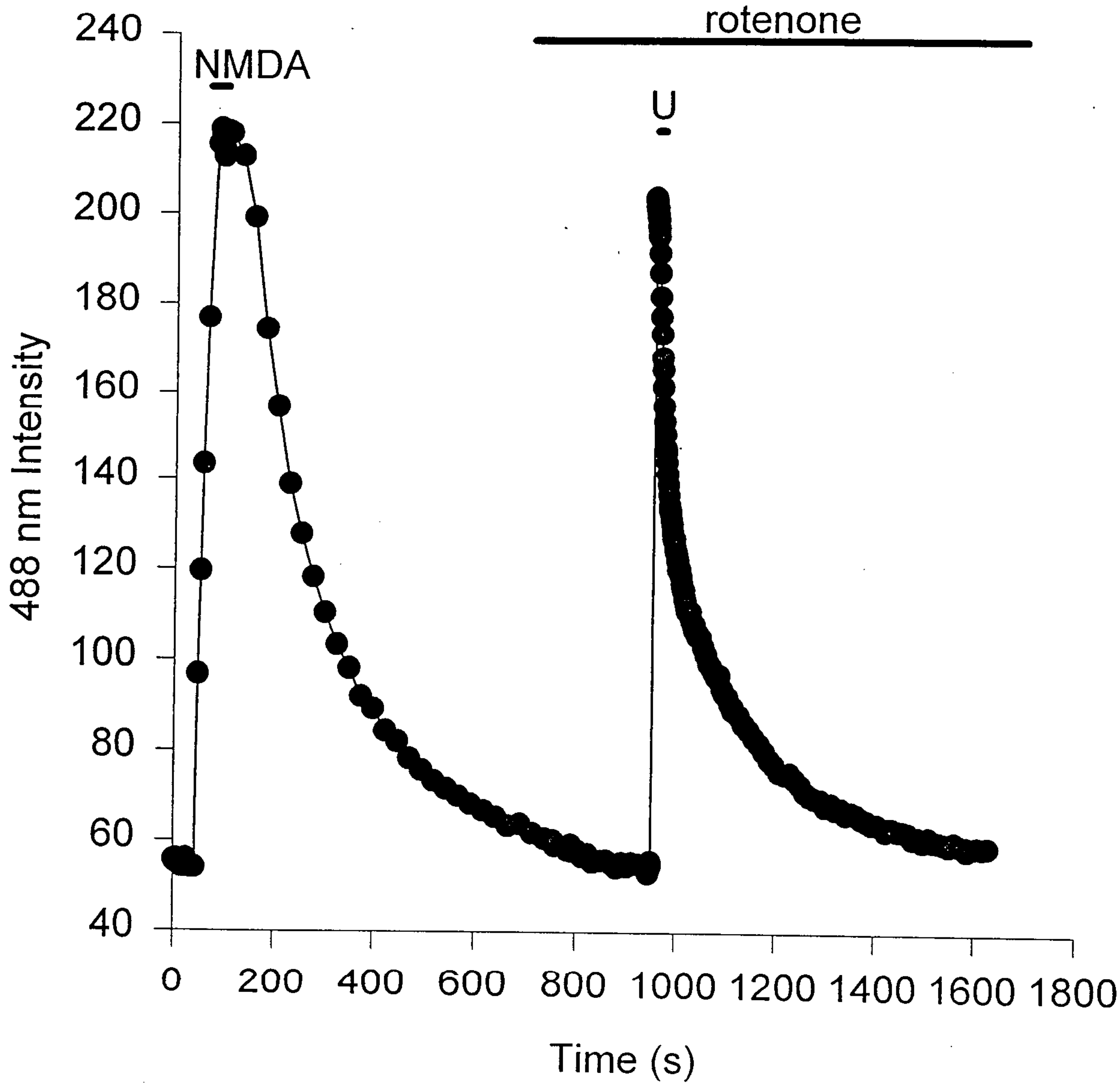
rotenone
NMDA
U
488 nm Intensity
240
220
200
180
160
140
120
100
80
60
40
0
200
400
600
800
1000
1200
1400
1600
1800
Time (s)

Figure 19: Background subtracted normalized data showing the influence of rotenone on Ca^{2+}-homeostasis.

Normalized mean response of two independent fields of neurons from sister cultures loaded with both fluo-3 and NP-EGTA. When 5 μM rotenone was superfused (□) (n=10) the resulting decay curve was significantly slower than controls (o) (n=16). (□ and o represent actual data points while the solid line represents the best fit double exponential decay curve.)

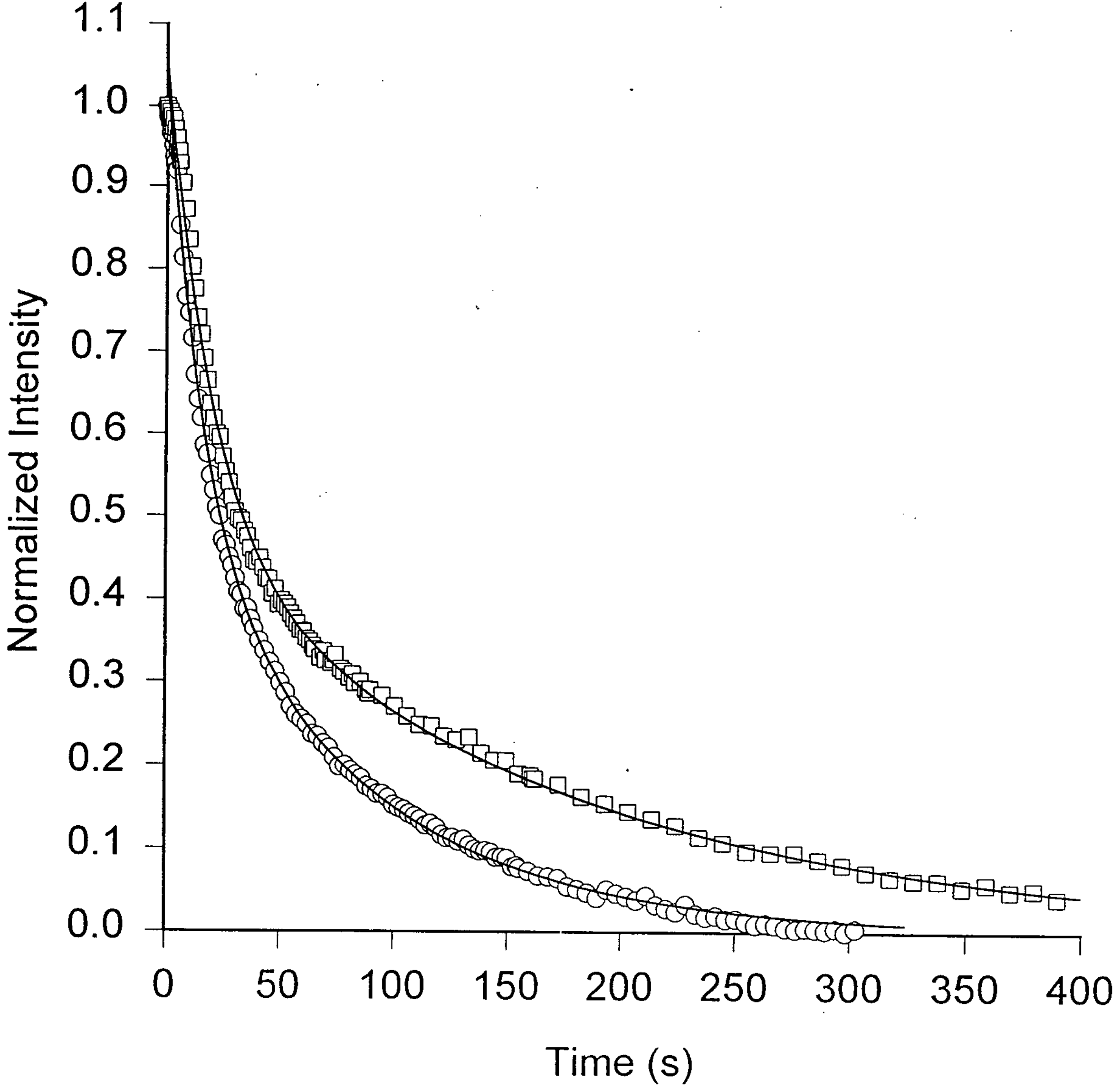
Normalized Intensity
1.1
1.0
0.9
0.8
0.7
0.6
0.5
0.4
0.3
0.2
0.1
0.0
0
50
100
150
200
250
300
350
400
Time (s)

Figure 20: The effect of thapsigargin on pH_i.

Mean response of a field of neurons (n=12) loaded with BCECF. pH_i was unaffected by the addition of 2 μM thapsigargin to the superfusate. Nigericin (10 μM) was added to the superfusate for calibration purposes (*).

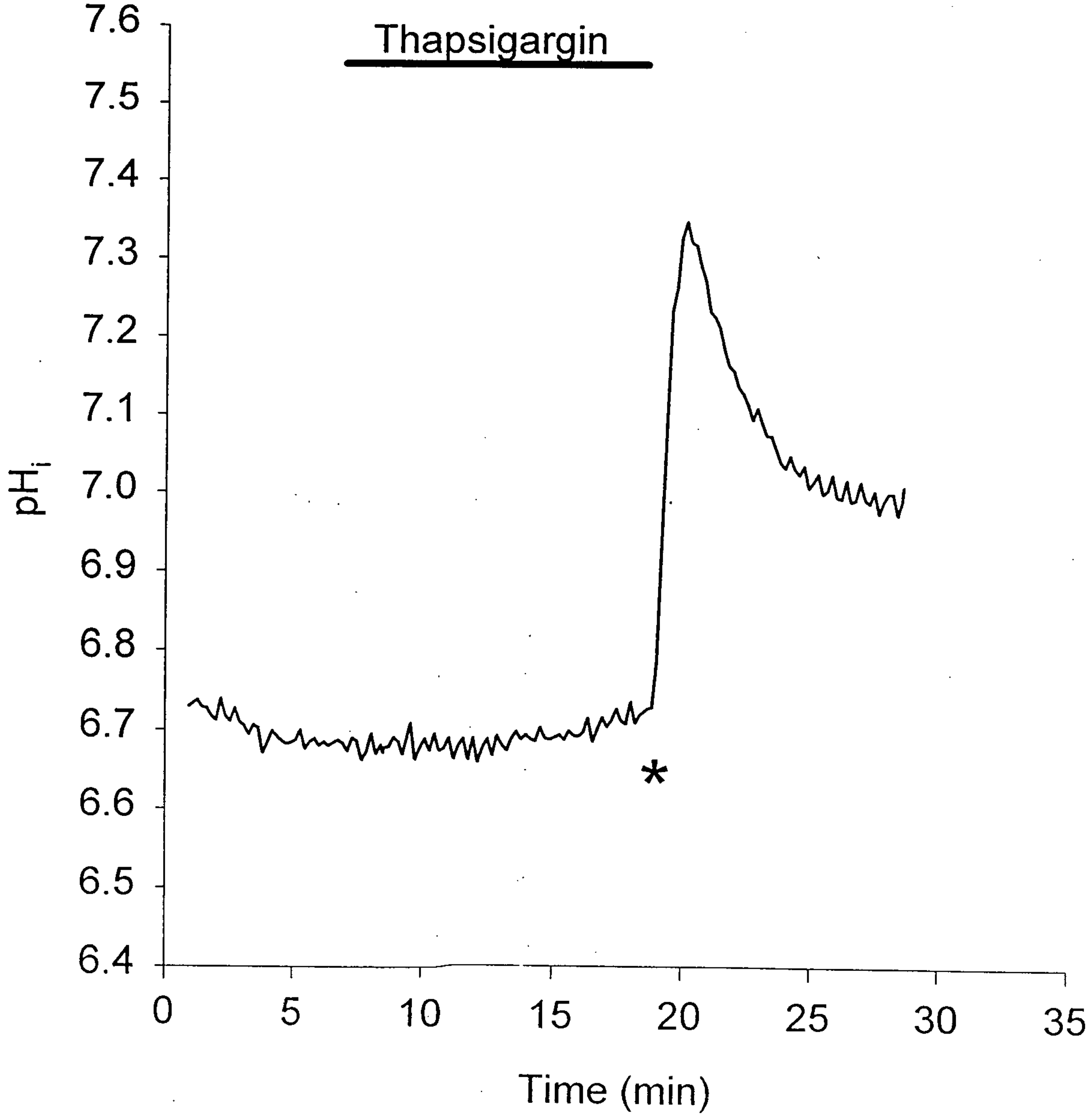
Thapsigargin
pH$_i$
7.6
7.5
7.4
7.3
7.2
7.1
7.0
6.9
6.8
6.7
6.6
6.5
6.4
*
0
5
10
15
20
25
30
35
Time (min)

Figure 21: The effect of CPA on pH$_i$.

Mean response of a field of neurons (n=13) loaded with BCECF. CPA (10 µM) was added to the superfusate for 10 minutes, during this time pH$_i$ was unaffected. Nigericin (10 µM) was added to the superfusate for calibration purposes (*).

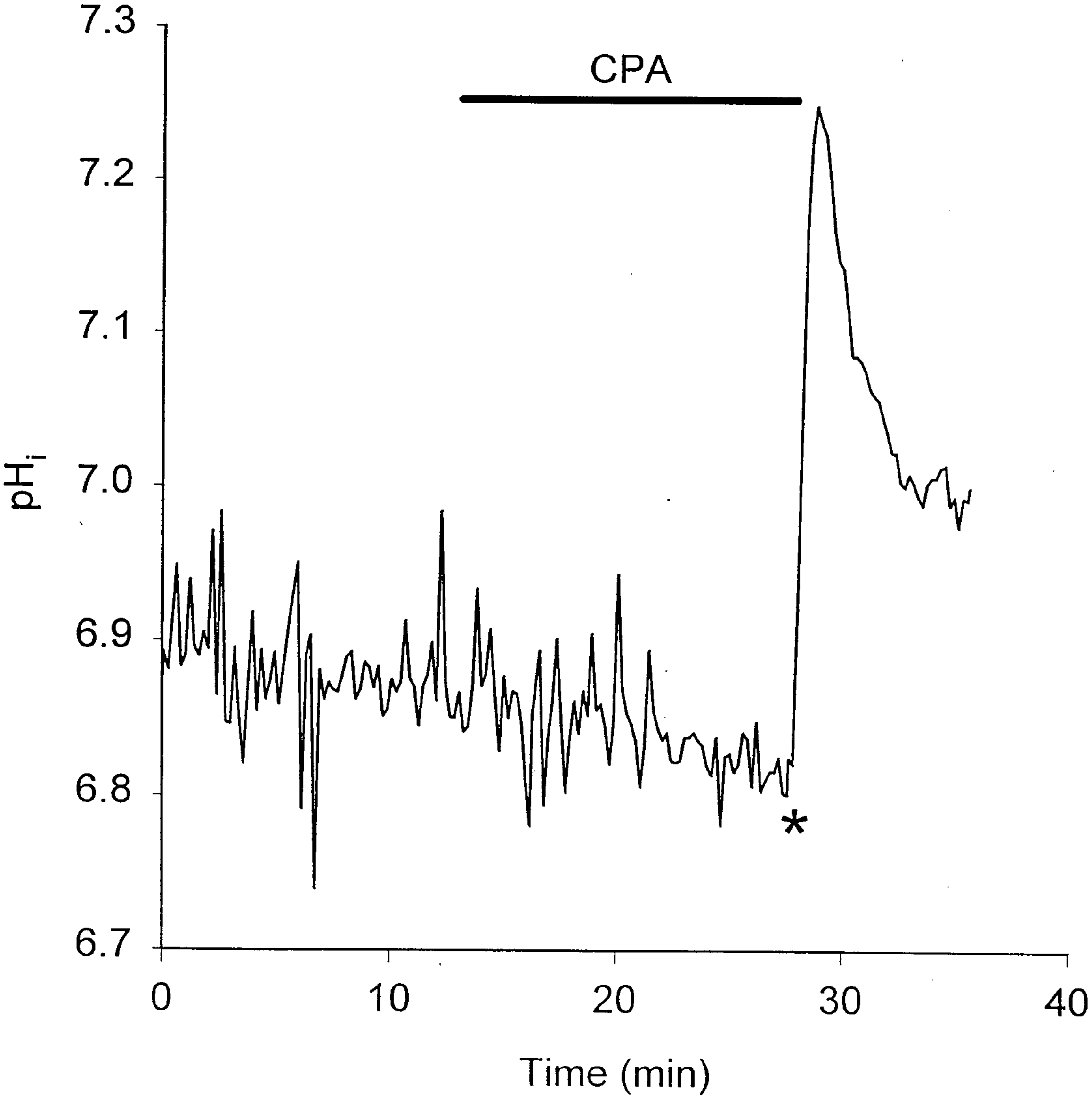
7.3
7.2
7.1
7.0
6.9
6.8
6.7
pH$_i$
CPA
*
0
10
20
30
40
Time (min)

Figure 22: The effect of ryanodine on pH_i.

Mean response of a field of neurons (n=29) loaded with BCECF. Ryanodine (20 μM) was added to the superfusate for 10 minutes, during this time pH_i was unaffected. Nigericin (10 μM) was added to the superfusate for calibration purposes (*).

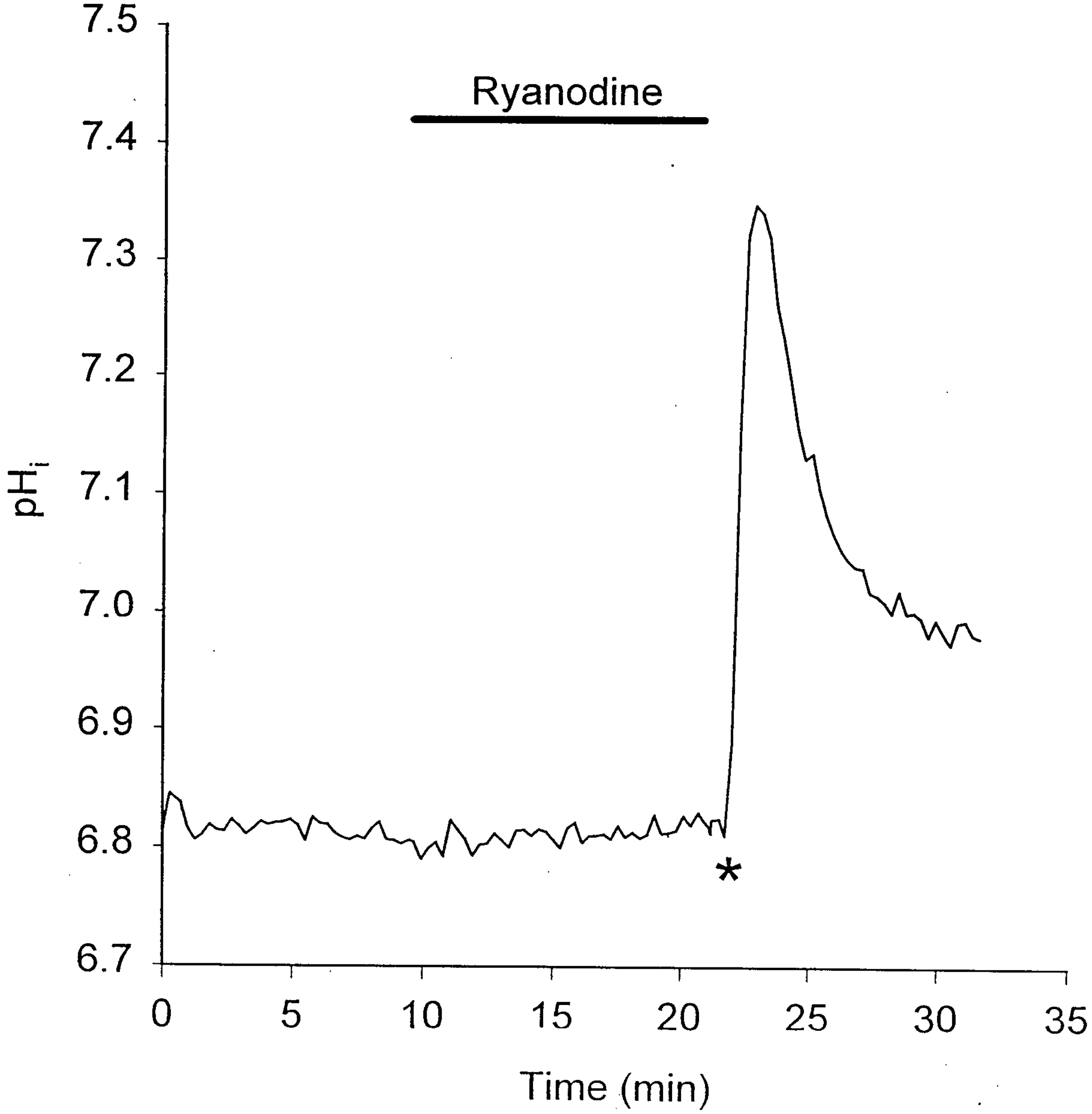
Ryanodine
pH$_i$
7.5
7.4
7.3
7.2
7.1
7.0
6.9
6.8
6.7
*
0
5
10
15
20
25
30
35
Time (min)

In view of the detrimental effects that changes in pH_i have on Ca^{2+}-homeostatic mechanism, attempts were made to 'clamp pH_i' using the K^+ ionophore nigericin (Fig. 23). In 19 neurons, following application of a high K^+/nigericin solution, Ca^{2+} levels increased as a result of plasma membrane depolarization and the resulting activation of VGCC. Following recovery to baseline $[Ca^{2+}]_i$, 40 μM NMDA was superfused for 5 s. In this situation, the observed responses were drastically different to those typically seen during NMDA application.

VI. Summary and statistical analysis of data

The following table lists the values obtained when individual Ca^{2+}-homeostatic mechanisms were inhibited prior to flash photolysis of NP-EGTA, the table lists the time constants for both the fast and slow components along with the statistical significance (students two-tailed unpaired ***t***-test) between experiments and controls:

Table 3: Statistical analysis of potential calcium homeostatic mechanisms

			FAST				SLOW	
	N	τ (s)	S.E.M.	SIG.		τ (s)	S.E.M.	SIG.
Control	33	15.82	1.37			57.12	4.20	
0 Na$^+$-NMDG	7	43.20	3.13	$p<0.001$		78.73	3.35	$p<0.001$
0 Na$^+$-NMDG + TMA	26	13.55	0.64	NS		66.70	5.62	NS
Control	10	7.49	1.03			27.86	1.69	
0 Na$^+$-Li$^+$ (4 min)	3	24.69	2.83	$P<0.05$		74.58	9.71	$p<0.05$
0 Na$^+$-Li$^+$ (12 min)	6	23.24	5.34	$P<0.05$		69.98	6.79	$p<0.001$
0 Na$^+$-Li$^+$ (25 min)	3	13.53	6.10	NS		44.07	2.45	$p<0.05$
0 Na$^+$-Li$^+$ (40 min)	2	11.15	1.41	NS		37.73	2.20	NS
Control	22	12.97	0.57			100.21	3.92	
CCCP	19	25.30	1.99	$p<0.001$		115.34	7.20	$p<0.05$
Control	11	15.62	2.47			62.22	1.94	
CCCP + TMA	3	36.63	4.86	$P<0.05$		102.85	7.93	$p<0.05$
CCCP + TMA + oligomycin	5	43.53	3.95	$p<0.001$		89.97	3.64	$p<0.001$
Control	16	14.94	0.92			79.93	1.58	
Rotenone	10	20.34	1.33	$P<0.05$		168.46	4.55	$p<0.001$

Figure 23: The effect of clamping pH_i using high K^+-nigericin during NMDA application.

Individual responses of 19 neurons loaded with both fluo-3 and NP-EGTA. A 5 s application of 40 μM NMDA produced a typical profile (see Fig. 1, 2, 3 for comparison) which subsequently decayed back to baseline values within 300 s. A high K^+-nigericin containing solution was then superfused for the remainder of the experiment. Following the depolarization of the plasma membrane and the subsequent entry of Ca^{2+} via voltage gated Ca^{2+}-channels, Ca^{2+}-levels decayed back to near resting levels. At this point 40 μM was applied for 5 s. The resulting responses were unlike any previously seen and many of the neurons did not recovery to baseline values during the next 300 s.

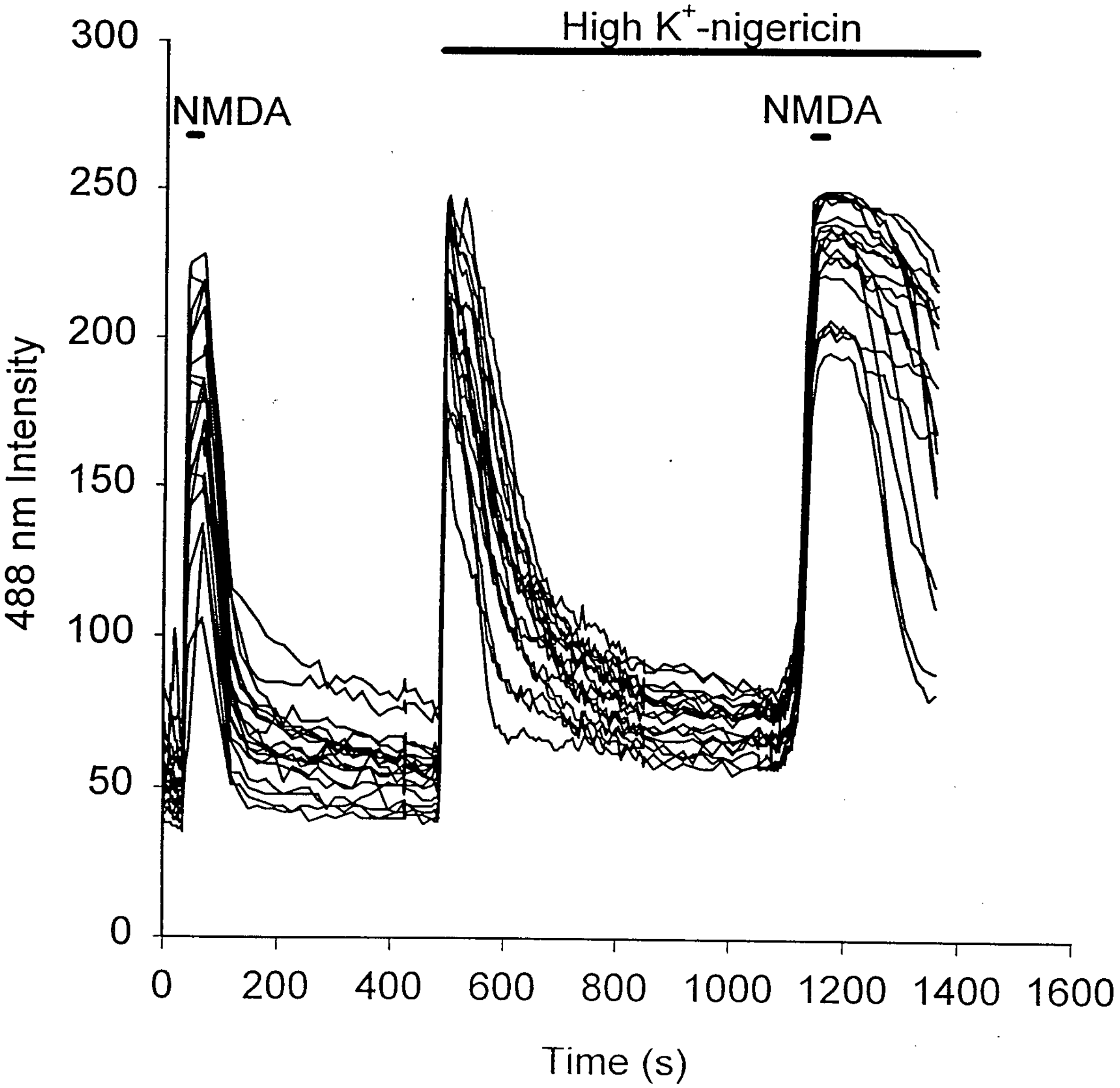
High K+-nigericin
NMDA
NMDA
488 nm Intensity
300
250
200
150
100
50
0
0
200
400
600
800
1000
1200
1400
1600
Time (s)

DISCUSSION

The aim of this study was, firstly, to develop a procedure to increase $[Ca^{2+}]_i$ using the caged Ca^{2+}-compound NP-EGTA, and secondly, to examine the potential Ca^{2+}-homeostatic mechanisms responsible for reducing background subtracted fluo-3 levels back to baseline values following flash photolysis of NP-EGTA. Because of the interrelationship between $[Ca^{2+}]_i$ and pH_i, and the potential effects of experimental manipulations on the latter, this study sought to maintain pH_i at a constant level thereby eliminating any of the effects that changes in pH_i have on Ca^{2+}-homeostatic mechanisms and fluorescent indicator dyes. The effects of drugs or ion substitutions on pH_i were compensated for by the addition of the appropriate amount of the weak base TMA determined using the pH sensitive dye BCECF in sister cultures. Of the Ca^{2+}-homeostatic mechanisms examined, only the inhibition of mitochondrial Ca^{2+}-uptake, by the protonophore CCCP and the electron transport chain inhibitor rotenone, significantly reduced the rate of recovery from Ca^{2+}-loads induced by flash photolysis of NP-EGTA. Inhibition of all other potential mechanisms (PM-Na^+/Ca^{2+} exchanger, PM-ATPase or ER-ATPase) failed to have any significant effect on the rate of recovery of Ca^{2+}-levels providing that pH_i was either maintained or restored to normal baseline values with the weak base TMA.

Loading with NP-EGTA and fluo-3

In order to induce increases in $[Ca^{2+}]_i$ and record the subsequent Ca^{2+}-decay curve, a method had to be developed which allowed for the co-loading of appropriate amounts of the caged Ca^{2+}-compound NP-EGTA and fluorescent indicator fluo-3. In order to determine the correct levels of fluo-3 to allow for both baseline and peak $[Ca^{2+}]_i$ determination with minimal influences on the Ca^{2+} decay curve, many empirical trials were performed with various loading times and concentrations (see Table 1). As fluo-3 has a relatively high K_d for Ca^{2+} (~ 80 nM), low levels could not be used as the signal from cells with low resting $[Ca^{2+}]_i$ would be undetectable. Similarly, high levels were not suitable as firstly, the mobile Ca^{2+}-buffering capacity of the cytosol would be altered thereby influencing the kinetics of the Ca^{2+}-decay curve and secondly, the fluo-3 fluorescence signal following photolysis would most likely saturate the camera thereby misjudging peak $[Ca^{2+}]_i$ along with the initial portions of the Ca^{2+}-decay curve (Ellis-Davies and Kaplan, 1994; Nerbonne, 1996). Loading parameters were therefore set at a level such that the neuronal Ca^{2+} buffering capacity was minimized while at the same time Ca^{2+}-levels were detectable in all neurons, even those with low resting $[Ca^{2+}]_i$.

Similar to the effects of fluo-3 on the neuronal calcium buffering capacity, unphotolyzed NP-EGTA, as discussed by Lamb and Stephenson (1995), may rebind Ca^{2+} thereby influencing the kinetics of the Ca^{2+}-decay curve; this problem will only be solved with the creation of caged Ca^{2+}-compounds with much higher affinities for Ca^{2+} (in the range of 1-10 nM) such that the majority of the chelator is bound to Ca^{2+} prior to photolysis (Nerbonne, 1996). In order to minimize this effect of NP-EGTA, the loading parameters were set at a level such that, firstly, following flash photolysis, significant increases in intracellular Ca^{2+}-levels were obtained, but secondly, that following flash photolysis the majority of the NP-EGTA present within the cytosol would be photolyzed thereby minimizing the influences of unphotolyzed NP-EGTA on the mobile Ca^{2+}-buffering capacity of the cytosol. This was partially achieved with the use of a 0.4 s flash of UV light despite the fact that the release of Ca^{2+} from NP-EGTA occurs within 200 μs (Nerbonne, 1996). By markedly increasing the required photolysis time, it was possible to ensure that the majority of the NP-EGTA within each neuron was photolyzed and, as a result, could not bind with Ca^{2+} and thereby influence the mobile Ca^{2+}-buffer capacity of the cytosol (see Fig. 2).

Empirical trials were also performed in order to determine the appropriate levels of NP-EGTA needed to produce moderate increases in $[Ca^{2+}]_i$ while at the same time minimizing the influences of NP-EGTA on the Ca^{2+}-buffering capacity of the cytoplasm. If high concentrations of NP-EGTA were used for loading, the increase in $[Ca^{2+}]_i$ following photolysis greatly exceeded the peak $[Ca^{2+}]_i$ reached during a 5 s application of 40 μM NMDA, suggesting that this increase in $[Ca^{2+}]_i$ was excessive in nature (data not shown). Determination of the appropriate loading conditions was further complicated by the relationship between caged compounds and fluorescent indicator dyes; the sensitivity of the fluorescent dye is changed depending on the concentration of the caged compound used and the ratio of the caged compound to fluorescent indicator (Zucker, 1992). As a result the relative amounts of fluo-3 and NP-EGTA were determined empirically to account for this phenomenon. The final loading concentrations of fluo-3-AM and NP-EGTA-AM were 3.1 μM and 8 μM respectively. Loading was for 1 hour at room temperature and photolysis was induced by a 0.4 s flash of unfiltered UV light.

NP-EGTA as a method for increasing $[Ca^{2+}]_i$

There are a number of properties of caged Ca^{2+}-compounds which have to be taken into consideration when they are used in an intracellular environment. These include their sensitivity to pH, their affinity for Ca^{2+} and selectivity of Ca^{2+}-binding with respect to other ions, especially Mg^{2+}, the relative binding of the native molecules with respect to their photolysis products, and the quantum yield for Ca^{2+} release (i.e. the proportion of caged Ca^{2+}-compound photolysed by UV light). DM-nitrophen, a derivative of the Ca^{2+}-chelator EDTA, has a high affinity for Ca^{2+}, a high quantum yield (0.18), and, following flash photolysis, the resulting products have a 6.0 x 10^5 fold decrease in the affinity for Ca^{2+}. However, it shares with its parent molecule EDTA, a high sensitivity to changes in pH and a high affinity for Mg^{2+}. Nitr-5, a derivative of BAPTA, is much more selective for Ca^{2+} over Mg^{2+}, is relatively insensitive to changes in pH, but has a relatively low affinity for Ca^{2+}, a low quantum yield (0.02), and only a 42-fold decrease in the affinity of the photolysis products for Ca^{2+}. When using nitr-5 to increase $[Ca^{2+}]_i$, it was apparent that significant increases in $[Ca^{2+}]_i$ were reached only when high levels of $[Ca^{2+}]_i$ were present immediately preceding photolysis (see Fig. 4); this is most likely due to the relatively high K_d of nitr-5 for Ca^{2+}. As a result it was necessary to utilize a caged Ca^{2+}-compound with much higher affinities for Ca^{2+}such that a larger percentage of the compound would be bound to Ca^{2+} prior to photolysis thereby negating the post-photolysis influences on the mobile Ca^{2+}-buffering capacity of the cytosol.

NP-EGTA, a relatively new caged Ca^{2+} compound, meets a number of important criteria not previously attained by nitr-5 or DM-nitrophen (Ellis-Davies and Kaplan, 1994; Nerbonne, 1996). NP-EGTA has a much lower affinity for Mg^{2+}, its flash photolysis products have a 1.2 x 10^4 fold decrease in affinity for Ca^{2+} and it has a high quantum yield (0.23). In addition, because it has a K_d close to the resting $[Ca^{2+}]_i$ of most cells (~ 80 nM in our neurons), at least 50% of the molecules would be in the Ca^{2+}-bound form thereby minimizing the post-photolysis effects on the mobile Ca^{2+}-buffering capacity of the cytosol. These properties have proved to be useful under physiological conditions, and flash photolysis of NP-EGTA has been previously used to induce successfully the endocytosis of secretory granules in mouse pancreatic β-cells (Eliasson *et al.*, 1996), contract chemically skinned skeletal muscle fibres in rabbit (Ellis-Davies and Kaplan, 1994), and induce exocytosis in rat pituitary melanotrophs (Parsons *et al.*, 1996).

In our experiments we have used NP-EGTA to assess neuronal Ca^{2+}-homeostasic mechanisms, and for this purpose there are many potential advantages over more traditional methods of increasing $[Ca^{2+}]_i$ such as the activation of VGCC or LGCC. Firstly, NP-EGTA can be loaded as an AM-ester and, after crossing the plasma membrane, is cleaved into free NP-EGTA which subsequently binds Ca^{2+} and equilibrates with the prevailing free Ca^{2+} concentration within the neuron. This is a useful property for the study of multiple cells simultaneously, especially when the preparation consists of multiple phenotypes as is the case with primary cultures of rat hippocampal neurons. Secondly, the release of Ca^{2+} as a result of photolysis is extremely rapid (< 200 μs) and the recovery following flash photolysis can be measured in the absence of any further influx (Nerbonne, 1996). Thirdly, NP-EGTA is freely diffusible and distributes evenly within the cytoplasm. The release of Ca^{2+} will therefore be uniform throughout the cytoplasm and large Ca^{2+}-gradients typically seen when increasing $[Ca^{2+}]_i$ via traditional methods (VGCC or LGCC) will be avoided. Fourthly, increasing Ca^{2+} via VGCCs and LGCCs results in relatively slow increases in $[Ca^{2+}]_i$ with continued Ca^{2+}-influx occurring at the same time as neuronal Ca^{2+}-homeostasic mechanisms being activated, an effect not seen with the use of NP-EGTA. Additionally, as previously mentioned, depending on the method used to increase $[Ca^{2+}]_i$, different Ca^{2+}-homeostatic mechanisms may be activated (White and Reynolds, 1995).

In addition to these advantages, with the use of NP-EGTA the 'nature' of the stimuli is unchanged between experiments and controls, and the Ca^{2+}-load will be very similar in both situations. For example, following replacement of all external-Na^+ with NMDG, two changes become apparent; firstly, pH_i decreases and secondly, the normal entry of Na^+ through LGCC, following application of NMDA, is absent. As a result, the Ca^{2+}-load induced in Na^+-free conditions differs from control situations not only as a result of the influences of pH_i on intracellular constituents but also as a result of the lack of Na^+ influx through VGCC or LGCC. This Na^+ influx will, in turn, influence $[Ca^{2+}]_i$ by way of a destabilization of Ca^{2+}-homeostatic mechanisms, in particular the PM-Na^+/Ca^{2+}exchanger (Kiedrowski *et al.*, 1994). In an attempt to minimize this influence, White and Reynolds (1995) applied 0 Na^+ solutions immediately following the application of high K^+ or glutamate but the timing involved in this procedure is virtually impossible to coordinate and, as a result, would not be reproducible between experiments.

Despite NP-EGTA being a marked improvement over other methods of increasing $[Ca^{2+}]_i$, there are some potential flaws in its use as a means of examining Ca^{2+}-homeostatic mechanisms. The homogeneous increase in $[Ca^{2+}]_i$, while allowing for an accurate assessment of Ca^{2+}-homeostatic mechanisms, is substantially different from the spatio-temporally graded signal that a neuron normally receives on activation of VGCC or LGCC. Those regions which receive higher amounts of Ca^{2+}-entry typically contain higher proportions of Ca^{2+}-homeostatic mechanisms as compared with regions with lower influx and, as a result, not all neuronal regions will be equipped to handle a global increase in $[Ca^{2+}]_i$ (Tymianski *et al.*, 1993; Rizzuto *et al.*, 1994; Reuter and Porzig, 1995; Stauffer *et al.*, 1997). The preferential location of the Na^+/Ca^{2+} exchanger in the synaptic regions of dendrites in hippocampal neurons is one example (Reuter and Porzig, 1995; Luther *et al.*, 1992). A second potential flaw is that the flash of light used for photolysis of NP-EGTA may not be constant between experiments, the intensity will change as the mercury arc-lamp ages and is replaced. These changes will influence the amount of Ca^{2+} released following photolysis and may not allow for reproducible results, particularly when comparing results obtained with a new rather than an old arc-lamp. Also, NP-EGTA, like its parent molecule EGTA, is pH sensitive, and a normal pH_i range must be maintained for NP-EGTA to be useful (Kao, 1994). Finally, the Ca^{2+}-buffering capacity of the cytosol will be influenced by both NP-EGTA and fluo-3. This problem is inherent with the use of all caged Ca^{2+}-compounds and fluorescent indicator dyes, but, by using the lowest concentration possible of both these compounds while still maintaining the capability to record accurate signals, even in those neurons with low resting $[Ca^{2+}]_i$, these influences were minimized.

While recognizing the influence of both NP-EGTA and fluo-3 on intra-neuronal Ca^{2+}, the use of day-matched controls for each experimental condition ensures that these effects are constant and other Ca^{2+}-homeostatic mechanisms can be measured in their presence. The other problems associated with the use of NP-EGTA, pH sensitivity and bulb aging, were both minimized by maintaining pH_i at a constant level with the use of TMA and by performing day and coverslip matched controls.

In order to obtain an accurate assessment of both baseline $[Ca^{2+}]_i$ and $[Ca^{2+}]_i$ following flash photolysis of NP-EGTA, the ratiometric dye fura-2 was used. Resting $[Ca^{2+}]_i$'s were found to be ~ 80 nm, consistent with values previously obtained in similar cultures (Abdel-Hamid and Baimbridge-submitted; Abdel-Hamid and Baimbridge-in press), and following photolysis, the peak $[Ca^{2+}]_i$ reached values ~ 800 nm, depending on the duration of the flash. Unfortunately, several problems exist with the use of fura-2 and NP-EGTA concurrently. Firstly, fura-2 is excited and bleached by the same wavelengths of light used to photolyse NP-EGTA and, conversely, the excitation of fura-2, may increase $[Ca^{2+}]_i$ by releasing Ca^{2+} from NP-EGTA (Zucker, 1992; Adams and Tsien, 1993). This continuous release of Ca^{2+} when measuring $[Ca^{2+}]_i$ with fura-2, may explain the minimal increases in $[Ca^{2+}]_i$ seen following flash photolysis of NP-EGTA, a large percentage of the Ca^{2+} held by NP-EGTA may have already been released (see Fig 5). Similarly, resting $[Ca^{2+}]_i$ may have been artificially raised by the continuous release of Ca^{2+} from NP-EGTA during fura-2 excitation. In order to demonstrate that significant increases in $[Ca^{2+}]_i$ could be reached with the concurrent use of fura-2 and NP-EGTA, neurons (loaded with fura-2 and NP-EGTA) were exposed to UV light for 0.5 s. This produced larger increases in $[Ca^{2+}]_i$, following photolysis, than were previously seen using a 0.4 s flash and further demonstrates that when imaging Ca^{2+}, using fura-2, in neurons loaded with NP-EGTA, the excitation wavelengths used for fura-2 release NP-EGTA from its cage, thereby decreasing the amount of NP-EGTA available for photolysis. As a result of the problems associated with the concurrent use of fura-2 and NP-EGTA, fura-red, which is excited at much longer wavelengths, was also utilized. This permitted the photolysis of NP-EGTA without any adverse effects on fura-red or, conversely, the excitation of fura-red without releasing Ca^{2+} from NP-EGTA. Using fura-Red, baseline $[Ca^{2+}]_i$ were found to be ~ 100 nM consistent with those obtained previously in identical neuronal cultures and peak $[Ca^{2+}]_i$ were found to be ~ 900 nM consistent with the physiological increases seen during a 5 s application of 20 μM NMDA (Abdel-Hamid and Baimbridge-submitted). For the majority of experiments, the single wavelength dye fluo-3 was used to assess $[Ca^{2+}]_i$. Reasons for using fluo-3 include, firstly, the excitation wavelength used for fluo-3 does not photolyze NP-EGTA, secondly, the marked lack of an effect that caged Ca^{2+}-compounds have on fluo-3 as opposed to ratiometric dyes (Zucker *et al.*, 1992; Hadley *et al.*, 1993), and thirdly, the much higher data acquisition rate of fluo-3 over ratiometric dyes allowing for much more accurate assessments of the kinetics of Ca^{2+}-decay curves.

Rates of recovery of [Ca^{2+}]$_i$ at 22° and 37° C

Decay curves recorded at 37 °C could always be resolved into double exponentials with fast and slow components which were similar but faster than those seen at room temperature, most likely reflecting increased enzymatic reaction speeds at higher temperatures. As temperature increases, the relative speed of a particular Ca^{2+}-homeostatic process will increase depending on its Q_{10} value (the fold increase in rate for a 10 °C increase in temperature). As a result it might have been possible to assign either the fast or the slow component to a particular homeostatic mechanism if the decrease in decay rates of one of the components, with increasing temperature, could be correlated to the Q_{10} value of a particular Ca^{2+}-homeostatic mechanism. For example it is known that the rate constant for mitochondrial Ca^{2+}-uptake increases by 60 % from 22 - 37 °C (Marengo *et al.*, 1997). However, numerous other factors are influenced by changes in temperature. For example, the K_d for Ca^{2+} of EGTA and BAPTA, the two principal compounds used to produce fluorescent Ca^{2+}-indicator dyes, are very temperature sensitive (Harrison and Bers, 1987). Additionally, the amount of Ca^{2+} released from NP-EGTA following flash photolysis would be different at room temperature versus 37 °C as a result of the temperature sensitivity of the binding of NP-EGTA to Ca^{2+}, and the kinetics of Ca^{2+}-transients has been shown to be altered at different temperatures (Shuttleworth and Thompson, 1991). As a result of the multitude of factors influenced by temperature, we have not attempted to assign either the fast or the slow component to a particular Ca^{2+}-homeostatic mechanism on the basis of differences in recovery rates recorded at different temperatures. Nonetheless, we can conclude that Ca^{2+}-decay curves are best-fit by a double exponential at both 37 °C and room temperature, and that the interpretation of our data collected mostly at room temperature is relevant to mechanisms active at 37 °C.

The influence of pH on Ca^{2+}-homeostatic mechansims

Intracellular pH (pH_i) in the majority of cell types is kept constant within the range of 6.8 to 7.2 (Putnam, 1995). Any prolonged deviations from this range are known to result in cellular toxicity and/or cellular death (Kraig *et al.*, 1987). In neurons, changes in pH_i have been shown to affect the activity of many enzymes and ion channels, the activities of VGCC and LGCC and the excitability of neurons (Chesler and Kaila, 1992). Additionally, cytoskeletal elements (cell shape and motility), cell-cell coupling, and membrane conductance are all dependent upon pH_i (Putnam, 1995). Of particular importance to the present study is the influences of pH_i on Ca^{2+}-regulatory mechanisms within neurons. For example, lowering pH_i inhibits the PM-ATPase (Carafoli, 1987), decreases the affinity of Ca^{2+}-binding proteins for Ca^{2+} (Ingersoll and Wasserman, 1971) and decreases mitochondrial Ca^{2+}-uptake (Gambassi *et al.*, 1993). Additionally, fluo-3, the fluorescent indicator dye used in this study, is very sensitive to changes in pH_i and its K_d for Ca^{2+} increases significantly (i.e. becomes less sensitive) as acidity increases (Martínez-Zaguilán *et al.*, 1996). Furthermore, as previously demonstrated by Koch and Barish (1994), intracellular acidification alone resulted in a greater than two-fold increase in the time required for $[Ca^{2+}]_i$ to return to baseline levels.

In many previous reports describing the Ca^{2+}-homeostatic mechanisms of living cells, the influences of ion substitutions or drugs on pH_i have been overlooked. For example, a common experimental method for inhibiting the Na^+/Ca^{2+} exchanger involves replacing all external Na^+ with either Li^+ or NMDG. On the basis of these experiments it has been concluded that the Na^+/Ca^{2+} exchanger contributes to the restoration of Ca^{2+} levels back to baseline values following relatively long (10-15 s) exposures to either high K^+ (Mironov *et al.*, 1993; Friel and

Tsien, 1994) or 3 μM glutamate (White and Reynolds, 1995). Our experiments clearly demonstrate one of the problems with this interpretation is that removing external Na^+ results in an intracellular acidification due to the inhibition of the Na^+/H^+ exchanger, which is an important acid extrusion mechanism in central neurons, exchanging one intracellular H^+ with one extracellular Na^+ (Schlue and Dörner, 1992; Koch and Barish, 1994; Baxter and Church, 1996; Bevensee *et al.*, 1996).

White and Reynolds (1995) suggested that replacement of Na^+ with Li^+ would not reduce pH_i, but, as we clearly show, this is not the case in our neuronal preparations. The effect of Li^+ substitution on pH_i are in fact time dependent. Initially there is a substantial fall in pH_i but, unlike substitution with NMDG, the pH_i slowly rises over a period of 30 minutes (Fig. 10). This delayed recovery of pH_i is a result of Li^+ being able to substitute for Na^+ in the Na^+/H^+ exchanger (Aronson, 1985). Additionally, White and Reynolds (1995) assumed that by adding HCO_3^- to a Na^+-free media (Na^+ replaced by NMDG) pH_i would be maintained due to the activity of the HCO_3^-/Cl^- exchanger, unfortunately they provided no evidence concerning the importance of the HCO_3^-/Cl^- exchanger in the control of pH_i in their neuronal cultures. Further evidence demonstrating the lack of concern over pH_i levels comes from experiments by Benham *et al.* (1992) and Mironov (1995) who both superfused pH 8.8 solutions in order to inhibit the Ca^{2+}-ATPase. While the Ca^{2+}-ATPase would undoubtedly be inhibited, these high pH solutions would also increase pH_i, influencing many intracellular constituents (fluorescent indicator dyes and Ca^{2+} homeostatic mechanisms), along with Ca^{2+}-entry via NMDA channels, thereby producing uninterpretable and confusing results (Tang *et al.*, 1990; Traynelis and Cull-Candy, 1990; Takadera *et al.*, 1992; Gottfried and Chesler, 1994).

We attempted to use the K^+ ionophore nigericin to clamp pH_i at a constant level in order to avoid the superfusion of TMA required to restore pH_i to resting levels following ion substitution or drug superfusion. However, nigericin superfusion increased $[Ca^{2+}]_i$ as a result of membrane depolarization due to the high K^+ solution and the concurrent activation of VGCC (see Fig. 24). While the neurons were being continually superfused with high K^+/nigericin, 40 μM NMDA was applied for 5 s. In this situation, the response observed was markedly different than that typically seen during NMDA application. In particular, in many neurons $[Ca^{2+}]_i$ did not return back to baseline values and for those neurons where some recovery in $[Ca^{2+}]_i$ did occur, the rate was greatly prolonged.

The role of the PM-Na⁺/Ca²⁺ exchanger

When the Na^+/Ca^{2+} exchanger was inhibited, under conditions in which the concomitant effects of pH_i are corrected for using TMA, we found no significant effect upon the rate of recovery of $[Ca^{2+}]_i$ following its release from NP-EGTA. Similar results were found when Na^+ was replaced by Li^+ (Table 3). Our results are in agreement with those of Benham *et al.* (1989), Duchen *et al.* (1990), Thayer and Miller (1990), Bleakman *et al.* (1993) and Stuenkel (1994), who all concluded that the PM-Na^+/Ca^{2+} exchanger was not important in reducing Ca^{2+}-loads in neurons. While the failure to take into account the effects on pH_i may explain the opposite conclusion reached by Mironov *et al.* (1993) and White and Reynolds (1995), it is possible that the contribution of PM-Na^+/Ca^{2+} exchange to Ca^{2+}-homeostasis varies considerably depending upon the particular neuronal phenotype. Indeed, White and Reynolds (1995), using cultured rat forebrain neurons, reported considerable variability in the degree of dependence of the PM-Na^+/Ca^{2+} exchanger in the recovery of an increase in $[Ca^{2+}]_i$ in individual neurons resulting from glutamate stimulation. Amiloride and its analogues, currently the most specific inhibitors for the

Na^+/Ca^{2+} exchanger, were not used as these compounds also inhibit the Na^+/H^+ exchanger and are fluorescent at wavelengths similar to those used in the excitation of fluo-3 (White and Reynolds, 1995).

Experiments in which Na^+ was replaced with Li^+ were particularly revealing in that the effects of Li^+ on pH_i are in fact time dependent. Initially there is a substantial fall in pH_i but, unlike substitution with NMDG, the pH_i does slowly recover and this recovery is more rapid and complete if experiments are performed at 37°C (Baxter and Church, 1996). We observed an apparent reduction of the rate of recovery of $[Ca^{2+}]_i$ following its release from NP-EGTA only when its effects upon pH_i was also apparent and not when pH_i had recovered. These experiments confirm the relatively unimportant role of the Na^+/Ca^{2+} exchanger in the overall Ca^{2+}-homeostasis of our neuronal preparations without the necessity of the use of TMA required to restore pH_i when Na^+ is replaced by NMDG.

The role of mitochondria

Ca^{2+} uptake into mitochondria occurs at the expense of ATP production. Mitochondria take up Ca^{2+} via a uniporter driven by the large electrochemical gradient across the mitochondrial inner membrane (Werth and Thayer, 1994). Ca^{2+} exits the mitochondria via a Na^+/Ca^{2+} exchanger, and Na^+ is then removed via a Na^+/H^+ exchanger, the net result being that two H^+ ions are prevented from entering the mitochondria via the ATP-synthase resulting in a decrease in ATP production. This study demonstrates that mitochondria are the principal mechanism responsible for sequestering Ca^{2+} in neonatal rat hippocampal neurons. Using 2 μM of the protonophore CCCP, we found a significant prolongation of the rate of recovery to baseline values following flash photolysis of NP-EGTA and this effect was still observed when the fall in pH_i induced by CCCP was restored with TMA. Similar results were found when mitochondrial Ca^{2+}-uptake was inhibited by superfusion of 5 μM of the respiratory chain inhibitor rotenone (see Table 3). The conclusion that mitochondrial Ca^{2+}-uptake is a major source of Ca^{2+}-sequestration is in agreement with Thayer and Miller (1990), Tatsumi and Katayama (1993), Stuenkel (1994), Werth and Thayer (1994) and White and Reynolds (1995).

When using protonophores such as CCCP consideration must be given to their effect on intracellular ATP levels in addition to their effect on pH_i. Protonophores are highly effective at collapsing the proton gradient across the mitochondrial inner membrane resulting in a reversal of the inner mitochondrial membrane ATP-synthase and the conversion of ATP to ADP and inorganic phosphate (Budd and Nicholls, 1996). In assessing Ca^{2+}-homeostatic mechanisms it is therefore necessary to distinguish between a direct inhibition of mitochondrial Ca^{2+}-uptake and an indirect inhibition of other potential mechanisms due to ATP depletion. Many groups have not accounted for ATP depletion following protonophore addition and as a result do not distinguish between longer recovery times to baseline levels as a result of inhibition of mitochondrial Ca^{2+}-uptake or those resulting from the ensuing inhibition of an ATP-dependent Ca^{2+}-homeostatic mechanism (Thayer and Miller, 1990; Wang and Thayer, 1994; Kiedrowski and Costa, 1995; White and Reynolds; 1995). Where others have simply measured ATP levels and, in doing so, have concluded that protonophores do not influence ATP stores (White and Reynolds, 1995) Budd and Nicholls (1996) demonstrated that it is the ATP/ADP ratio which is important for the functioning of many enzymes and not the absolute ATP level. In order to limit ATP depletion, we superfused our neuronal preparations with the ATP-synthase inhibitor oligomycin. When doing so, ATP/ADP levels are transiently maintained (most likely due to glycolysis) and any changes in Ca^{2+}-extrusion rates can be attributed to inhibition of mitochondrial Ca^{2+}-uptake rather than ATP depletion (Budd and Nicholls, 1996). Under these conditions we still observed a marked prolongation of the recovery rate of background subtracted fluo-3 fluorescence levels following Ca^{2+}-release from NP-EGTA (see Table 3).

We have also considered the possibilities that protonophores may influence non-mitochondrial Ca^{2+}-pools or may permeabilize the plasma membrane allowing H^+ ions to move towards their Nernst electrochemical equilibrium, consequently influencing pH_i or potentially depolarizing the plasma membrane thereby promoting Ca^{2+}-entry via VGCC (Duchen, 1990; Jensen and Rehder, 1991; White and Reynolds, 1995; Budd and Nicholls, 1996b). Jensen and Rehder (1991) showed that in *Helisoma* neurons, FCCP induced an increase in $[Ca^{2+}]_i$ that lasted indefinitely and was not influenced by earlier depletion of mitochondrial Ca^{2+}-stores, and White and Reynolds (1995) showed that increases in $[Ca^{2+}]_i$, in cultured rat cortical neurons, induced by FCCP application, were decreased when VGCC blockers were superfused. In our experiments, CCCP produced a small fall in pH_i and only a transient increase in $[Ca^{2+}]_i$ (see Fig. 15) suggesting that in neonatal rat hippocampal neurons, only minimal amounts of Ca^{2+} are released from the mitochondria. This transient increase in $[Ca^{2+}]_i$ may originate from three other potential sources; firstly, inhibition of mitochondrial Ca^{2+}-uptake, secondly, Ca^{2+}-entry via VGCC secondary to a depolarization of the plasma membrane, and thirdly, a release of Ca^{2+} from non-specific Ca^{2+} binding sites within the cytoplasm secondary to a decrease in pH_i. Following the addition of TMA, this increase in $[Ca^{2+}]_i$ reversed and declined (see Fig. 15) suggesting that the majority of the increase was pH related and occurred most likely as a result of protons dislodging Ca^{2+} from nonspecific intracellular binding sites and not as a result of further Ca^{2+}-entry as a result of membrane depolarization (Meech and Thomas, 1977; Ou Yang *et al.*, 1995). This pH related increase in Ca^{2+} following superfusion of 2 μM CCCP is further strengthened by the fact that when pH_i was not corrected for, superfusion of 2 µM CCCP produced a long-lasting increase in $[Ca^{2+}]_i$ (see Fig. 14). Similarly, following rotenone superfusion, which does not change pH_i, baseline $[Ca^{2+}]_i$ did not change (see Fig. 18) further strengthening our conclusion that rises in $[Ca^{2+}]_i$ following CCCP superfusion which does change pH_i levels, were in fact due to a reduction in pH_i.

We conclude from our observations that mitochondria are the major Ca^{2+}-homeostatic mechanism available to cultured post-natal hippocampal neurons for the reduction of increases in $[Ca^{2+}]_i$ to baseline values following flash photolysis of NP-EGTA. When inhibiting mitochondrial Ca^{2+}-uptake with CCCP, $[Ca^{2+}]_i$ never fully recovered to baseline levels most likely as a result of the effects of pH. On the other hand, when using rotenone to inhibit mitochondrial Ca^{2+} uptake, baseline values were restored in the majority of neurons measured. We believe that the principal reason for this discrepancy is the dramatically different effects of these two compounds on pH_i.

In view of the fact that, following inhibition of mitochondrial Ca^{2+}-uptake, Ca^{2+}-levels begin to decay towards baseline values, other mechanisms are most likely involved in the restoration of baseline Ca^{2+}-levels. During control situations, when mitochondrial Ca^{2+}-uptake is not inhibited, mitochondria sequester the majority of the Ca^{2+}-increase induced by flash photolysis of NP-EGTA but, following inhibition of mitochondrial Ca^{2+}-uptake, other previously unimportant mechanisms (Na^+/Ca^{2+} exchanger, PM-ATPase, ER-ATPase) may begin to sequester Ca^{2+} in order to return Ca^{2+}-levels to near baseline values. This explains the recovery of Ca^{2+}-levels seen following flash photolysis of NP-EGTA in neurons in which mitochondrial Ca^{2+}-uptake has been inhibited with CCCP or rotenone.

The role of the ER

It has been reported that the caffeine sensitive Ca^{2+} stores may be substantially different in their magnitudes when comparing central (including hippocampal), and peripheral neurons (Shmigol *et al.*, 1994). In the latter, caffeine results in a significant intracellular release of Ca^{2+} whereas in central neurons it is relatively ineffective. We used ryanodine, CPA and thapsigargin in attempts to inhibit the uptake of Ca^{2+} into intracellular stores such as the ER. The results of these experiments were quite variable and in some cases we even observed a small increase in the rate of recovery of fluo-3 fluorescence during application of these drugs. However, taken as a whole, we found no consistent evidence to suggest that the ER-ATPase was an important contributor to the homeostasis of Ca^{2+}-loads induced by photolysis of NP-EGTA. A similarly negative conclusion resulted from experiments designed to determine the role of the PM-ATPase in Ca^{2+}-buffering by inhibiting its activity with vanadate. Eosin, a potent and specific inhibitor of the PM-ATPase (Gatto *et al.*, 1995), is fluorescent at the excitation wavelength used for fluo-3, and as a result it could not be used to assess the contributions of the PM-ATPase to Ca^{2+}-homeostasis using our methods.

Conclusions, limitations and future directions

From this study we conclude that following flash photolysis of NP-EGTA, the principal Ca^{2+}-homeostatic mechanism responsible for reducing $[Ca^{2+}]_i$ levels back to baseline values is mitochondrial Ca^{2+}-uptake. Inhibition of all other potential Ca^{2+}-homeostatic mechanisms did not influence the decay back to baseline values once normal pH_i was either maintained or restored. There are however, several limitations associated with the above conclusions. Firstly,

$[Ca^{2+}]_i$ was measured from the cell bodies of hippocampal neurons whereas many Ca^{2+}-homeostatic mechanisms, for example the Na^+/Ca^{2+} exchanger, have been shown to be preferentially localized to nerve terminals and presynaptic boutons (Luther *et al.*, 1992; Reuter and Porzig, 1995). As a result inhibition of the Na^+/Ca^{2+} exchange in the cell bodies may have had little effect as the highest proportion of PM-Na^+/Ca^{2+} exchangers may have been found in other neuronal regions. Secondly, all experiments were performed at room temperature to improve the resolution of Ca^{2+}-transients, decrease dye-leakage and decrease dye-compartmentalization. As the Q_{10} values for Ca^{2+}-homeostatic mechanism are very temperature sensitive, this decreased temperature may not have demonstrated the true contributions of Ca^{2+}-homeostatic mechanisms such as the Na^+/Ca^{2+} exchanger, ER-ATPase or PM-ATPase to Ca^{2+}-transients. Instead these potential homeostatic mechanism may have been operating at a lower rate as compared with those seen at physiological temperatures.

This study found that mitochondrial Ca^{2+}-uptake was the principal mechanism responsible for reducing $[Ca^{2+}]_i$ back to baseline values. Using the fluorescent indicator dye rhod-2, which is selectively taken up by mitochondria, direct evidence for mitochondrial Ca^{2+}-uptake could be obtained and is an attractive option for further experiments. Our conclusions are also limited by the lack of information regarding the absolute levels of $[Ca^{2+}]_i$, obtained by the photolysis of NP-EGTA, especially in relation to levels that might be achieved under more physiological conditions. It would therefore be useful to reexamine the effect of mitochondrial inhibitors following the release of variable amounts of Ca^{2+} obtained by varying the concentration of NP-EGTA within neurons. Under these conditions it might be possible to determine a threshold $[Ca^{2+}]_i$, beyond which mitochondrial sequestration of Ca^{2+} becomes significant.

Following inhibition of mitochondrial Ca^{2+}-uptake, Ca^{2+}-levels decay towards initial levels suggesting that other homeostatic mechanisms may play a role in the restoration of baseline values. Experiments where multiple Ca^{2+}-homeostatic mechanisms are simultaneously inhibited would demonstrate which of the potential Ca^{2+}-homeostatic mechanism(s) may be operating during inhibition of mitochondrial Ca^{2+}-uptake.

Abdel-Hamid, K.M. & Baimbridge, K.G. (1997). The effects of artificial calcium buffers on calcium responses and glutamate-mediated excitotoxicity in cultured hippocampal neurons. *Neuroscience* In Press.

Adams, S.R. & Tsien, R.Y. (1993). Controlling cell chemistry with caged compounds. *Annual Review of Physiology* **55**, 755-784.

Ahmed, Z. & Connor, J.A. (1988). Calcium regulation by and buffer capacity of molluscan neurons during calcium transients. *Cell Calcium* **9**, 57-69.

Akerman, K.E.O., Wikstrom, M.K.F. & Saris, N.E. (1977). Effects of inhibitors on the sigmoidicity of the calcium ion transport kinetics in rat liver mitochondria. *Biochimica et Biophysica Acta* **464**, 287-294.

Aronson, P.S. (1985). Kinetic properties of the plasma membrane Na^+/H^+ exchanger. *Annual Review of Physiology* **47**, 545-560.

Augustine, G.J., Charlton, M.P. & Smith, S.J. (1987). Calcium action in synaptic transmitter release. *Annual Review of Neuroscience* **10**, 633-693.

Baimbridge, K.G., Celio, M.R. & Rogers, J.H. (1992). Calcium-binding proteins in the nervous system. *Trends in Neurosciences* **15**, 303-308.

Bassani, J.W.M., Bassani, R.A. & Bers, D.M. (1995). Calibration of indo-1 and resting intracellular $[Ca]_i$ in intact rabbit cardiac myocytes. *Biophysical Journal* **68**, 1453-1460.

Baxter, K.A. & Church, J. (1996). Characterization of acid extrusion mechanisms in cultured fetal rat hippocampal neurones. *Journal of Physiology* **493**, 457-470.

Bean, B.P. (1989). Classes of calcium channels in vertebrate cells. *Annual Review of*

Physiology **51**, 367-384.

Benham, C.D., Evans, M.L. & McBain, C.J. (1992). Ca^{2+} efflux mechanisms following depolarization evoked calcium transients in cultured rat sensory neurones. *Journal of Physiology* **455**, 567-583.

Berridge, M.J. (1997). Elementary and global aspects of calcium signalling. *Journal of Physiology* **499**, 291-306.

Bevensee, M.O., Cummins, T.R., Haddad, G.G., Boron, W.F. & Boyarsky, G. (1996). pH regulation in single CA1 neurons acutely isolated from the hippocampi of immature and mature rats. *Journal of Physiology* **494**, 315-328.

Blaustein M.P. (1988). Calcium transport and buffering in neurons. *Trends in Neurosciences* **11**, 438-443.

Blaustein, M.P. & Hodgkin, A.L. (1969). The effect of cyanide on the efflux of calcium from squid axons. *Journal of Physiology* **198**, 46-48.

Bleakman, D., Roback, J.D., Wainer, B.H., Miller, R.J. & Harrison, N.L. (1993). Calcium homeostasis in rat septal neurons in tissue culture. *Brain Research* **600**, 257-267.

Brandl, C.J., Green, N.M., Korczak, B. & MacLennan, D.H. (1986). Two Ca^{2+}-ATPase genes: homologies and mechanistic implications of deduced amino acid sequences. *Cell* **44**, 597-607.

Bright, G.R., Fisher, G.W., Rogowska, F. & Taylor, D.L. (1987). Fluorescence ratio imaging microscopy: Temporal and spatial measurements of cytoplasmic pH. *Journal of Cell Biology* **104**, 1019-1033.

Budd, S.L. & Nicholls, D.G. (1996). A Reevaluation of the role of mitochondria in neuronal Ca^{2+} homeostasis. *Journal of Neurochemistry* **66**, 403-411.

Budd, S.L. & Nicholls, D.G. (1996b) Mitochondria, calcium regulation, and acute glutamate excitotoxicity in cultured cerebellar granule cells. *Journal of Neurochemistry* **67**, 2282-2291.

Carafoli, E. (1987). Intracellular calcium homeostasis. *Annual Review of Biochemistry* **56**, 395-433.

Carafoli, E. (1991). The Calcium pumping ATPase of the plasma membrane. *Annual Review of Physiology* **53**, 531-547.

Caroni, P., Villani, F. & Carafoli, E. (1981). The cardiotoxic antibiotic doxorubicin inhibits the Na^+/Ca^{2+} exchange of dog heart. *FEBS Letters* **130**, 184-186.

Chaillet, J.R. & Boron, W.F. (1985). Intracellular calibration of a pH-sensitive dye in isolated, perfused salamander proximal tubules. *Journal of General Physiology* **86**, 765-94.

Chard, P.S., Bleakman, J.D., Christakos, D., Fullmer, C.S. & Miller, R.J. (1993). Calcium buffering properties of Calbindin D28k and parvalbumin in rat sensory neurones. *Journal of Physiology* **472**, 341-357.

Chesler, M. & Kaila, K. (1992). Modulation of pH by neuronal activity. *Trends in Neurosciences* **15**, 396-402.

De Luca, H.F. & Engström, G.W. (1961). Calcium uptake by rat kidney mitochondria. *Proceedings of the National Academy of Sciences of the United States of America* **47**, 1744-1750.

Dipolo, R. & Beauge, L. (1979). Physiological Role of ATP-driven calcium pump in squid axon. *Nature* **278**, 271-273.

Duchen, M.R., Valdeolmillos, M., O'Neill, S.C. & Eisner, D.A. (1990). Effects of metabolic blockade on the regulation of intracellular calcium in dissociated mouse sensory neurones. *Journal of Physiology* **424**, 411-426.

Duchen, M.R. (1990). Effects of metabolic inhibition on the membrane properties of isolated mouse primary sensory neurones. *Journal of Physiology* **424**, 387-409.

Dunham, E.T. & Glynn, I.M. (1961). Adenosine-triphosphatase activity and the active movements of alkali metal ions. *Journal of Physiology* **156**, 274-293.

Ebashi, S. & Lippman, F. (1962). Adenosine triphosphate-linked concentration of calcium ions in a particulate fraction of rabbit muscle. *Journal of Cell Biology* **14**, 389-400.

Eliasson, L., Proks, P., Ämmälä, C., Ashcroft, F.M., Bokvist, K, Renström, E., Rorsman, P. & Smith, P.A. (1996). Endocytosis of secretory granules in mouse pancreatic β-cells evoked by transient elevation of cytosolic calcium. *Journal of Physiology* **493**, 755-767.

Ellis-Davies, G.C.R. & Kaplan, J.H. (1994). Nitrophenyl-EGTA, a photolabile chelator that selectively binds Ca^{2+} with high affinity and releases it rapidly upon photolysis. *Proceedings of the National Academy of Sciences of the United States of America* **93**, 187-191.

Fabiato, A. (1983). Calcium-induced release of calcium from the cardiac sarcoplasmic reticulum. *American Journal of Physiology* **245**, C1-14.

Farber, J.L. (1981). The role of calcium in cell death. *Life Science* **29**, 1289-1295.

Friel, D.D. & Tsien, R.W. (1994). An FCCP-sensitive Ca^{2+} store in bullfrog sympathetic neurons and its participation in stimulus-evoked changes in $[Ca^{2+}]_i$. *The Journal of Neuroscience* **14**, 4007-4024.

Gambassi, G., Hansford, R.G., Sollott, S.J., Hogue, B.A., Lakatta, E.G. & Capogrossi, M.C. (1993). Effects of acidosis on resting cytosolic and mitochondrial Ca^{2+} in mammalian myocardium. *Journal of General Physiology* **102**, 575-597.

Gatto, C., Hale, C.C., Xu, W. & Milanick, M.A. (1995) Eosin, a potent inhibitor of the plasma membrane Ca pump, does not inhibit the Cardiac Na-Ca exchanger. *Biochemistry* **34**, 965-972.

Gleason, E., Borges, S. & Wilson, M. (1995). Electrogenic Na^+-Ca^{2+} exchange clears Ca^{2+} loads from retinal amacrine cells in culture. *The Journal of Neuroscience* **15**, 3612-3621.

Goeger, D.E., Riley, R.T. & Dorner, J.W. (1988). Cyclopiazonic acid inhibition of the Ca^{2+}-transport ATPase in rat skeletal muscle sarcoplasmic reticulum vesicles. *Biochemical Pharamcology* **37**, 978-981.

Gopinath, R.M. & Vincenzi, F.F. (1977). Phosphodiesterase protein activator mimics red blood cell cytoplasmatic activator of the (Ca^{2+} + Mg^{2+}) ATPase. *Biochemical and Biophysical Research Communications* **77**, 1203-1209.

Gottfried, J.A. & Chesler, M. (1994). Endogenous H^+ modulation of NMDA receptor-mediated EPSCs revealed by carbonic anhydrase inhibition in rat hippocampus. *Journal of Physiology* **478**, 373-378.

Grynkiewica, G., Poenie, M. & Tsien, R.Y. (1985). A new generation of Ca^{2+} indicators with greatly improved fluorescence properties. *Journal of Biological Chemistry* **260**, 3440-3450.

Gunter, T.E., Gunter, K.K., Sheu, S.S. & Gavin, C.E. (1994). Mitochondrial calcium transport: physiological and pathological relevance. *American Journal of Physiology* **267**, C313-339.

Gunter, T.E. & Pfeiffer, D.R. (1990). Mechanisms by which mitochondria transport calcium. *American Journal of Physiology* **258**, C755-C786.

Hadley, R.W., Kirby, M.S., Lederer, W.J. & Koa, J.P.Y. (1993). Does the use of DM-nitrophen, nitr-5, or diazo-2 interfere with the measurement of indo-1 fluorescence. *Biophysical Journal* **65**, 2537-2546.

Harrison, S.M. & Bers, D.M. (1987). The effect of temperature and ionic strength on the apparent Ca-affinity of EGTA and the analogous Ca-chelators BAPTA and dibromo-BAPTA. *Biochimica et Biophysica Acta* **925**, 133-143.

Hehl, S., Golard, A., & Hille, B. (1996). Involvement of mitochondria in intracellular calcium sequestration by rat gonadotropes. *Cell Calcium* **20**, 515-524.

Herrington, J., Park, Y.B., Babcock, D.F. & Hille, B. (1996). Dominant role of mitochondria in clearance of large Ca^{2+} loads from rat adrenal chromaffin cells. *Neuron* **16**, 219-228.

Hess, P. (1990). Calcium channels in vertebrate cells. *Annual Review of Neuroscience* **13**, 337-356.

Hirning, L.D., Fox, A.P., McCleskey, E.W., Oliver, B.M., Thayer, S.A., Miller, R.J. & Tsien, R.W. (1988). Dominant role of N-type Ca^{2+} channels in evoked release of norepinephrine from sympathetic neurons. *Science* **239**, 57-61.

Holliday, J., Adams, R.J., Sejnowski, T.J. & Spitzer, N.C. (1991). Calcium-induced release of calcium regulates differentiation of cultured spinal neurons. *Neuron* 7, 787-796.

Huettner, J.E. & Baughman, R.W. (1986). Primary cultures of identified neurons from the visual cortex of postnatal rats. *Journal of Neuroscience* **6**, 3044-3060.

Hodgkin A.L. & Keynes R.D. (1957). Movements of labeled calcium in squid giant axons. *Journal of Physiology* **134**, 253-281.

Holzapfel, S.W. (1968). The isolation and structure of cylopiazonic acid, a toxic metabolite of penicillium cylopium westling. *Tetrahedron* **24**, 2101-2119.

Inesi, G. & Sagara, Y. (1994). Specific inhibitors of intracellular Ca^{2+}-transport ATPases. *The Journal of Membrane Biology* **141**, 1-6.

Ingersoll, R.J. & Wasserman, R.H. (1971). Vitamin D3-induced calcium-binding protein binding characteristics, conformational effects, and other properties. *Journal of Biological Chemistry* **246**, 2808-2814.

Jensen, J.R. & Rehder, V. (1991). FCCP Releases Ca^{2+} from a non-mitochondrial store in an identified *Helisoma* neuron. *Brain Research* **551**, 311-314.

Kao, J.P.Y., Harootunian, A.T. & Tsien, R.Y. (1989). Photochemically generated cytosolic calcium pulses and their detection by fluo-3. *Journal of Biological Chemistry* **264**, 8179-8184.

Kao, J.P.Y. (1994). Practical aspects of measuring $[Ca^{2+}]$ with fluorescent indicators. *Methods in Cell Biology* **40**, 155-181.

Katz, S. & Blostein, R. (1975). Ca^{2+}-stimulated membrane phosphorylation and ATPase activity of the human erythrocyte. *Biochimica et Biophysica Acta* **389**, 314-324.

Katz, B. & Miledi, R. (1969). Tetrodotoxin-resistant electric activity in presynaptic terminals. *Journal of Physiology* **203**, 459-487.

Kennedy, H.J. & Thomas, R.C. (1995). Intracellular calcium and its sodium-independent regulation in voltage-clamped snail neurones. *Journal of Physiology* **484**, 533-548.

Kennedy, H.J. & Thomas, R.C. (1996). Effects of injection calcium-buffer solutions on $[Ca^{2+}]_i$ in Voltage-clamped snail neurons. *Biophysical Journal* **70**, 2120-2130.

Kiedrowski, L. & Costa, E. (1995). Glutamate-induced destabilization of intracellular calcium concentration homeostasis in cultured cerebellar granule cells: role of mitochondria in calcium buffering. *Molecular Pharmacology* **47**, 140-147.

Kiedrowski, L., Brooker, G., Costa, E. & Wroblewski, J.T. (1994). Glutamate impairs neuronal calcium extrusion while reducing the sodium gradient. *Neuron* **12**, 295-300.

Knauf, P.A., Proverbio, F. & Hoffmann, J.F. (1974). Electrophoretic separation of different phosphoproteins associated with Ca^{2+}-ATPase and Na^+, K^+-ATPase in human red cells ghosts. *Journal of General Physiology* **63**, 324-336.

Koch, R.A. & Barish, M.E. (1994). Perturbation of intracellular calcium and hydrogen ion regulation in cultured mouse hippocampal neurons by reduction of the sodium ion concentration gradient. *The Journal of Neuroscience* **14**, 2585-2593.

Kostyuk, P.G., Mironov, S.L., Tepikin, A.L. & Belan, P.V. (1989). Cytoplasmic free Ca in isolated snail neurons as revealed by fluorescent probe Fura-2: Mechanisms of Ca recovery after Ca Load and Ca Release from intracellular stores. *The Journal of Membrane Biology* **110**, 11-18.

Kraig, R., Petito, C., Plum, F. & Pulsinelli, W. Hydrogen ions kill brain at concentrations reached in ischemia. *Journal of Cerebral Blood Flow & Metabolism* **7**, 379-386.

Kretsinger, R.H., Nockolds, C.E. (1973). Carp muscle calcium-binding protein. II. Structure determination and general description. *Journal of Biological Chemistry* **248**, 3313-3326.

Lamb, G.D., & Stephenson, D.G. (1995). Activation of ryanodine receptors by flash photolysis of caged Ca^{2+}. *Biophysical Journal* **68**, 946-948.

Lledo, P.M. Somasundaram, B., Morton, A.J., Emson, P.C., & Mason, W.T. (1992). Stable transfection of Calbindin-D28k into the GH3 cell line alters calcium currents and intracellular calcium homeostasis. *Neuron* **9**, 943-954.

Llinas, R., Sugimori, M., Lin, J.W. & Cherksey, B. (1989). Blocking and isolation of a calcium channel from neurons in mammals and cephalopods utilizing a toxin fraction (FTX) from funnel-web spider poison. *Proceedings of the National Academy of Sciences of the United States of America* **86**, 1689-1693.

Luther, P.W., Yip, R.K., Bloch, R.J., Ambesi, A., Lindenmayer, G.E. & Blaustein, M.P. Presynaptic localization of sodium/calcium exchangers in neuromuscular preparations. *The Journal of Neuroscience* **12**, 4898-4904.

Lynch, T.J. & Cheung, W.Y. (1979). Human erythrocyte (Ca^{2+} Mg^{2+})-ATPase: mechanism of stimulation by Ca^{2+}. *Archives of Biochemistry and Biophysics* **194**, 195-170.

Lynch, G., Larson, J., Kelso, S., Barrionuevo, G. & Schottler, F. (1983). Intracellular injections of EGTA block induction of hippocampal long-term potentiation. *Nature* **305**, 719-21.

MacLennan, D.H., Brandl, C.J., Korczak, B. & Green, N.M. (1985). Amino-acid sequence of a Ca^{2+}-Mg^{2+} dependent ATPase from rabbit muscle sarcoplasmic reticulum, deduced from its complementary DNA sequence. *Nature* **316**, 696-700.

Madison, D., Fox, A.P. & Tsien, R.W. (1987). Adenosine reduces an inactivating component of calcium current in hippocampal CA3 neurons. *Biophysical Journal* **51**, 30a.

Marengo, F.D., Wang, S.Y. & Langer, G.A. (1997). The effects of temperature upon calcium exchange in intact cultured cardiac myocytes. *Cell Calcium* **21**, 263-273.

Martínez-Zaguilán, R., Parnami, G. & Lynch, R.M. (1996). Selection of fluorescent ion indicators for simultaneous measurements of pH and Ca^{2+}. *Cell Calcium* **19**, 337-349.

Mayer, M.L., & Westbrook, G.L. (1987). Permeation and block of N-methyl-D-aspartic acid receptor channels by divalent cations in mouse cultured central neurons. *Journal of Physiology* **394**, 501-527.

McBurney R.N. & Neering I.R. (1987). Neuronal calcium homeostasis. *Trends in*

Neurosciences **10**, 164-169.

Meech, R.W. & Thomas, R.C. (1977). The effect of calcium injection on the intracellular sodium and pH of snail neurones. *Journal of Physiology* **265**, 867-879.

Meech, R.W. (1978). Calcium-dependent potassium activation in nervous tissues. *Annual Review of Biophysics & Bioengineering* 7, 1-18.

Milanick, M.A. (1990). Proton fluxes associated with the Ca pump in human red-blood-cells. *American Journal of Physiology* **258**, C552-C562.

Miller, R.J. (1991). The control of neuronal Ca^{2+} homeostasis. *Progress in Neurobiology* **37**, 255-285.

Miller R.J. (1992). Voltage-sensitive Ca^{2+}-channels. *Journal of Biological Chemistry* **267**, 1403-1406.

Minta, A., Kao, J.P.Y. & Tsien, R.Y. (1989). Fluorescent indicators for cytosolic calcium based on rhodamine and fluorescein. *Journal of Biological Chemistry* **264**, 8171-8178.

Mintz, I.M., Venema, V.J., Swiderek, K.M., Lee, T.D., Bean, B.P. & Adams, M.E. (1992). P-type calcium channels blocked by the spider toxin *omega*-Aga-IVA. *Nature* **355**, 827-829.

Mironov, S.L. (1995). Plasmalemmal and intracellular Ca pumps as main determinants of slow Ca buffering in rat hippocampal neurones. *Neuropharmacology* **9**, 1123-1132.

Mironov, S.L., Usachev, Y.M. & Lux, H.D. (1993). Spatial and temporal control of intracellular free Ca^{2+} in chick sensory neurons. *Pflugers Archives* **424**, 183-191.

Mitchell, P. (1966). Chemiosmotic coupling in oxidative and photosynthetic phosphorylation.

Biological Reviews of the Cambridge Philosophical Society **41**, 445-502.

Moore, G.A., McConkey, D.J., Kass, G.E., O'Brien, P.J. & Orrenius, S. (1987). 2,5-di(tert-butyl)-1,4-benzohydroquinone-a novel inhibitor of liver microsomal Ca^{2+} sequestration. *FEBS Letters* **224**, 331-336.

Morgan, J.I., & Curran, T. (1988). Calcium as a modulator of the immediate-early gene cascade in neurons. *Cell Calcium* **9**, 303-311.

Morita, K., North, R.A. & Tokimasa, T. (1982). The calcium activated potassium conductance in guinea-Pig myenteric neurones. *Journal of Physiology* **329**, 341-354.

Nelson S.R. & Foltz F.M. (1983). Hypocalcemia and motor neuron degeneration in paraphysectomized frogs. *Experimental Neurology* **79**, 763-772.

Nerbonne, J.M. (1996). Caged Compounds: tools for illuminating neuronal responses and connections. *Current Opinion in Neurobiology* **6**, 379-386.

Nicholls, D.G. (1985). A role for the mitochondrion in the protection of cells against calcium overload? *Progress in Brain Research* **63**, 97-106.

Nicholls, D.G. (1986). Intracellular calcium homeostasis. *British Medical Bulletin* **42**, 353-358.

Niggli, V., Sigel, E. & Carafoli, E. (1982). The purified Ca^{2+} pump of human-erythrocyte membranes catalyzes an electroneutral Ca^{2+}-H^{+} exchange in reconstituted liposomal systems. *Journal of Biological Chemistry* **257**, 2350-2356.

Nowycky, M.C., Fox, A.P. & Tsien, R.W. (1985). Three types of neuronal calcium channel with different calcium agonist sensitivity. *Nature* **316**, 440-443.

Oberholtzer, J.C., Baettger, C., Summers, M.C. & Matschinsky, F.M. (1988). The 28 kDa calbindin is a major calcium binding protein in the basilar papilla of the chick. *Proceedings of the National Academy of Sciences of the United States of America* **85**, 3387-3391.

Osterrieder, W., Brum, G., Hescheler, J., Trautwein, W., Flockerzi, V. & Hofmann, F. (1982). Injection of subunits of cyclic AMP-dependent protein kinase into cardiac myocytes modulates Ca^{2+} current. *Nature* **298**, 576-578.

Ou Yang, Y., Kristián, T., Kristiánová, V., Mellergård, P. & Siesjö, B.K. (1995). The influence of calcium transients on intracellular pH in cortical neurons in primary culture. *Brain Research* **676**, 307-313.

Park, Y.B., Herrington, J., Babcock, D.F. & Hille, B. (1996). Ca^{2+} clearance mechanisms in isolated rat adrenal chromaffin cells. *Journal of Physiology* **492**, 329-346.

Parsons, T.D., Ellis-Davies, G.C.R. & Almers, W. (1996). Millisecond studies of calcium-dependent exocytosis in pituitary melanotrophs: comparison of the photolabile calcium-chelators nitrophenyl-EGTA and DM-nitrophen. *Cell Calcium* **19**, 185-192.

Plummer, M.R., Logothetis, D.E. & Hess, P. (1989). Elementary properties and pharmacological sensitivities of calcium channels in mammalian peripheral neurons. *Neuron* **2**, 1453-1463.

Putnam, R.W. (1995). Intracellular pH regulation. *Cell Physiology Source Book* 212-229.

Randall, R.D. & Thayer, S.A. (1992). Glutamate-induced calcium transient triggers delayed calcium overload and neurotoxicity in rat hippocampal neurons. *Journal of Neuroscience* **12**, 1882-1895.

Rasmussen, U., Christensen, S.B. & Sanberg, F. (1978). Thapsigargin and thapsigargicine, two new histamine liberators from *Thapsia garganica L. Acta Pharmaceutica Suecica* **15**, 133-140.

Reeves, J.P. & Sutko, J.L. (1980). Sodium-calcium exchange activity generates a current in cardiac membrane vesicles. *Science* **208**, 1461-1464.

Regan, L.J., Sah, D.Y.W., & Bean, B.P. (1991). Ca channels in rat central and peripheral neurons: high-threshold current resistant to dihydropyridine blockers and ω-conotoxin. *Neuron* **6**, 269-280.

Regehr, W.G. & Mintz, I.M. (1994). Participation of multiple calcium channel types in transmission at single climbing fiber to Purkinje cell synapses. *Neuron* **12**, 605-613.

Reuter, H. & Porzig, H (1995). Localization and functional significance of the Na/Ca exchanger in presynaptic boutons of hippocampal cells in cultures. *Neuron* **15**, 1077-1084.

Reuter, H., Seitz, N. (1968). The dependence of calcium efflux from cardiac muscle on temperature and external ion composition. *Journal of Physiology* **195**, 451-470.

Reuter, H., Stevens, C.F., Tsien, R.W. & Yellen, G. (1982). Properties of single calcium channels in cardiac cell culture. *Nature* **297**, 501-504.

Rizzuto, R., Simpson, A.W.M., Brini, M. & Pozzan, T. (1992). Rapid changes of mitochondrial Ca^{2+} revealed by specifically targeted recombinant aequorin. *Nature* **358**, 325-327.

Rizzuto, R., Bastianutto, S., Brini, M., Murgia, M. & Pozzan, T. (1994). Mitochondrial Ca^{2+} homeostasis in intact cells. *The Journal of Cell Biology* **126**, 1183-1194.

Ronner, P., Gazzotti, P. & Carafoli, E. (1977). A lipid requirement for the (Ca^{2+} Mg^{2+})-activated ATPase of erythrocyte membranes. *Archives of Biochemistry and Biophysics* **179**, 578-583.

Ross, W.N., Stockbridge, L.L. & Stockbridge, N.L. (1986). Regional properties of calcium entry in barnacle neurons determined with Arsenazo III and a photodiode array. *Journal of Neuroscience* **6**, 1148-1159.

Ross W.N. (1993) Calcium on the level. *Biophysical Journal* **64**, 1655-1656.

Sala, F. & Hernandez-Cruz, A. (1990). Calcium diffusion modeling in a spherical neuron: Relevance of buffering properties. *Biophysical Journal* **57**, 313-324.

Sanchez-Armass, S. & Blaustein, M.P. (1987). Role of sodium-calcium exchange in regulation of intracellular calcium in nerve terminals. *American Journal of Physiology* **252**, C595-C603.

Schatzmann, H.J. (1966) ATP-dependent Ca++ extrusion from human red cells. *Experimentia* **22**, 364-368.

Schlue, W.R. & Dörner, R. (1992). The regulation of pH in the central nervous system. *Canadian Journal of Physiology and Pharmacology* **70**, S278-S285.

Schwiening, C.J., Kennedy, H.J. & Thomas R.C. (1993) Calcium-hydrogen exchange by the plasma membrane Ca-ATPase of voltage-clamped snail neurons. *Proceedings of the Royal Society London* **253**, 285-289.

Schwiening, C.J. & Boron, W.F. (1994). Regulation of intracellular pH in pyramidal neurones from the rat hippocampus by Na^+-dependent Cl^--HCO_3^-exchange. *Journal of Physiology* **475**, 59-67.

Seidler, N.W., Jona, I., Vegh, M. & Martonosi, A. (1989). Cyclopiazonic acid is a specific inhibitor of the Ca^{2+}-ATPase of sarcoplasmic reticulum. *Journal of Biological Chemistry* **264**, 17816-17823.

Shmigol, A, Kirischuk, S., Kostyuk, P. & Verkhratsky, A. (1994). Different properties of caffeine-sensitive Ca^{2+} stores in peripheral and central mammalian neurones. *Pflugers Archives* **426**, 174-176.

Shuttleworth, T.J. & Thompson, J.L. (1991). Effect of Temperature on receptor-activated changes in $[Ca^{2+}]_i$ and their determination using fluorescent probes. *Journal of Biological Chemistry* **266**, 1410-1414.

Sidky, A.O. & Baimbridge, K.G. (1997). Na^+/Ca^{2+} exchange is not involved in the fast recovery of Ca^{2+} levels in neurons in which normal pH_i is restored. *Canadian Journal of Physiology and Pharmacology* **75** Axvii.

Siegl, P.K.S., Cragoe, E.J., Trumble, M.J. & Kaczorowski, G.J. (1984). Inhibition of Na^+/Ca^{2+} exchange in membrane vesicle and papillary muscle preparations from guinea pig heart by analogs of amiloride. *Proceedings of the National Academy of Sciences of the United States of America* **81**, 3238-3242.

Simpson, P.B., Challiss, R.A.J. & Nahorski, S.R. (1993). Involvement of intracellular stores in the Ca^{2+} responses to N-Methyl-D-aspartate and depolarization in cerebellar granule cells. *Journal of Neurochemistry* **61**, 760-763.

Simpson, P.B., Challiss R.A.J. & Nahorski, S.R. (1995). Neuronal Ca^{2+} stores: activation and function. *Trends in Neurosciences* **18**, 299-306.

Smallwood, J.I., Waisman, D.M., Lafreniere, D. & Rasmussen, H. (1983). Evidence that the erythrocyte calcium pump catalyzes a Ca^{2+}:nH^+ exchange. *Journal of Biological Chemistry* **258**, 1092-1097.

Snutch, T.P., Leonard, J.P., Gilbert, M.M., Lester, H.A. & Davidson, N. (1990). Rat brain expresses a heterogeneous family of calcium channels. *Proceedings of the National Academy of Sciences of the United States of America* **87**, 3391-3395.

Stauffer, T.P., Guerini, D., Celio, M.R. & Carafoli, E. (1997). Immunolocalization of the plasma membrane Ca^{2+} pump isoforms in the rat brain. *Brain Research* **748**, 21-29.

Stuenkel, E.L. (1994). Regulation of intracellular calcium and calcium buffering properties of rat isolated neurohypophysial nerve endings. *Journal of Physiology* **481**, 251-271.

Takadera, T., Shimada, Y. & Mohri, T. (1992). Extracellular pH modulates N-methyl-D-aspartate receptor-mediated neurotoxicity and calcium accumulation in rat cortical cultures. *Brain Research* **572**, 126-131.

Tang, C.M., Dichter, M. & Morad, M. (1990). Modulation of the N-methyl-D-aspartate channel by extracellular H^+. *Proceedings of the National Academy of Sciences of the United States of America* **87**, 6445-6449.

Tatsumi, H. & Katayama, Y. (1993). Regulation of the intracellular free calcium concentration in acutely dissociated neurones from rat nucleus basalis. *Journal of Physiology* **464**, 165-181.

Thastrup, O., Dawson, A.P., Scharff, O., Foder, B., Cullen, P.J., Drobak, B.K., Bjerrum, P.J., Christensen, S.B. & Hanley, M.R. (1989). Thapsigargin, a novel molecular probe for studying intracellular calcium release and storage. *Agents & Actions* **27**, 17-23.

Thayer, S.A. & Miller, R.J. (1990). Regulation of the intracellular free calcium concentration in single rat dorsal root ganglion neurones *in vitro. Journal of Physiology* **425**, 85-115.

Traynelis, S.F. & Cull-Candy, S.G. (1990). Proton inhibition of N-methyl-D-aspartate receptors in cerebellar neurons. *Nature* **345**, 347-350.

Tsien, R.W., Lipsombe, D., Madison, D.V., Bley, K.R. & Fox, A.P. (1988). Multiple types of neuronal calcium channels and their selective modulation. *Trends in Neurosciences* **11**, 431-438.

Tsien, R.W. & Tsien, R.Y. (1990). Calcium channel stores and oscillations. *Annual review of*

Cell Biology **6**, 715-760.

Tsien, R.W. Ellinor, P.T. & Horne, W.A. (1991). Molecular diversity of voltage dependent Ca^{2+} channels. *Trends in Neurosciences* **12**, 349-354.

Tymianski, M. Charlton, M.P., Carlen, P.L. & Tator, C.H. (1993). Source specificity of early calcium neurotoxicity in cultured embryonic spinal neurons. *The Journal of Neuroscience* **13**, 2085-2104.

Vasington, F.D., Murphy, J. (1961). *Federation Proceedings* **20**, 146.

Wang, G.J., Randall, R.D. & Thayer, S.A. (1994). Glutamate induced intracellular acidification of cultured hippocampal neurons demonstrates altered energy metabolism resulting from Ca^{2+} loads. *Journal of Neurophysiology* **72**, 2563-2569.

Wasserman, R.H. & Taylor, A.N. (1966). Vitamin D3-induced calcium-binding protein in chick intestinal mucosa. *Science* **152**, 791-793.

Werth, J.L. & Thayer, S.A. (1994). Mitochondria buffer physiological calcium loads in cultured rat dorsal root ganglion neurons. *The Journal of Neuroscience* **14**, 348-356.

Werth, J.L., Usachev, Y.M. & Thayer, S.A. (1996). Modulation of calcium efflux from cultured rat dorsal root ganglion neurons. *The Journal of Neuroscience* **16**, 1008-1015.

White, R.J. & Reynolds, I.J. (1995). Mitochondria and Na^{+}/Ca^{2+} exchange buffer glutamate-induced calcium loads in cultured cortical neurons. *The Journal of Neuroscience* **15**, 1318-1328.

Widdowson, E.M. & Dickerson, J.W. (1964). Mineral Metabolism 2, 1-247.

Zavoico, G.B. & Cragoe, E.J. (1988). Ca^{2+} mobilization can occur independent of acceleration of Na^+/H^+ exchange in thrombin-stimulated human platelets. *Journal of Biological Chemistry* **263**, 9635-9639.

Zucker, R.S. (1992). Effects of photolabile calcium chelators on fluorescent calcium indicators. *Cell Calcium* **13**, 29-40.